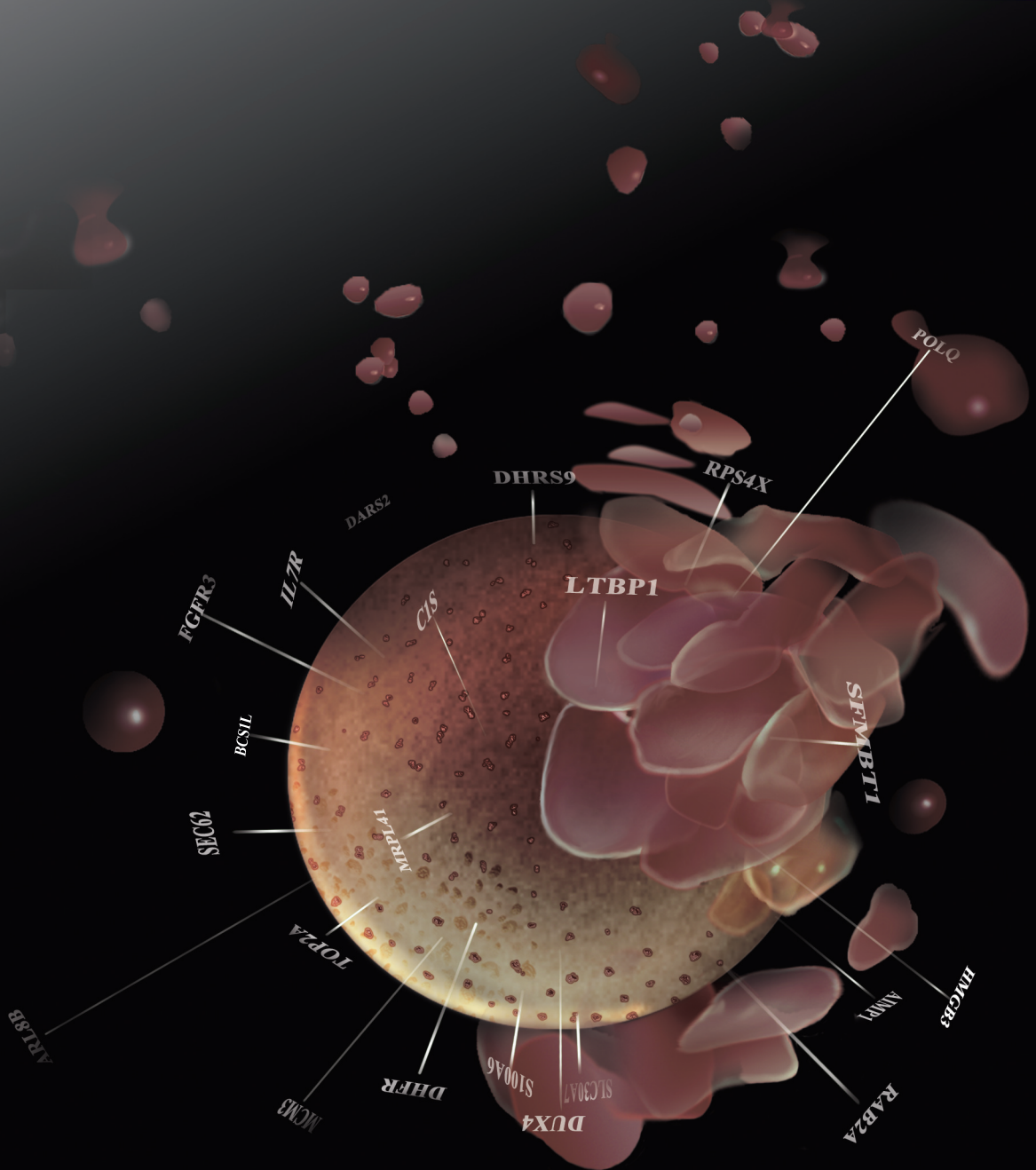


# Gene expression based risk classification in multiple myeloma

Rowan Kuiper





***Gene expression based  
risk classification  
in multiple myeloma***

***Rowan Kuiper***

Gene expression based risk classification in multiple myeloma

Copyright ©2018 Rowan Kuiper, Rotterdam, The Netherlands. All rights reserved. No part of this thesis may be reproduced, stored in a retrieval system or transmitted in any form or by any means, without permission of the author. The copyright of articles that have been published or accepted for publication has been transferred to the respective journal.

Cover design: Marleen van Es

Layout: Manon Kuiper and Rowan Kuiper

Printing: Ridderprint BV | [www.ridderprint.nl](http://www.ridderprint.nl)

***Risicoclassificatie in multipel myeloom gebaseerd  
op gen expressie***

***Gene expression based risk classification in  
multiple myeloma***

**Proefschrift**

ter verkrijging van de graad van doctor aan de  
Erasmus Universiteit Rotterdam  
op gezag van de  
rector magnificus

Prof.dr. R.C.M.E. Engels

en volgens besluit van het College voor Promoties.  
De openbare verdediging zal plaatsvinden op

donderdag 20 december 2018 om 11.30 uur

door

**Rowan Kuiper**  
geboren te Vlaardingen

## Promotiecommissie

**Promotor:** Prof.dr. P. Sonneveld

**Overige leden:** Prof.dr. A.G. Uitterlinden  
Prof.dr. H.R. Delwel  
Prof.dr. S. Zweegman

**Co-promotor:** Dr. M. van Duin







# Table of contents

	<b>Page</b>
<b>1 General introduction</b>	<b>1</b>
<b>2 EMC92: A risk classifier for multiple myeloma</b>	<b>31</b>
<b>3 EMC92-ISS risk stratification in multiple myeloma</b>	<b>55</b>
<b>4 SKY92 risk in elderly newly diagnosed multiple myeloma</b>	<b>77</b>
<b>5 Nopaco: A Non-Parametric concordance test</b>	<b>99</b>
<b>6 CRBN in Thalidomide treated NDMM patients</b>	<b>117</b>
<b>7 Genetic predisposition to BiPN in MM</b>	<b>129</b>
<b>8 Novel locus associated with BiPN in myeloma</b>	<b>141</b>
<b>9 General discussion</b>	<b>157</b>
<b>10 Summaries</b>	<b>171</b>
<b>Abbreviations</b>	<b>185</b>



# CHAPTER

**General introduction**

---

# MULTIPLE MYELOMA

1

Multiple myeloma (MM) is a malignant plasma cell disorder in the bone marrow. Plasma cells are antibody producing cells. In the majority of MM patients a monoclonal protein is detected, the so-called M-protein that is produced by the clonal plasma cells. This disease accounts for 13% of all hematologic malignancies. MM had a crude incidence rate of 6.6 out of 100.000 individuals in 2015, corresponding to 1100 new patients a year in the Netherlands.<sup>1</sup> The incidence is age dependent with 80% of patients being older than 60 years.<sup>1</sup> MM is a genetically heterogeneous disease, characterized by various recurrent aberrations. Patients demonstrate a large variation in response to treatment, survival and adverse treatment effects.

## Diagnosis

The diagnosis of MM is based on the presence of either more than 10% abnormal plasma cells in the bone marrow or plasmacytoma proven by biopsy. In addition, either end organ damage that can be attributed to the underlying plasma cell proliferative disorder must be present or at least one of three myeloma defining events (MDE). End organ damage is defined by the CRAB criteria: c) increased levels of calcium ( $\geq 11.5$  mg/100 ml); r) renal insufficiency indicated by increased serum creatinine ( $> 1.73$  mmol/L); a) anemia (hemoglobin  $< 6.2$  mmol/L) and b) bone lesions ( $\geq 1$  by X-ray, CT or PET-CT). MDE consists of 1)  $\geq 60\%$  clonal plasma cells on bone marrow examination; 2) a free light chain ratio of  $\geq 100$ ; 3) more than one focal lesion on magnetic resonance imaging (MRI) that is  $\geq 5$  mm in size.<sup>2</sup> These MDEs were recently included in the myeloma defining criteria to allow early diagnosis and initiation of therapy before end-organ damage.

## Disease stages

Most MM cases are thought to develop from the precursor stages monoclonal gammopathy of undetermined significance (MGUS) and smoldering MM (Figure 1).<sup>3,4</sup> MGUS is estimated to occur in approximately 1-3% of the population above 50 years.<sup>5,6</sup> These patients have detectable mono-clonal protein (M-protein, see also below, MGUS:  $< 3$ g/dL M-protein) without clinical symptoms and without

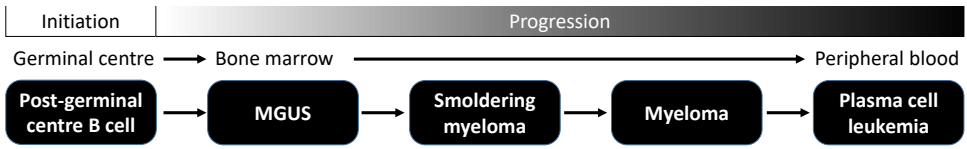


**Figure 1. Disease stages in MM.** (Source: Morgan et al. 2012)<sup>3</sup>

MDE (Table 1). MGUS evolves into myeloma at a rate of approximately 1% per year.<sup>7</sup> Smoldering myeloma (SMM) is characterized by higher levels of M-protein (>3g/dL, comparable to symptomatic myeloma) however, these patients do not demonstrate end-organ damage or MDE. The rate of progression from smoldering MM to clinical MM is 10% in the first 5 years after diagnosis, decreasing to 3% per year over the following 5 years, and 1.5% per year thereafter.<sup>5,8</sup> Some patients with MM may progress to plasma cell leukemia (PCL). PCL cells are no longer restricted to the bone marrow and are able to survive in the peripheral blood. Diagnostic criteria for PCL are > 20% circulating plasma cells and an absolute count > 2 × 10<sup>9</sup> plasma cells/L in peripheral blood in addition to the MM diagnostic criteria.<sup>9</sup>

**Table 1. Clinical staging of multiple myeloma** (as reported by Rajkumar et al. (2016)).<sup>2</sup>

Stage	Serum M-protein (g/dl)	BM plasma cells(%)	End-organ damage (CRAB)
MGUS	Increased but <3	<10	No
SMM	>3	10-60	No
MM	No criteria	>60	No
	No criteria	>10	Yes

## Treatments

Newly diagnosed patients are split into two groups based on being eligible for high-dose Melphalan combined with autologous stem cell transplantation (HDM/ASCT). This distinction is based on age and fitness of the patient, with an age cut-off of either 65 years or 70 years old used routinely.<sup>34</sup> Patients below this age limit are considered to be sufficiently fit to undergo the combined HDM/ASCT procedure. For transplantation eligible patients, treatment consists of a sequence of variable phases, including induction, HDM/ASCT (1x or 2x), consolidation and maintenance.<sup>35</sup>

**Table 2. Drugs in MM**

Drug	Class	Ref.
Melphalan	Alkylating agents	10
Cyclophosphamide		
Dexamethasone	Corticosteroids	11,12
Prednisone		
Bortezomib (Velcade)	Proteasome inhibitors (PI)	13
Carfilzomib (Kyprolis)		14
Ixazomib (Ninlaro)		15
Oprozomib		16
Thalidomide	Immunomodulatory (IMiD) / CRBN interaction	17,18
Lenalidomide (Revlimid)		17,19
Pomalidomide (Pomalyst)		20,21
Daratumumab (Darzalex)	CD38 antibody	22–24
Isatuximab	CD38 antibody	25
Elotuzumab	SLAMF7 (CD319) antibody	26–28
Pembrolizumab (Keytruda)	PD-1 antibody	21,29
Venetoclax	Bcl2 inhibitor	30
Panabinstat (Farydak)	HDAC inhibitor	31
CAR-T-BCMA	Chimeric antigen T cell receptor against BCMA	32,33

In recent years a large number of new drugs have become available (see Table 2).<sup>36–38</sup> Three important classes of drugs are proteasome inhibitors (PI) (e.g., Bortezomib), immunomodulatory drugs (Imid) (e.g., Thalidomide) and monoclonal antibodies (e.g., daratumumab). For transplantation eligible patients, induction treatment includes combinations such as Bortezomib, Dexamethasone and Thalidomide (VTD) and Bortezomib, Cyclophosphamide and Dexamethasone (VCD). Transplant ineligible patients are now often treated with the doublet Lenalidomide with Dexamethasone (Rd).<sup>39</sup> Treatment choice depends on various considerations including reported efficacy, tolerance, patient condition and performance, cost effectiveness and availability. These factors are reviewed and summarized in the local guidelines. Side effects of treatment such as peripheral neuropathy, myelosuppression, thrombosis or cardiac toxicity frequently occur, and may lead to dose reduction or even treatment discontinuation. Peripheral neuropathy (PNP) associated with Bortezomib and Thalidomide treatment is discussed in this thesis.<sup>40</sup> PNP was shown to be reduced by changing the mode of Bortezomib administration from intravenous to subcutaneous.<sup>41</sup> Newer PIs

were reported to cause much less PNP, compared to Bortezomib. In a study which compared Bortezomib to Carfilzomib containing treatment, PNP was found in 32% of Bortezomib treated patients compared to only 6% of Carfilzomib treated patients.<sup>42,43</sup>

## Prognostic factors

Use of new drugs as outlined above has resulted in a vast improvement in survival of MM patients. Improvement in 5-year relative survival rates (1993-97 vs 2008-12) are seen among patients of all age and race/ethnicity groups (Figure 2). Among patients <65 years of age RSR increased from 38% to 62%, for 65 to 74 years of age from 29% to 48%, and  $\geq 75$  years of age from 21% to 34%.<sup>44</sup> However, MM is still considered an incurable disease.<sup>45</sup> Although the median overall survival (OS) is 6.1 years, there is a large variation ranging from less than two years to over twenty years.<sup>46-49</sup> An estimation of the risk for individual patients can be made using prognostic factors. These are clinical or biological characteristics that are objectively measurable in an untreated individual or that are intrinsic to the host (e.g., age, comorbidities, fitness) and that provide information on the likely outcome of the disease.<sup>50</sup> In the following sections the most important prognostic factors are discussed.

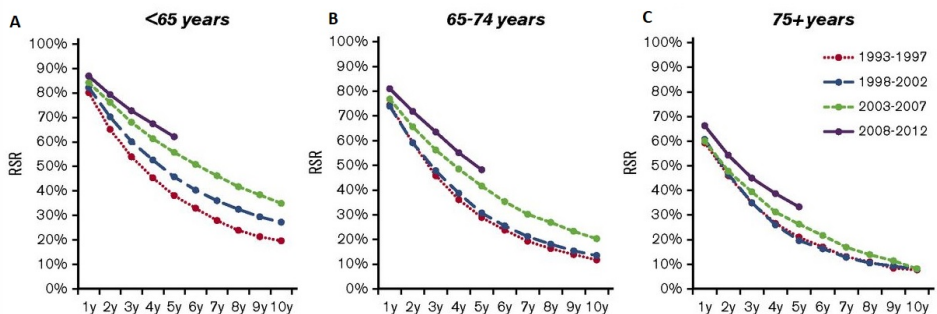


**Figure 2. Relative survival rates (RSR) in MM.** Changes in the RSRs of patients diagnosed with MM in the United States grouped by age: A) diagnosed at age <65 years, B) diagnosed at age 65 to 74 years or C) diagnosed at age  $\geq 75$  years. (Source: Costa et al. 2017)<sup>44</sup>

## Serum markers

Serum markers are easily obtained and thus minimally invasive. Important serum proteins for MM include M-protein, serum free light chains, beta-2-microglobulin (B2m), creatinine, albumin and lactate dehydrogenase (LDH). MM is characterized by an increase in monoclonal plasma cells which all produce an immunoglobulin (Monoclonal protein, M-protein). An elevated M-protein level measured in serum or urine is therefore a marker of tumor load and indicator for MM. Immunoglobulins are made up of two light and two heavy chains. Each myeloma clone produces either a kappa or a lambda light chain. As a result, in the serum of MM patients the ratio of free light chains is affected, with either kappa or lambda highly overrepresented. B2m is a subunit of the MHC class-I molecule which is present on all nucleated cells. The normal level in serum is less than 2mg/L but B2m is often elevated in diseases associated with increased cell turnover, such as MM. Creatinine is a byproduct of muscle metabolism, which is excreted by the kidneys. In case of renal failure, creatinine levels will rise and are used as an indirect measure of renal function. Typically, creatinine levels are 0.5-1.0 mg/dL for women and 0.7-1.2 mg/dL for men. Albumin reflects systemic dysregulation. Lower levels have shown to be correlated to increased levels of interleukin 6 (IL6) - activating the growth of MM cells.<sup>51</sup> The normal range of albumin is 3.5-5 g/dL. Finally, cancer cells often have an increased energy requirement which is met by an elevated glycolysis. LDH is an enzyme involved in glycolysis, and can therefore be correlated to tumor growth. The normal range is 135-225 U/L.

**Table 3. The International Staging System criteria and median survival** as reported by Greipp *et al.* (2005).<sup>52</sup>

Stage	Criteria	Median Survival
I	Serum B2m < 3.5 mg/L and serum albumin ≥ 3.5 g/dL	62 months
	A. Serum B2m < 3.5 mg/L and serum albumin < 3.5 g/dL	44 months
II	B. or serum B2m 3.5 to < 5.5 mg/L irrespective of the serum albumin level	
III	Serum B2m ≥ 5.5 mg/L	29 months



**Table 4. Recurrent cytogenetic aberrations in MM and their prognosis.**

Aberration	Incidence by FISH	Oncogene	Prognosis	Ref.
t(4;14)(p16;q32)	14 to 16%	FGFR3 and MMSET	Unfavorable	54–57
t(6;14)(p21;q32)	3 to 4%	CCND3	Uncertain	56,57
t(8;14)(q24;q32)	3%	MYC	Unknown	57,58
t(11;14)(q13;q32)	15 to 16%	CCND1	Uncertain	56
t(14;16)(q32;q23)	3 to 5%	c-MAF	Uncertain	56,57
t(14;20)(q32;q12)	2%	MAFB	Uncertain	56,57
del(13q)	50%	RB	Unfavorable	57
del(17)(p13)	10%	TP53	Unfavorable	54
del(1p)	30%	Unknown	Unfavorable	59
gain(1q)	30%	Unknown	Unfavorable	57,59,60
Hyperdiploidy	50%	Unknown	Favorable	54,57

## International Staging System

The International Staging System (ISS) is currently widely accepted as a measure reflecting tumor burden, renal function and fitness.<sup>52,53</sup> ISS classifies patients into three grades, based on the serum levels of B2m and albumin (Table 3). Higher ISS stages are associated with increased risk, also in patients treated with current treatment modalities.

## Cytogenetics

In addition to aberrant serum markers, tumor specific recurrent cytogenetic aberrations can be observed in MM.<sup>4</sup> Important for MM development, as for other cancer types, are defects in the mechanisms that control cell division.<sup>61</sup> A number of cytogenetic aberrations directly or indirectly reflect this pathway, e.g., upregulation of cyclin-D1 (Figure 3).

Some aberrations are present at diagnosis in a substantial number of patients such as translocations involving the IgH-locus on chromosome 14q32 (Table 4) or a hyperdiploid karyotype of many of the odd numbered chromosomes. These are considered to be primary events in contrast to the secondary events - such as deletion of the p53 locus, gain of chromosome 1q or a loss of chromosome 13q - which are usually seen during disease progression. Characteristic for MM are the primary translocating events affecting the IgH-locus.<sup>4,63</sup> Being the highest expressed locus in antibody producing plasma cells, juxtaposition of proto-

oncogenes to the IgH enhancer results in strong overexpression of the IgH gene, leading to M-protein production.<sup>4,64</sup> Recurrent translocations include t(4;14) and t(11;14), observed in approximately 14% and 16% of newly diagnosed MM patients respectively.<sup>4,65–67</sup> The translocation t(4;14)<sup>68</sup> is an important prognos-

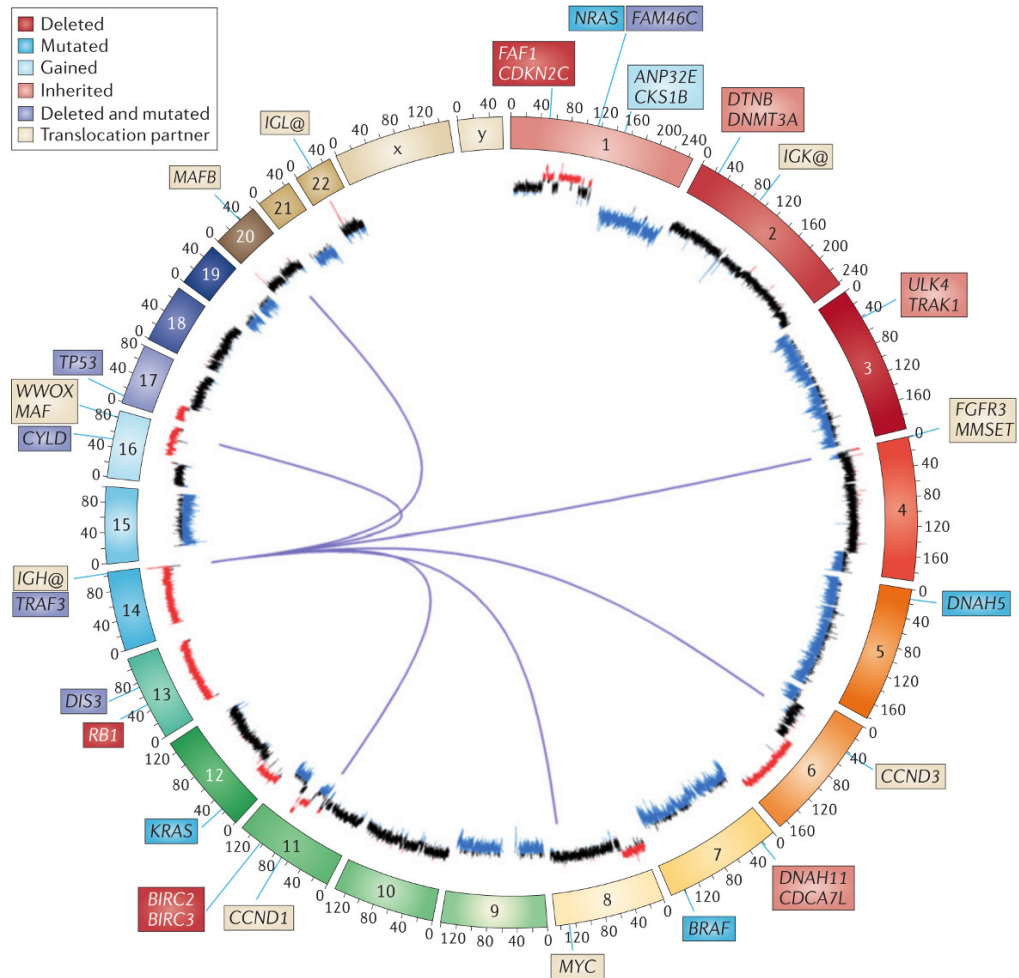


**Figure 3. Circos plot showing key genetic events encountered in MM.** Each chromosome is depicted on a circle starting on the top with chromosome 1 and ending with 22, X and Y. The length of a chromosome corresponds to the number of nucleotides it contains. Translocations of the immunoglobulin heavy chain locus (IGH@) on chromosome 14 are shown as lines to their chromosomal binding partner. Copy-number alterations are color-coded inside the circle as red (deletion), black (normal copy-number) and blue (gain). The target genes are on the outside of the circle. (Source: Morgan et al. 2012)<sup>3</sup>

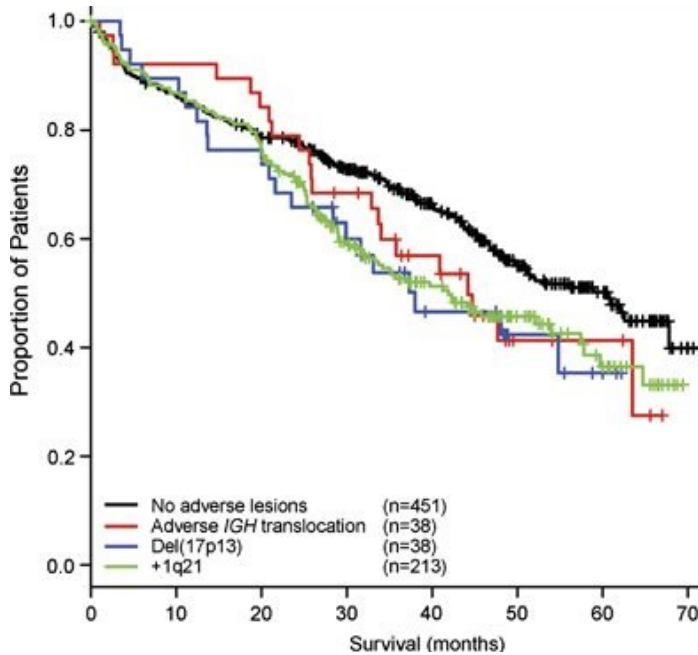


**Figure 4. Overall survival in the MRC Myeloma IX Trial.** OS for some adverse FISH lesions when they occur in isolation compared with samples lacking any adverse lesions. (Source: Boyd et al. 2012)<sup>62</sup>

tic factor, associated with a poor outcome (Figure 4). It causes an upregulation of the histone methyltransferase myeloma SET domain protein (MMSET) and in 70% of the cases the fibroblast growth factor receptor 3 (FGFR3) is also affected. Recently, a newly discovered small RNA gene SCARNA22 was found to be co-expressed with MMSET; this gene is localized in MMSET intron 20. SCARNA22 knockdown experiments demonstrated impaired cell proliferation and deregulated oxidative stress response, raising the question whether SCARNA22 may play a role in t(4;14) patients.<sup>69,70</sup> The translocation t(11;14) fuses the cyclin-D1 gene (CCND1) to the IgH-locus thereby possibly disrupting the G1-S cell-cycle boundary; t(11;14) patients are reported to have a relatively favorable prognosis.<sup>64</sup> Recently it was shown that the Bcl-2 targeting drug Venetoclax was exceptionally effective in this patient group.<sup>71</sup> This creates the possibility of precision medicine.

Other less common recurrent translocations in MM are t(6;14), t(8;14), t(14;16) and t(14;20).<sup>66,67</sup> In addition to translocations, other aberrations like

---

gains and deletions are frequently observed. MM patients with a deletion of the short arm of chromosome 17 locus (del(17p13)), containing the TP53 gene, have worse survival than patients without this deletion (Figure 4). P53 is a multifaceted transcription factor affecting many key cellular processes such as apoptosis, proliferation, DNA repair, metabolism, cell migration and autophagy.<sup>72,73</sup> It is recognized as the most frequently inactivated tumor suppressor in human cancers. In MM approximately 8% of patients have this deletion at the time of diagnosis and this frequency increases during progression of the disease with increasing number of cases with bi-allelic inactivation.<sup>74</sup> More frequently identified aberrations include deletion of chromosome 13 del(13) seen in 50% of newly diagnosed myeloma, gain(1q) (30%) and deletion of chromosome 1p (30%). These are usually associated with a poor outcome. A favorable aberration is hyperdiploid myeloma (50%) in which many of the odd numbered chromosomes (3, 5, 7, 9, 11, 15, 19 and 21) have an additional copy. Initially it was thought that a hyperdiploid genotype and IGH translocations were mutually exclusive.<sup>64</sup> However, recent research showed that hyperdiploidy may precede IGH translocation in a proportion of patients such that both coexist.<sup>75</sup> The effect of coexisting hyperdiploidy and translocations on prognosis is not entirely clear, but may depend on the nature of the hyperdiploidy, with trisomies 3 and 5 conferring a reduction of the poor risk commonly associated with t(4;14) whereas trisomy 21 has the opposite effect.<sup>54</sup>

## Gene expression

Gene expression arrays provide a widely accepted method to determine the expression of most known genes simultaneously. The resulting data has been analyzed in the context of various clinical and biological features resulting in unsupervised molecular subtyping and supervised classifiers.

## Molecular classifications

MM is biologically variable, and is likely to have distinct subtypes, including those described by gene expression profiling. Activation of cyclin D genes is common in MM, and the rationale behind the translocation/Cyclin D (TC) classification.<sup>64,76</sup> Based on CCND1, CCND2, CCND3, FGFR3, MMSET, MAF, ITGB7

and CX3XR1 expression, tumors were classified in eight subgroups. Using an unsupervised hierarchical clustering approach of gene expression profiles, novel putative subgroups were identified by Zhan *et al.* (2006) and Broijl *et al.* (2010) denoted as the UAMS and EMC clustering respectively. The UAMS clustering resulted in seven clusters (CD1, CD2, MS, MF, HY, PR and LB). Just as the TC classification most groups were strongly influenced by known genetic lesions, such as c-MAF/MAFB (MF cluster), Cyclin genes (primarily CD1 and -2 clusters), MMSET-activating translocations (MS cluster) and hyperdiploidy (HY cluster; Table 5).<sup>77</sup> Other clusters with less clear gene associations were found to be enriched with a low incidence of focal bone disease (LB group) and increased expression of proliferation-associated genes (PR) group. The EMC clustering found three additional clusters in addition to the seven UAMS clusters. These showed an increased expression in the nuclear factor kappa light-chain-enhancer of activated B cells pathway (NF $\kappa$ B group), cancer testis antigens without over expression of proliferation genes (CTA group) and up-regulation of protein tyrosine phosphatases PRL-3 and PTPRZ1 as well as SOCS3 (PRL3 group), respectively. Kuehl *et al.* (2012) published a comparison of these three classifications in terms of cytogenetic characteristics.<sup>78</sup>

**Table 5. Comparison of different molecular classifications in MM** according to Kuehl *et al.* (2012)<sup>78</sup>

Group	Gene	TC <sup>76</sup>	UAMS <sup>77</sup>	EMC <sup>79</sup>
Cyclin D transl.	CCND1	11q13	CD1,CD2	CD1,CD2
		6p21	CD1,CD2	CD1,CD2
MMSET transl.	MMSET	4p16	MS	MS
MAF transl.	MAF, MAFA, MAFB	MAF	MF	MF
		CCND1+CCND2	D1+D2 PR	PR, CTA
Hyperdiploid	CCND1	D1	HY	HY, CD1, NF $\kappa$ B, CTA, PRL3
		CCND1+CCND2	D1+D2 PR	PR, CTA
Other	no CCND1	None	PR	PR, CTA
		CCND2	D2	PR, LB
			LB, CTA, PRL3	

Some of these subgroups have been linked to treatment outcome and prognosis. Bergsagel *et al.* reported a median overall survival of 26 months for TC 4p16 (t(4;14)) patients versus 33 months for patients with a non-TC 4p16 subgroup designation. This was confirmed in independent studies.<sup>80</sup> The MMSET (MS; t(4;14)), MAF (MF; t(14;16)/t(14;20)) and proliferation (PR) groups have been

reported to have shorter survival relative to the other subgroups in two independent reports.<sup>77,81</sup> These reports further describe a survival benefit of the MS subgroup when treated with novel drugs as compared to conventional drugs.<sup>11,81</sup>

## 1 Gene expression based prognosis

Gene expression profiling of tumor cells can be used for the development of algorithms specifically intended to estimate prognosis in cancer patients, as initially demonstrated for breast cancer patients and later in acute lymphoblastic leukaemia.<sup>82-84</sup> As described in more detail below, the development of prognostic algorithms, or prognostic classifiers, consists of two phases: a training phase and a validation phase. In the training phase a classifier is generated by finding genes which combined have a strong link to survival of the patients within that set. The validation set is then used to evaluate whether the identified combination of genes has value in independent data. The UAMS70-gene classifier was the first of such prognostic classifiers described for MM. Prognostic value was derived by combining 70 genes, or even a reduced set of 17 genes.<sup>85</sup> Selected MM classifiers are shown in Table 6.

**Table 6. Prognostic gene classifiers in multiple myeloma.**

Classifier	#Groups	Risk proportion (%)	Platform	Ref.
GPI50	2	51 / 39 / 10	Affymetrix U133 2.0	86,87
HM19	3	44 / 48 / 8	Affymetrix U133 2.0	88
IFM15	2	75 / 25	Custom design	89
MILLENNIUM100	2	50 / 50	Affymetrix U133 A+B	90
MRCIX6	2	95 / 5	Affymetrix U133 2.0	91
UAMS17	2	88 / 12	Affymetrix U133 2.0	85
UAMS70	2	91 / 9	Affymetrix U133 2.0	85
UAMS80	2	92 / 8	Affymetrix U133 2.0	92

### Risk stratification using prognostic markers

To achieve more accurate prognostication, individual markers are often combined. The ISS (see Table 3) is an example in which combining two serum markers resulted in improved prognostic strength.<sup>52</sup> In addition, improved prognostication can be achieved by grouping patients with different high-risk cytogenetic

**Table 7. Updated mSmart risk stratification.** These criteria are continuously updated. The definition in this table is from Mikhael *et al.* (2013).<sup>93</sup> PCLI = Plasma cell labeling index.

Risk group	Criteria	Proportion	Median OS
Standard-risk	t(11;14)	60 %	8-10 yrs
	t(6;14)		
No intermediate- or high-risk			
Intermediate-risk	t(4;14)	20%	4-5 yrs
	del(13)		
	Hypodiploidy		
PCLI ≥ 3%			
High-risk*	del(17p)	20%	3 yrs
	t(14;16)		
	t(14;20)		
High-risk gene expression profile			

\*In the presence of concurrent trisomies, patients with high-risk cytogenetics should be considered standard-risk

**Table 8. Prognostic ISS + cytogenetics risk stratification** according to Avet-Loiseau *et al.* (2013)<sup>94</sup>

Risk group	Criteria	Proportion	OS at 4yr
Low-risk	ISS < 3 and not del(17p) and not t(4;14)	54%	71%
Intermediate-risk	ISS < 3 and [ del(17p) or t(4;14) ]	28%	45%
	or		
High-risk	ISS = 3 and not del(17p) and not t(4;14)	18%	33%
	del(17p)		

**Table 9. Prognostic revised ISS (R-ISS)** according to Palumbo *et al.* (2015)<sup>95</sup>

Risk group	Criteria	Proportion	OS at 5yr
R-ISS:I (Low-risk)	ISS = I and not del(17p) and not t(4;14) and not t(14;16) and normal LDH	28%	82%
R-ISS:II (Intermediate-risk)	No R-ISS-I and no R-ISS-III	62%	62%
R-ISS:III (High-risk)	ISS = 3 and [ del(17p) or t(4;14) or t(14;16) or High LDH]	10%	40%

---

markers, for instance having any of the following markers: del(17p), t(4;14) and/or t(14;16).<sup>96,97</sup> Alternatively, patients with only 1 high-risk marker were shown to have a favorable prognosis compared to patients positive for 2 or more high-risk marker.<sup>98</sup> The Mayo Clinic has introduced the Mayo stratification for myeloma and risk-adapted therapy classification (Table 7).<sup>93</sup> Based on cytogenetics, gene expression and a plasma cell labeling index (i.e., a measure of proliferating cells), patients are stratified into three risk groups. The composition of this stratification is based on expert opinion and regularly updated but so far not independently validated.<sup>93</sup> Other risk stratification methods include the combination of ISS together with cytogenetics (Table 8) and the revised ISS (R-ISS) which combines ISS, cytogenetics and LDH (Table 9).<sup>94,95</sup> In the R-ISS, a subset of the ISS-I or ISS-III patients is reclassified as R-ISS-II resulting in a higher proportion of these intermediate-risk patients.



# Bioinformatics

Organisms can be reduced to large networks of interacting molecules. Analysis of resulting data structures requires bioinformatics.<sup>99</sup> Here we will focus very briefly on bioinformatic topics relevant to this thesis.

1

## Introduction to microarrays

In our studies we mostly made use of the gene expression profiling and genome wide genotyping; for both techniques microarrays were used. To characterize the mRNA which is expressed by a cell at a specific point in time or under specific conditions, microarrays were developed for transcriptome analysis.<sup>100</sup> Microarrays allow measurements of large amounts of many short RNA sequences simultaneously. They are glass or silica slides that have large number of oligonucleotides probes (i.e., short stretches of (c)DNA) with known sequences bound to their surface. Here, microarrays with cDNA probes for specific RNAs were used, and microarrays with DNA probes specific for detection of single nucleotide polymorphisms (SNPs). In both cases, the probes are organized in spots such that each position on the array corresponds to a unique sequence. Hybridization of RNA obtained from the MM cells of a patient to the cDNA probes gives an estimation of the quantity of a specific RNA in the MM cells of that patient. Alternatively, hybridization of DNA obtained from peripheral blood samples to sequence specific probes gives an estimation of the SNPs specific for that patient (and alternatively can be used for copy number analyses). The focus of this thesis is on the Affymetrix Human Genome U133 arrays used for gene expression profiling. The U133 plus 2.0 is the most widely applied Affymetrix human gene chip. It contains 54675 probe-sets of which 44754 overlap with the probe sets used on the U133 A and B chips combined. After a sample has been hybridized to a microarray (Figure 5), a high resolution image file (DAT file) is obtained by scanning it. In the image, each probe is identified and assigned an expression value proportional to the corresponding spot intensities. Subsequent processing prior to bioinformatic analyses usually involve normalization and correction for batch effects to allow comparisons between array and between batches respectively.

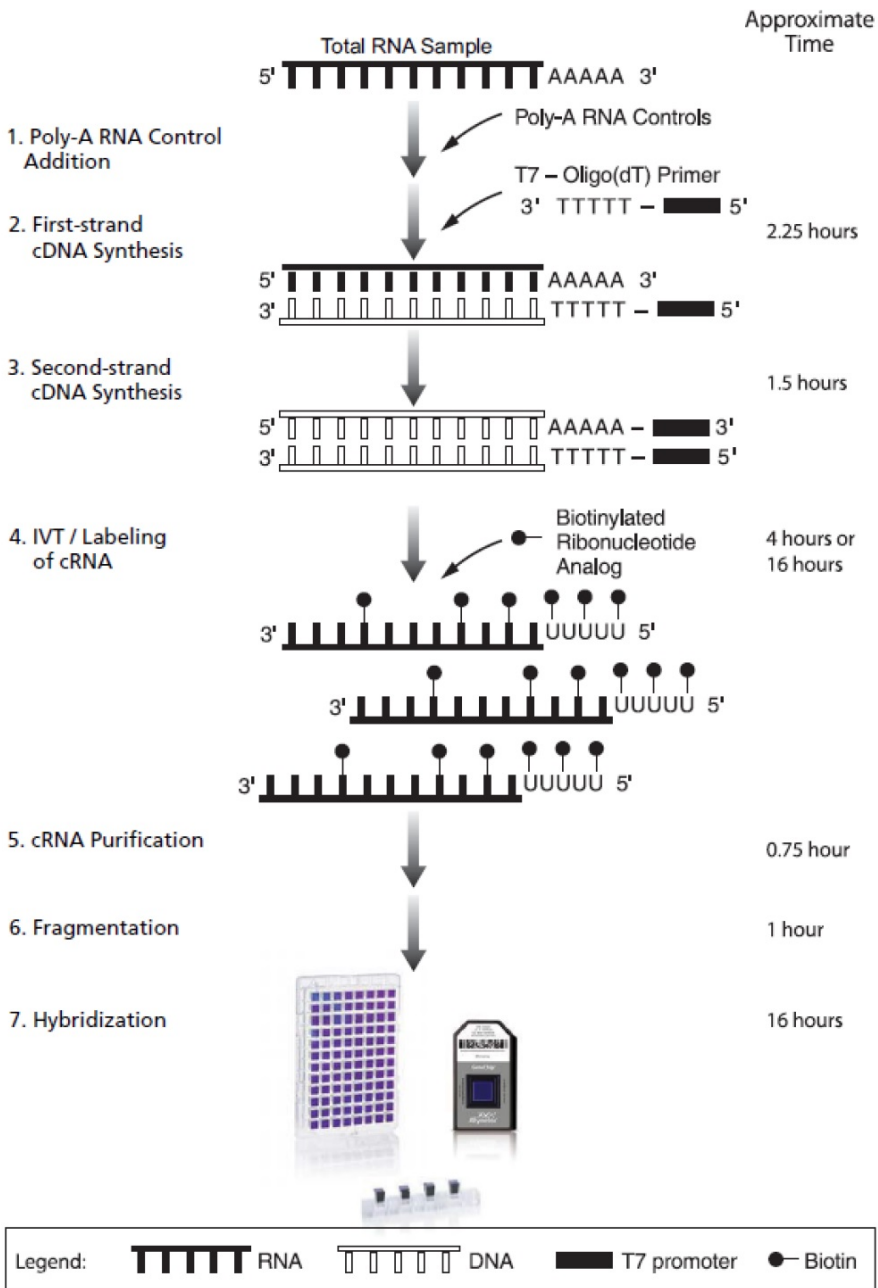


**Figure 5. Affymetrix Microarray Assay Workflow IVT PLUS Amplification and Labeling process.** (Source: Affymetrix manual)

## Normalization

In general, three basic normalization steps are distinguished: 1) background-correction, 2) summarization and 3) normalization (Table 10). Several methods exist such as the normalization used by the Affymetrix microarray suite 5.0 (MAS5), model-based expression intensities (MBEI) or robust multi-array averaging (RMA) and its extensions involving adjustment for non-specific binding (GCRMA) and a multi-array approach using a frozen reference set (FRMA).<sup>101-108</sup> In this thesis MAS5 was used as a standard because of its simplicity and applicability to single arrays.

**Table 10. Normalization steps, their aim and a brief description on the MAS5 method.**<sup>102</sup>

Step	Aim	MAS5
Background correction	Correcting for technical noise	The lowest 2% of probe intensity values represent background noise.
Summarization	Combining intensities of probes that map to the same transcript	Tukey's Bi-Weight
Normalization	Reducing inter-array variance	Scaling the intensities of each array (note: single array)

## Batch effect correction

Due to many causes (e.g., changes in RNA extraction, temperature differences, labeling, handling by technician), differences between series of microarray experiments may occur.<sup>103,109</sup> If left uncorrected, batches rather than biological differences can be the greatest source of differential expression in high throughput RNA analyses.<sup>110</sup> This may lead to false or confusing conclusions. A review with examples and consequences is given by Leek *et al.*<sup>110</sup> Avoiding batch effects is usually not possible but appropriately designing the experiment by randomizing cases and controls over dates and sites, may allow batch correction. It turns out that a simple mean centering and scaling to unit variance for each batch separately, often removes most of the batch effect. More complex and computationally intensive algorithms were developed based on higher dimensional analysis techniques, making use of singular value decompositions<sup>111,112</sup> and weighted discrimination analysis.<sup>113</sup> The batch effect correction method Combat<sup>114</sup> was developed to overcome some major disadvantage of the above methods, and is

---

thought to be more robust against outliers and applicable in the context of smaller sample sizes ( $n > 6$ ).<sup>115</sup> It uses a Bayesian model to estimate the batch parameters which can be used to adjust the data, by pooling information across genes to shrink magnitude of estimates toward their overall mean. Instead of shrinking towards the mean, a modified combat (M-Combat) has been published which shrinks toward a reference batch instead of averaging over multiple batches.<sup>116</sup> This is desirable in case of a classification setting where a training set can be used as the reference batch.

## Model building

To extract data for model building, machine learning tools have been developed.<sup>117</sup> These tools are aimed at finding ways to predict phenotypical characteristics by associating them to gene expression data. A model is a representation which approximates a variable of interest (e.g., risk-group) in terms of other, more easily observable, variables. A patients' survival is unknown at diagnosis but may be found to correlate to the expression of certain genes at diagnosis. This way single genes or combinations of genes can be found with predictive ability (Figure 6).

## Overtraining

Over-interpretation of the training-data can result in a model that fits the training data, but has no applicability on unseen, independent data. This phenomenon is termed overtraining and is often evident when a model is too complex.<sup>118</sup> E.g., when a linear classifier is applied to a training set with two patients, one high-risk, one low-risk, it is clear that a model can be found, based on a single gene only, which perfectly separates the two risk groups. However, due to the scarce evidence provided by the data, this model is likely to fail to separate risk groups when applied to other patient samples (test data). Similarly, two genes are able to perfectly separate the two risk groups in case of three patients (one from one class and two from the other). In general,  $n$  patients can be perfectly separated into two risk groups by a  $(n-1)$  dimensional linear boundary.<sup>119</sup> The larger the number of variables included in a model relative to the number of patients available to fit the model, the easier it becomes to find a (likely false) separation in

the data. A classifier based on a single variable is more likely to correctly classify future samples if it correctly classified 100 training patients as compared to a training set of only 2 patients. Overtraining is recognized when the prediction error of a model is low in the training-data but high when applied to other data, i.e., has a low generalizability (Figure 7).<sup>117</sup>

## Cross-validation

Cross-validation is a common procedure in model building to prevent overtraining. It estimates the performance of a model in unseen data based on its training set. In a cross-validation the training-data is randomly split into a number of fold of approximately equal size. The model is built on all but one fold and subsequently tested on the fold that was left out. This procedure is repeated until all folds were excluded once. Summarization of each folds' performance

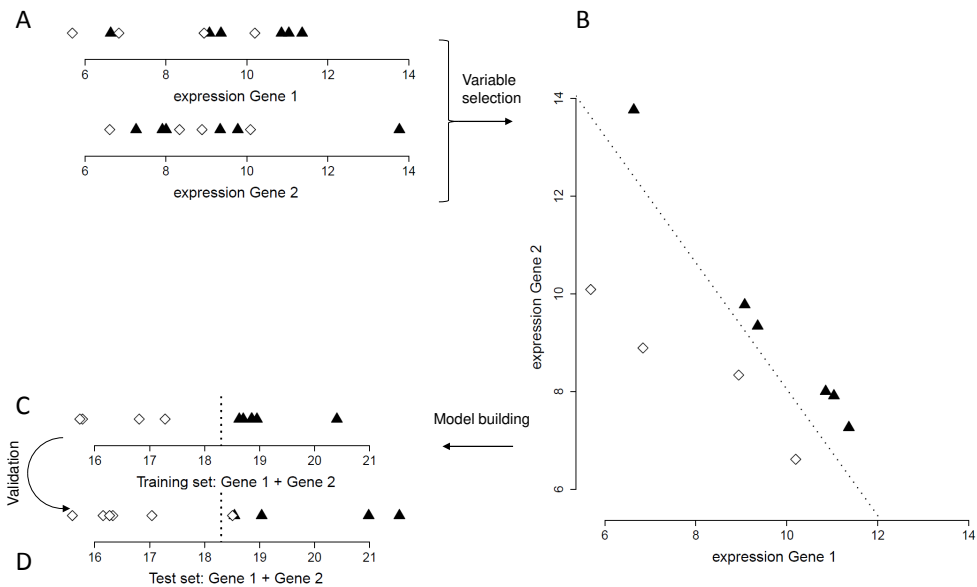


**Figure 6. Example of model building on hypothetical data.** The expression of two genes are measured at diagnosis for ten training patients which belong to either one of two classes: alive (white diamonds) or dead (black triangles) within 2 years. A) The individual genes themselves are poor class separators. B) Combining both genes, however, results in a perfect class separation, indicated by the dotted line. C) Generation of a simple linear model (high-risk if  $[\text{gene1} + \text{gene2}] > 18.3$ ). D) Validation of the model in independent data, i.e., patients who were not part of the training set (prediction error: 1 out of 10).

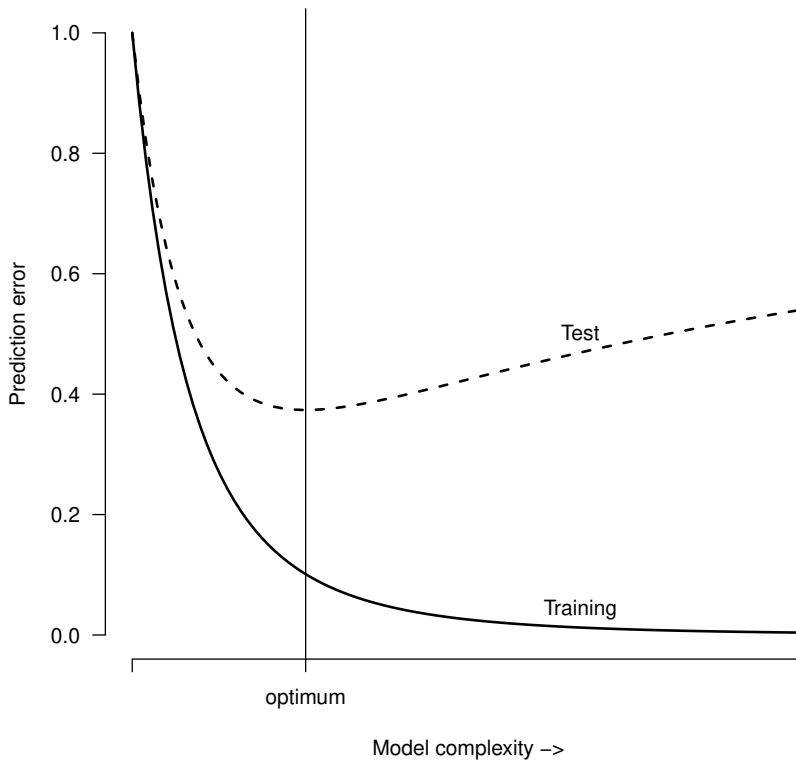


**Figure 7. Generalization error.** The complexity of a model (e.g., number of variables) is related to the performance in the training-data and test-data (or unseen data). Adapted from a figure in Hastie et al.(2009)<sup>117</sup>

into an overall estimate is then used as a rough estimate of the expected performance on unseen data using a given model-building approach. Often model-building incorporates feature selection (e.g., which and how-many probe-sets to include) and/or setting of hyper-parameters (e.g., the regularization parameter in lasso/ridge regression)<sup>120,121</sup> that tune the model. These parameters determine the complexity of the model, and consequentially these will affect the generalizability of the model. A nested cross-validation is often used in which these parameters are optimized within the inner-loop and performance is estimated in an outer-loop. Despite termed validation, cross-validation estimates model performance, but true validation (i.e., replication) to unseen data is still required.

## Scope and outline of this thesis

The work in this thesis focuses on multiple myeloma patients. A main question was whether it is possible to find patterns in biological data sets, which can be used for the prognosis of MM patients. Despite continuous development of novel treatments, a large variety in survival is observed in MM patients. Are these differences related to tumor biology such that prognostic information can be obtained from plasma cells? Further, many prognostic factors have been described but their optimal use is unknown. Given the current set of prognostic factors, can we define a strong prognostic classifier by combining them in one of many ways? Side effects, such as peripheral neuropathy during Bortezomib treatment seriously affects quality of life of a patient. Being able to identify susceptibility to side effects would be useful. Can we recognize susceptible patients prior to treatment by genetic predisposition?

Chapter 2 describes the development and validation of a prognostic gene expression classifier. By gene expression profiling of 290 MM patients included in the HOVON-65/GMMG-HD4 clinical trial, a 92 gene classifier (EMC92) was developed, enabling the classification of patients into high- or standard risk. This classifier was validated in four external patient cohorts (newly diagnosed and relapsed) in which its performance was shown to be independent of other prognostic factors. Chapter 3 discusses the ability of combining prognostic factors and ranking these in terms of performance. By exploiting the value of twenty known prognostic factors, which were systematically combined pair-wisely, we selected those combinations that improved prognostication. Among the most promising was the EMC92-ISS combination, enabling the classification of patients into four risk groups. The combinations that were found in the discovery phase were then validated in a similar group of patients that were left out of the discovery phase prior to the analysis. In Chapter 4 the EMC92 classifier was evaluated in elderly patients. Although approximately 65% of newly diagnosed MM patients are older than 65 years and thus likely non-transplant eligible, the EMC92-gene classifier has been validated using mainly newly diagnosed transplant eligible or relapsed patients. Only in a subset of the MRC-IX, newly diagnosed non-transplant eligible patients were included. Therefore, we applied the EMC92-gene classifier

---

to 178 patients included in the HOVON-87 trial with a median age of 73 years. Also in this setting the classifier has a strong performance, independent of other prognostic factors. Chapter 5 focuses on an important aspect of classifiers, i.e., concordance. Upon repeatedly classifying a patient under similar conditions, the resulting outcome should remain the same. We have described a method to quantify the concordance between repeated measurements and a test for equal concordances. In Chapter 6, the relation between expression of the protein cereblon (CRBN) with clinical outcome was evaluated. CRBN was found to be essential for the activity of the immune modulatory drugs, including Thalidomide and Lenalidomide. Using 96 Thalidomide treated patients of the HOVON-65/GMMG-HD4 trial, we showed that higher levels CRBN gene expression were significantly associated with longer progression-free survival. In contrast, no association between CRBN expression and survival was observed in the arm with Bortezomib maintenance. Chapters 7 and 8 deal with the putative genetic predisposition to the side effect peripheral neuropathy (PNP). Patients with high grades of PNP require dose-reduction or even discontinuation of the treatment (in this case Bortezomib). Identification of patients with an increased risk of developing PNP could help treatment decisions. Therefore we tested in Chapter 7 the association between germline single nucleotide polymorphisms (SNPs) and the occurrence of PNP during Bortezomib treatment in the IFM-2015-01 clinical trial. In Chapter 8, the Bortezomib treated patients of the HOVON65/GMMG-HD4 were re-genotyped using a more recent type of SNP array with unbiased design (more than 900.000 SNPs). A SNP mapping to the 3' UTR of PKNOX1 was among the highest associations in the IFM discovery cohort that could be validated in the HOVON-65/GMMG-HD4 validation data.



## REFERENCES

1. IKN. Integraal Kankercentrum Nederland. 2015.
2. Rajkumar SV. Multiple myeloma: 2016 update on diagnosis, risk-stratification, and management. *Am J Hematol* . 2016; **91**(7):719–34.
3. Morgan GJ, Walker BA, & Davies FE. The genetic architecture of multiple myeloma. *Nat Rev Cancer* . 2012; **12**(5):335–48.
4. Kuehl WM & Bergsagel PL. Multiple myeloma: evolving genetic events and host interactions. *Nat Rev Cancer* . 2002; **2**(3):175–87.
5. Rajkumar SV, Dimopoulos MA, Palumbo A, *et al*. International Myeloma Working Group updated criteria for the diagnosis of multiple myeloma. *Lancet Oncol* . 2014; **15**(12):e538–48.
6. Landgren O, Kyle RA, Pfeiffer RM, *et al*. Monoclonal gammopathy of undetermined significance (MGUS) consistently precedes multiple myeloma: a prospective study. *Blood* . 2009; **113**(22):5412–7.
7. Kyle RA, Therneau TM, Rajkumar SV, *et al*. A long-term study of prognosis in monoclonal gammopathy of undetermined significance. *N Engl J Med* . 2002; **346**(8):564–9.
8. Kyle RA, Remstein ED, Therneau TM, *et al*. Clinical course and prognosis of smoldering (asymptomatic) multiple myeloma. *N Engl J Med* . 2007; **356**(25):2582–90.
9. de Larrea FC, Kyle RA, Durie BG, *et al*. Plasma cell leukemia: consensus statement on diagnostic requirements, response criteria and treatment recommendations by the International Myeloma Working Group. *Leukemia* . 2013; **27**(4):780–91.
10. Voorhees PM & Usmani SZ. The role of high-dose melphalan and autologous stem cell transplant in the rapidly evolving era of modern multiple myeloma therapy. *Clin Adv Hematol Oncol* . 2016; **14**(9):719–28.
11. Kervoelen C, Menoret E, Gomez-Bougie P, *et al*. Dexamethasone-induced cell death is restricted to specific molecular subgroups of multiple myeloma. *Oncotarget* . 2015; **6**(29):26922–34.
12. Alexanian R, Barlogie B, & Dixon D. High-dose glucocorticoid treatment of resistant myeloma. *Ann Intern Med* . 1986; **105**(1):8–11.
13. Sonneveld P, Schmidt-Wolf IG, van der Holt B, *et al*. Bortezomib induction and maintenance treatment in patients with newly diagnosed multiple myeloma: results of the randomized phase III HOVON-65/ GMMG-HD4 trial. *J Clin Oncol* . 2012; **30**(24):2946–55.
14. Sheng Z, Li G, Li B, Liu Y, & Wang L. Carfilzomib-containing combinations as frontline therapy for multiple myeloma: A meta-analysis of 13 trials. *Eur J Haematol* . 2017; **98**(6):601–607.
15. Kumar S, Moreau P, Hari P, *et al*. Management of adverse events associated with ixazomib plus lenalidomide/dexamethasone in relapsed/refractory multiple myeloma. *Br J Haematol* . 2017; **178**(4):571–582.
16. Zang Y, Thomas SM, Chan ET, *et al*. The next generation proteasome inhibitors carfilzomib and oprozomib activate prosurvival autophagy via induction of the unfolded protein response and ATF4. *Autophagy* . 2012; **8**(12):1873–4.

- 
17. Lindner S & Kronke J. The molecular mechanism of thalidomide analogs in hematologic malignancies. *J Mol Med (Berl)* . 2016; **94**(12):1327–1334.
  18. Millrine D & Kishimoto T. A Brighter Side to Thalidomide: Its Potential Use in Immunological Disorders. *Trends Mol Med* . 2017; **23**(4):348–361.
  19. Raza S, Safyan RA, & Lentzsch S. Immunomodulatory Drugs (IMiDs) in Multiple Myeloma. *Curr Cancer Drug Targets* . 2017; **17**(9):846–857.
  20. Moreau P, Weisel KC, Song KW, *et al*. Relationship of response and survival in patients with relapsed and refractory multiple myeloma treated with pomalidomide plus low-dose dexamethasone in the MM-003 trial randomized phase III trial (NIMBUS). *Leuk Lymphoma* . 2016; **57**(12):2839–2847.
  21. Badros A, Hyjek E, Ma N, *et al*. Pembrolizumab, pomalidomide and low dose dexamethasone for relapsed/refractory multiple myeloma. *Blood* . 2017; **130**(10):1189–1197.
  22. Cejalvo MJ, Ribas P, & de la Rubia J. The safety of daratumumab for the treatment of multiple myeloma. *Expert Opin Drug Saf* . 2017; **16**(6):753–760.
  23. Usmani SZ, Diels J, Ito T, Mehra M, Khan I, & Lam A. Daratumumab monotherapy compared with historical control data in heavily pretreated and highly refractory patients with multiple myeloma: An adjusted treatment comparison. *Am J Hematol* . 2017; **92**(8):e146–e152.
  24. McEllistrim C, Krawczyk J, & O'Dwyer ME. New developments in the treatment of multiple myeloma - clinical utility of daratumumab. *Biologics* . 2017; **11**:31–43.
  25. Zagouri F, Terpos E, Kastiris E, & Dimopoulos MA. Emerging antibodies for the treatment of multiple myeloma. *Expert Opin Emerg Drugs* . 2016; **21**(2):225–37.
  26. Friend R, Bhutani M, Voorhees PM, & Usmani SZ. Clinical potential of SLAMF7 antibodies - focus on elotuzumab in multiple myeloma. *Drug Des Devel Ther* . 2017; **11**:893–900.
  27. Magen H & Muchtar E. Elotuzumab: the first approved monoclonal antibody for multiple myeloma treatment. *Ther Adv Hematol* . 2016; **7**(4):187–95.
  28. Dimopoulos MA, Lonial S, White D, *et al*. Elotuzumab plus lenalidomide/dexamethasone for relapsed or refractory multiple myeloma: ELOQUENT-2 follow-up and post-hoc analyses on progression-free survival and tumour growth. *Br J Haematol* . 2017; **178**(6):896–905.
  29. Sidaway P. Haematological cancer: Pembrolizumab is effective in multiple myeloma. *Nat Rev Clin Oncol* . 2017; **14**(7):393.
  30. Wu J, Ross J, Peale J F V, *et al*. A Favorable BCL-2 Family Expression Profile May Explain the Increased Susceptibility of the t(11;14) Multiple Myeloma Subgroup to Single Agent Venetoclax. *Blood* . 2016; **128**(22):5613.
  31. Moore D. Panobinostat (Farydak): A Novel Option for the Treatment of Relapsed Or Relapsed and Refractory Multiple Myeloma. *P T* . 2016; **41**(5):296–300.
  32. Tai YT & Anderson KC. Targeting B-cell maturation antigen in multiple myeloma. *Immunotherapy* . 2015; **7**(11):1187–99.
  33. Sidaway P. Haematological cancer: Anti-BCMA CAR T cells show promise in MM. *Nat Rev Clin Oncol* . 2016; **13**(9):530.
  34. Palumbo A, Bringhen S, Mateos MV, *et al*. Geriatric assessment predicts survival and toxicities

- in elderly myeloma patients: an International Myeloma Working Group report. *Blood* . 2015; **125**(13):2068–74.
35. Lee HS & Min CK. Optimal maintenance and consolidation therapy for multiple myeloma in actual clinical practice. *Korean J Intern Med* . 2016; **31**(5):809–19.
  36. Boudreault JS, Touzeau C, & Moreau P. Triplet combinations in relapsed/refractory myeloma: update on recent phase 3 trials. *Expert Rev Hematol* . 2017; **10**(3):207–215.
  37. Rosinol L, Oriol A, Teruel AI, *et al*. Superiority of bortezomib, thalidomide, and dexamethasone (VTD) as induction pretransplantation therapy in multiple myeloma: a randomized phase 3 PETHEMA/GEM study. *Blood* . 2012; **120**(8):1589–96.
  38. Jakubowiak AJ, Chari A, Lonial S, *et al*. Daratumumab (DARA) in combination with carfilzomib, lenalidomide, and dexamethasone (KRd) in patients (pts) with newly diagnosed multiple myeloma (MMY1001): An open-label, phase 1b study. *ASCO Annual Meeting Abstract* . 2017; **35**(Suppl 15):8000.
  39. Benboubker L, Dimopoulos MA, Dispenzieri A, *et al*. Lenalidomide and dexamethasone in transplant-ineligible patients with myeloma. *N Engl J Med* . 2014; **371**(10):906–17.
  40. Delforge M, Blade J, Dimopoulos MA, *et al*. Treatment-related peripheral neuropathy in multiple myeloma: the challenge continues. *Lancet Oncol* . 2010; **11**(11):1086–95.
  41. Moreau P, Pylypenko H, Grosicki S, *et al*. Subcutaneous versus intravenous administration of bortezomib in patients with relapsed multiple myeloma: a randomised, phase 3, non-inferiority study. *Lancet Oncol* . 2011; **12**(5):431–40.
  42. Bringhen S, De Wit E, & Dimopoulos MA. New Agents in Multiple Myeloma: An Examination of Safety Profiles. *Clin Lymphoma Myeloma Leuk* . 2017; **17**(7):391–407.
  43. Dimopoulos MA, Moreau P, Palumbo A, *et al*. Carfilzomib and dexamethasone versus bortezomib and dexamethasone for patients with relapsed or refractory multiple myeloma (ENDEAVOR): a randomised, phase 3, open-label, multicentre study. *Lancet Oncol* . 2016; **17**(1):27–38.
  44. Costa LJ, Brill IK, Omel J, Godby K, Kumar SK, & Brown EE. Recent trends in multiple myeloma incidence and survival by age, race, and ethnicity in the United States. *Blood Adv* . 2017; **1**(4):282–287.
  45. San-Miguel JF & Mateos MV. Can multiple myeloma become a curable disease? *Haematologica* . 2011; **96**(9):1246–8.
  46. Kumar SK, Dispenzieri A, Lacy MQ, *et al*. Continued improvement in survival in multiple myeloma: changes in early mortality and outcomes in older patients. *Leukemia* . 2014; **28**(5):1122–8.
  47. Neben K, Jauch A, Bertsch U, *et al*. Combining information regarding chromosomal aberrations t(4;14) and del(17p13) with the International Staging System classification allows stratification of myeloma patients undergoing autologous stem cell transplantation. *Haematologica* . 2010; **95**(7):1150–7.
  48. Brenner H, Gondos A, & Pulte D. Recent major improvement in long-term survival of younger patients with multiple myeloma. *Blood* . 2008; **111**(5):2521–6.

- 
49. Alexanian R, Delasalle K, Wang M, Thomas S, & Weber D. Curability of multiple myeloma. *Bone Marrow Res* . 2012; **2012**:916479.
  50. Italiano A. Prognostic or predictive? It's time to get back to definitions! *J Clin Oncol* . 2011; **29**(35):4718; author reply 4718-9.
  51. Kim JE, Yoo C, Lee DH, Kim SW, Lee JS, & Suh C. Serum albumin level is a significant prognostic factor reflecting disease severity in symptomatic multiple myeloma. *Ann Hematol* . 2010; **89**(4):391-7.
  52. Greipp PR, San Miguel J, Durie BG, *et al*. International staging system for multiple myeloma. *J Clin Oncol* . 2005; **23**(15):3412-20.
  53. Engelhardt M, Terpos E, Kleber M, *et al*. European Myeloma Network recommendations on the evaluation and treatment of newly diagnosed patients with multiple myeloma. *Haematologica* . 2014; **99**(2):232-42.
  54. Chretien ML, Corre J, Lauwers-Cances V, *et al*. Understanding the role of hyperdiploidy in myeloma prognosis: which trisomies really matter? *Blood* . 2015; **126**(25):2713-9.
  55. Xie Z, Bi C, Chooi JY, Chan ZL, Mustafa N, & Chng WJ. MMSET regulates expression of IRF4 in t(4;14) myeloma and its silencing potentiates the effect of bortezomib. *Leukemia* . 2015; **29**(12):2347-54.
  56. Chesi M & Bergsagel PL. Molecular pathogenesis of multiple myeloma: basic and clinical updates. *Int J Hematol* . 2013; **97**(3):313-23.
  57. Corre J, Munshi N, & Avet-Loiseau H. Genetics of multiple myeloma: another heterogeneity level? *Blood* . 2015; **125**(12):1870-6.
  58. Dib A, Gabrea A, Glebov OK, Bergsagel PL, & Kuehl WM. Characterization of MYC translocations in multiple myeloma cell lines. *J Natl Cancer Inst Monogr* . 2008; **2008**(39):25-31.
  59. Chang H, Qi X, Jiang A, Xu W, Young T, & Reece D. 1p21 deletions are strongly associated with 1q21 gains and are an independent adverse prognostic factor for the outcome of high-dose chemotherapy in patients with multiple myeloma. *Bone Marrow Transplant* . 2010; **45**(1):117-21.
  60. An G, Xu Y, Shi L, *et al*. Chromosome 1q21 gains confer inferior outcomes in multiple myeloma treated with bortezomib but copy number variation and percentage of plasma cells involved have no additional prognostic value. *Haematologica* . 2014; **99**(2):353-9.
  61. Hanahan D & Weinberg RA. The hallmarks of cancer. *Cell* . 2000; **100**(1):57-70.
  62. Boyd KD, Ross FM, Chiecchio L, *et al*. A novel prognostic model in myeloma based on cosegregating adverse FISH lesions and the ISS: analysis of patients treated in the MRC Myeloma IX trial. *Leukemia* . 2012; **26**(2):349-55.
  63. Bergsagel PL & Chesi M. Molecular classification and risk stratification of myeloma. *Hematol Oncol* . 2013; **31**(Suppl 1):38-41.
  64. Bergsagel PL & Kuehl WM. Molecular pathogenesis and a consequent classification of multiple myeloma. *J Clin Oncol* . 2005; **23**(26):6333-8.
  65. Moreau P, Facon T, Leleu X, *et al*. Recurrent 14q32 translocations determine the prognosis of multiple myeloma, especially in patients receiving intensive chemotherapy. *Blood* . 2002; **100**(5):1579-83.

66. Fonseca R, Debes-Marun CS, Picken EB, *et al.* The recurrent IgH translocations are highly associated with nonhyperdiploid variant multiple myeloma. *Blood* . 2003; **102**(7):2562–7.
67. Avet-Loiseau H, Attal M, Moreau P, *et al.* Genetic abnormalities and survival in multiple myeloma: the experience of the Intergroupe Francophone du Myelome. *Blood* . 2007; **109**(8):3489–95.
68. Keats JJ, Reiman T, Maxwell CA, *et al.* In multiple myeloma, t(4;14)(p16;q32) is an adverse prognostic factor irrespective of FGFR3 expression. *Blood* . 2003; **101**(4):1520–9.
69. Chu L, Su MY, Maggi J L B, *et al.* Multiple myeloma-associated chromosomal translocation activates orphan snoRNA ACA11 to suppress oxidative stress. *J Clin Invest* . 2012; **122**(8):2793–806.
70. Mirabella F, Wu P, Wardell CP, *et al.* MMSET is the key molecular target in t(4;14) myeloma. *Blood Cancer J* . 2013; **3**(5):e114.
71. Kumar S, Kaufman JL, Gasparetto C, *et al.* Efficacy of venetoclax as targeted therapy for relapsed/refractory t(11;14) multiple myeloma. *Blood* . 2017; **130**:2401–2409.
72. Muller PA & Vousden KH. Mutant p53 in cancer: new functions and therapeutic opportunities. *Cancer Cell* . 2014; **25**(3):304–17.
73. Reed SM & Quelle DE. p53 Acetylation: Regulation and Consequences. *Cancers (Basel)* . 2014; **7**(1):30–69.
74. Chavan SS, He J, Tytarenko R, *et al.* Bi-allelic inactivation is more prevalent at relapse in multiple myeloma, identifying RB1 as an independent prognostic marker. *Blood Cancer J* . 2017; **7**(2):e535.
75. Pawlyn C, Melchor L, Murison A, *et al.* Coexistent hyperdiploidy does not abrogate poor prognosis in myeloma with adverse cytogenetics and may precede IGH translocations. *Blood* . 2015; **125**(5):831–40.
76. Bergsagel PL, Kuehl WM, Zhan F, Sawyer J, Barlogie B, & Shaughnessy J J. Cyclin D dysregulation: an early and unifying pathogenic event in multiple myeloma. *Blood* . 2005; **106**(1):296–303.
77. Zhan F, Huang Y, Colla S, *et al.* The molecular classification of multiple myeloma. *Blood* . 2006; **108**(6):2020–2028.
78. Kuehl WM & Bergsagel PL. Molecular pathogenesis of multiple myeloma and its premalignant precursor. *J Clin Invest* . 2012; **122**(10):3456–63.
79. Broyl A, Hose D, Lokhorst H, *et al.* Gene expression profiling for molecular classification of multiple myeloma in newly diagnosed patients. *Blood* . 2010; **116**(14):2543–53.
80. Kalf A & Spencer A. The t(4;14) translocation and FGFR3 overexpression in multiple myeloma: prognostic implications and current clinical strategies. *Blood Cancer J* . 2012; **2**(9):e89.
81. Broijl A. Molecular profiling in multiple myeloma (page 96). Ph.D. thesis, Erasmus University. 2012.
82. van 't Veer LJ, Dai H, van de Vijver MJ, *et al.* Gene expression profiling predicts clinical outcome of breast cancer. *Nature* . 2002; **415**(6871):530–6.
83. Den Boer ML, van Slegtenhorst M, De Menezes RX, *et al.* A subtype of childhood acute lym-

- phoblastic leukaemia with poor treatment outcome: a genome-wide classification study. *Lancet Oncol* . 2009; **10**(2):125–34.
84. van der Veer A, Waanders E, Pieters R, *et al*. Independent prognostic value of BCR-ABL1-like signature and IKZF1 deletion, but not high CRLF2 expression, in children with B-cell precursor ALL. *Blood* . 2013; **122**(15):2622–9.
  85. Shaughnessy JJ D, Zhan F, Burington BE, *et al*. A validated gene expression model of high-risk multiple myeloma is defined by deregulated expression of genes mapping to chromosome 1. *Blood* . 2007; **109**(6):2276–2284.
  86. Hose D, Reme T, Hielscher T, *et al*. Proliferation is a central independent prognostic factor and target for personalized and risk-adapted treatment in multiple myeloma. *Haematologica* . 2011; **96**(1):87–95.
  87. Hose D, Reme T, Meissner T, *et al*. Inhibition of aurora kinases for tailored risk-adapted treatment of multiple myeloma. *Blood* . 2009; **113**(18):4331–40.
  88. Reme T, Hose D, Theillet C, & Klein B. Modeling risk stratification in human cancer. *Bioinformatics* . 2013; **29**(9):1149–57.
  89. Decaux O, Lode L, Magrangeas F, *et al*. Prediction of survival in multiple myeloma based on gene expression profiles reveals cell cycle and chromosomal instability signatures in high-risk patients and hyperdiploid signatures in low-risk patients: a study of the Intergroupe Francophone du Myelome. *J Clin Oncol* . 2008; **26**(29):4798–4805.
  90. Mulligan G, Mitsiades C, Bryant B, *et al*. Gene expression profiling and correlation with outcome in clinical trials of the proteasome inhibitor bortezomib. *Blood* . 2007; **109**(8):3177–3188.
  91. Dickens NJ, Walker BA, Leone PE, *et al*. Homozygous deletion mapping in myeloma samples identifies genes and an expression signature relevant to pathogenesis and outcome. *Clin Cancer Res* . 2010; **16**(6):1856–1864.
  92. Shaughnessy JJ D, Qu P, Usmani S, *et al*. Pharmacogenomics of bortezomib test-dosing identifies hyperexpression of proteasome genes, especially PSMD4, as novel high-risk feature in myeloma treated with total therapy 3. *Blood* . 2011; **118**:3512–3524.
  93. Mikhael JR, Dingli D, Roy V, *et al*. Management of newly diagnosed symptomatic multiple myeloma: updated Mayo Stratification of Myeloma and Risk-Adapted Therapy (mSMART) consensus guidelines 2013. *Mayo Clin Proc* . 2013; **88**(4):360–76.
  94. Avet-Loiseau H, Durie BG, Cavo M, *et al*. Combining fluorescent in situ hybridization data with ISS staging improves risk assessment in myeloma: an International Myeloma Working Group collaborative project. *Leukemia* . 2013; **27**(3):711–7.
  95. Palumbo A, Avet-Loiseau H, Oliva S, *et al*. Revised International Staging System for Multiple Myeloma: A Report From International Myeloma Working Group. *J Clin Oncol* . 2015; **33**(26):2863–9.
  96. Avet-Loiseau H, Attal M, Campion L, *et al*. Long-term analysis of the IFM 99 trials for myeloma: cytogenetic abnormalities [t(4;14), del(17p), 1q gains] play a major role in defining long-term survival. *J Clin Oncol* . 2012; **30**(16):1949–52.
  97. Grzasko N, Hajek R, Hus M, *et al*. Chromosome 1 amplification has similar prognostic value

- to del(17p13) and t(4;14)(p16;q32) in multiple myeloma patients: analysis of real-life data from the Polish Myeloma Study Group. *Leuk Lymphoma* . 2017; **58**(9):2089–2100.
98. Shah V, Sherborne AL, Walker BA, *et al*. Prediction of outcome in newly diagnosed myeloma: a meta-analysis of the molecular profiles of 1905 trial patients. *Leukemia* . 2018; **32**(1):102–110.
  99. Hogeweg P. The roots of bioinformatics in theoretical biology. *PLoS Comput Biol* . 2011; **7**(3):e1002021.
  100. Zhao S, Fung-Leung WP, Bittner A, Ngo K, & Liu X. Comparison of RNA-Seq and microarray in transcriptome profiling of activated T cells. *PLoS One* . 2014; **9**(1):e78644.
  101. Hubbell E, Liu WM, & Mei R. Robust estimators for expression analysis. *Bioinformatics* . 2002; **18**(12):1585–92.
  102. Irizarry RA, Hobbs B, Collin F, *et al*. Exploration, normalization, and summaries of high density oligonucleotide array probe level data. *Biostatistics* . 2003; **4**(2):249–64.
  103. Irizarry RA, Warren D, Spencer F, *et al*. Multiple-laboratory comparison of microarray platforms. *Nat Methods* . 2005; **2**(5):345–50.
  104. Cope LM, Irizarry RA, Jaffee HA, Wu Z, & Speed TP. A benchmark for Affymetrix GeneChip expression measures. *Bioinformatics* . 2004; **20**(3):323–31.
  105. Zhu Q, Miecznikowski JC, & Halfon MS. Preferred analysis methods for Affymetrix GeneChips. II. An expanded, balanced, wholly-defined spike-in dataset. *BMC Bioinformatics* . 2010; **11**(1):285.
  106. Dabney AR & Storey JD. A reanalysis of a published Affymetrix GeneChip control dataset. *Genome Biol* . 2006; **7**(3):401.
  107. Wu Z, Irizarry R, Gentleman R, Murillo F, & Spencer F. A model based background adjustment for Oligonucleotide expression arrays. *Journal of the American Statistical Association* . 2004; **99**(468):909–917.
  108. Wu Z & Irizarry RA. Stochastic models inspired by hybridization theory for short oligonucleotide arrays. *J Comput Biol* . 2005; **12**(6):882–93.
  109. Kitchen RR, Sabine VS, Simen AA, Dixon JM, Bartlett JM, & Sims AH. Relative impact of key sources of systematic noise in Affymetrix and Illumina gene-expression microarray experiments. *BMC Genomics* . 2011; **12**(1):589.
  110. Leek JT, Scharpf RB, Bravo HC, *et al*. Tackling the widespread and critical impact of batch effects in high-throughput data. *Nat Rev Genet* . 2010; **11**(10):733–9.
  111. Alter O, Brown PO, & Botstein D. Singular value decomposition for genome-wide expression data processing and modeling. *Proc Natl Acad Sci U S A* . 2000; **97**(18):10101–6.
  112. Nielsen TO, West RB, Linn SC, *et al*. Molecular characterisation of soft tissue tumours: a gene expression study. *Lancet* . 2002; **359**(9314):1301–7.
  113. Benito M, Parker J, Du Q, *et al*. Adjustment of systematic microarray data biases. *Bioinformatics* . 2004; **20**(1):105–14.
  114. Johnson WE, Li C, & Rabinovic A. Adjusting batch effects in microarray expression data using empirical Bayes methods. *Biostatistics* . 2007; **8**(1):118–27.

- 
115. Chen C, Grennan K, Badner J, *et al.* Removing batch effects in analysis of expression microarray data: an evaluation of six batch adjustment methods. *PLoS One* . 2011; **6**(2):e17238.
  116. Stein CK, Qu P, Epstein J, *et al.* Removing batch effects from purified plasma cell gene expression microarrays with modified ComBat. *BMC Bioinformatics* . 2015; **16**(63).
  117. Hastie T, Tibshirani R, & Friedman J. The elements of statistical learning, volume 2. Springer: 2009.
  118. Babyak M. What You See May Not Be What You Get: A Brief, Nontechnical Introduction to Overfitting in Regression-Type Models. *Psychosomatic Medicine* . 2004; **66**(3):411–421.
  119. Cover TM. Geometrical and statistical properties of systems of linear inequalities with applications in pattern recognition. *Electronic Computers, IEEE Transactions on* . 1965; **EC14**(3):326–334.
  120. Tibshirani R. Regression shrinkage and selection via the lasso. *Journal of the Royal Statistical Society. Series B (Methodological)* . 1996; :267–288.
  121. Hoerl AE & Kennard RW. Ridge regression: Biased estimation for nonorthogonal problems. *Technometrics* . 1970; **12**(1):55–67.



# CHAPTER

# 2

## A Gene Expression Signature for High-risk Multiple Myeloma

Rowan Kuiper\*, Annemiek Broyl\*, Yvonne de Knegt,  
Martin H. van Vliet, Erik H. van Beers, Bronno van der Holt,  
Laila el Jarari, George Mulligan, Walter Gregory, Gareth Morgan, Hartmut  
Goldschmidt, Henk M. Lokhorst,  
Mark van Duin & Pieter Sonneveld

\*These authors contributed equally to this work

---

## ABSTRACT

There is a strong need to better predict survival of patients with newly diagnosed multiple myeloma (MM). As gene expression profiles (GEPs) reflect the biology of MM in individual patients, we built a prognostic signature based on GEPs.

GEPs obtained from newly diagnosed MM patients included in the HOVON-65/GMMG-HD4 trial ( $n = 290$ ) were used as training data. Using this set, a prognostic signature of 92 genes (EMC92-gene signature) was generated by supervised principal components analysis combined with simulated annealing.

Performance of the EMC92-gene signature was confirmed in independent validation sets of newly diagnosed (TT2,  $n = 351$ ; TT3,  $n = 142$ ; MRC-IX,  $n = 247$ ) and relapsed patients (APEX,  $n = 264$ ). In all sets, patients defined as high-risk by the EMC92-gene signature show a clearly reduced overall survival with hazard-ratios (HR) of 3.4 (95%CI: [2.2 – 5.3]) for the TT2 study, HR: 5.2 [2.5 – 11] for the TT3 study, HR: 2.4 [1.7 – 3.4] for the MRC-IX study and HR: 3.0 [2.1 – 4.4] for the APEX study ( $p < 1 \times 10^{-4}$  in all studies). In multivariate analyses this signature was proven independent of currently used prognostic factors.

The EMC92-gene signature is better or comparable to previously published signatures. This signature contributes to risk assessment in clinical trials and could provide a tool for treatment choices in high-risk multiple myeloma patients.

## INTRODUCTION

Multiple myeloma (MM) is characterized by accumulation of malignant monoclonal plasma cells in the bone marrow. The median overall survival (OS) for newly diagnosed patients treated with high dose therapy varies from 4 to 10 years.<sup>1,2</sup>

The International Staging System (ISS), based on serum  $\beta$ 2-microglobulin and albumin, is widely used as a prognostic system for patients with newly diagnosed MM. ISS has been confirmed as a solid prognostic factor in clinical trials.<sup>1</sup> Additional clinical factors to define high-risk disease have not been consistently reproduced, with the exception of extensive disease represented by renal failure and plasma cell leukemia.<sup>2,3</sup> In addition to ISS, cytogenetic aberrations such as deletion of 17p (del(17p)), translocations t(4;14) and t(14;16) were shown to be associated with an adverse prognosis. The combination of prognostic markers t(4;14), del(17p) and ISS enabled further delineation of patients into prognostic subgroups.<sup>4</sup>

A strategy to include genetic characteristics of MM is the translocation and cyclin D (TC) classification, which distinguishes eight subgroups based on genes which are deregulated by primary immunoglobulin H translocations and transcriptional activation of cyclin D genes.<sup>5</sup> Subsequently, the University of Arkansas for Medical Sciences (UAMS) generated a molecular classification of myeloma based on gene expression profiles of patients included in their local trials. The UAMS molecular classification of myeloma identifies seven distinct gene expression clusters, including the translocation clusters MS, MF, CD-1, CD-2, a hyperdiploid cluster (HY), a cluster with proliferation-associated genes (PR), and a cluster characterized by low percentage of bone disease (LB).<sup>6</sup> More recently, we extended this classification based on the HOVON-65/GMMG-HD4 prospective clinical trial and identified additional molecular clusters, i.e. NF $\kappa$ B, CTA and PRL3.<sup>7</sup> Because these clusters were discriminated based on disease specific gene expression profiles (GEP), we and others hypothesized that they may be relevant for therapy outcome. Indeed, the UAMS defined clusters MF, MS and PR were found to identify high-risk disease in the Total Therapy 2 trial.<sup>6</sup>

Several survival signatures were developed based on samples from clini-

---

cal trials, such as the UAMS70, the related UAMS17 and the recently published UAMS80 signature which have value in prognostication of MM.<sup>8-10</sup> Other signatures include the Medical Research Council (MRC) gene signature based on the MRC-IX trial, the French Intergroupe Francophone du Myélome (IFM) signature and the Millennium signature based on relapse patients.<sup>11-13</sup> Recently, a GEP based proliferation index was reported.<sup>14</sup> So far, none of these signatures have been introduced in general clinical practice.

The additional and independent prognostic significance of a prognosticator based on gene expression has been acknowledged in mSMART (Mayo Stratification for Myeloma And Risk-adapted Therapy). Hereby, a high-risk MM population can be defined for which alternative treatment is proposed although this has not been validated in prospective clinical trials.<sup>15</sup>

The aim of the present study was to develop a prognostic signature for overall survival in MM patients. This investigation was prospectively included as a secondary analysis of a randomized clinical trial for newly diagnosed, transplant-eligible patients with multiple myeloma (HOVON-65/GMMG-HD4).

## MATERIALS AND METHODS

### Patients

As training set the HOVON-65/GMMG-HD4 study (ISRCTN64455289) was used. Details of the training set are given in the online supplemental document A.<sup>16</sup> Informed consent to treatment protocols and sample procurement was obtained for all cases included in this study, in accordance with the Declaration of Helsinki. Use of diagnostic tumor material was approved by the institutional review board of the Erasmus Medical Center. Arrays used for analysis passed extensive quality controls, as described previously.<sup>7</sup> Of the 328 gene arrays deposited at the NCBI-GEO repository, clinical outcome data was available for 290 patients (accession number: GSE19784).

Four independent datasets were used as validation of which both survival data were available as well as GEPs of purified plasma cells obtained from bone marrow aspirates of myeloma patients. The datasets Total Therapy 2 (UAMS-TT2,  $n = 351$ , GSE2658, NCT00573391), Total Therapy 3 (UAMS-TT3,  $n = 142$ , E-TABM-1138, NCT00081939) and MRC-IX ( $n = 247$ , GSE15695, ISRCTN6845-4111) were obtained from newly diagnosed patients. The APEX dataset ( $n = 264$ , GSE9782, registered under M34100-024, M34100-025 and NCT00049478 / NCT00048230) consisted of relapsed myeloma cases (see online supplemental document A).<sup>11,17-23</sup>

### Gene expression pre-processing

To allow gene expression analysis in the HOVON-65/GMMG-HD4, plasma cells were purified from bone marrow aspirates obtained at diagnosis, using immune-magnetic beads. Only samples with a plasma cell purity of  $\geq 80\%$  were used. Gene expression was determined on an Affymetrix GeneChip® Human Genome U133 Plus2.0 Array (Affymetrix, Santa Clara, CA, USA).

To allow for validation across different studies, only probe sets present on both the U133 Plus2.0 and the U133 A/B platforms were included ( $n = 44754$ ). Probe sets having an expression value below the lowest 1% bioB hybridization control in more than 95% of the samples are excluded. This resulted in 27680

---

probe sets to be analyzed. All data were MAS5 normalized,  $\log_2$  transformed and mean-variance scaled, using default settings in the Affy package in Bioconductor.<sup>24</sup>

The normalized validation gene expression data sets were downloaded from the repositories NCBI-GEO (APEX, MRC-IX and UAMS-TT2) and ArrayExpress (UAMS-TT3). Datasets UAMS-TT2, UAMS-TT3 and MRC-IX were generated using the U133 Plus2.0 (Affymetrix, Santa Clara, CA, USA) platform whereas the Affymetrix HG U133 A/B platform was used in the APEX study. The IFM dataset was not included in our analysis due to an incompatible, custom platform.

The strong batch effect that exists between these GEPs studies was successfully removed by ComBat using the non-parametric correction option.<sup>25</sup> APEX was run on a different array platform with an incomplete overlap in probe sets with the other datasets, and as a result ComBat correction was applied in two separate runs with one run for all analyses involving the APEX data set and an additional run for all other analyses.

## Survival signature

The HOVON-65/GMMG-HD4 data were used as a training set. GEP and PFS data were combined for building a GEP based survival classifier. PFS was used for generating a classifier for OS since PFS was the primary endpoint of the HOVON-65/GMMG-HD4 study and PFS demonstrated a higher number of events compared to OS (179 PFS vs. 99 OS events in total in the HOVON-65/GMMG-HD4). All evaluations of the signature are based on OS data in training and validation sets. Analyses were performed using R with the survival package for survival analyses.<sup>26</sup> Out of 27680 probe sets tested, 1093 probe sets were associated to PFS in univariate Cox regression analyses (false discovery rate (FDR) < 10%; for probe sets and survival data see online supplemental document B). Subsequently, this set was used as input into a supervised principal component analysis (SPCA) framework in combination with simulated annealing (online supplemental documents A and B).<sup>27</sup> This analysis yielded a model of 92 probe sets, termed the EMC92 signature. The survival signature is a continuous score, i.e. the sum of standardized expression values multiplied by the probe set specific weighting coefficient (online Table S1, R-script and supplemental document C). High-risk

disease was defined as the proportion of patients with an overall survival of less than two years in the training set.

## Validation of the EMC92 signature

A multivariate Cox regression analysis was performed for patients with available covariates. Covariates with  $< 10\%$  of the data missing were used as input in a backward stepwise selection procedure ( $p < 0.05$ ).

The EMC92 signature together with seven previously described, external signatures for OS in multiple myeloma have been analyzed in a pair-wise comparison using a multivariate Cox regression analysis. This analysis was performed for all pair-wise comparisons on the pooled datasets excluding the training sets for the signatures being tested. The models were stratified for study.

Pathway analysis was performed using the 92 genes corresponding to the EMC92 signature as well as the 1093 genes generated by univariate PFS analysis ( $FDR < 10\%$ ) with the probe sets used as input for the analysis as a reference set ( $n = 27680$ , Ingenuity Systems, [www.ingenuity.com](http://www.ingenuity.com)).  $p$ -values were derived from right-tailed Fisher exact tests and corrected for multiple testing by a Benjamini-Hochberg correction.<sup>28</sup>

---

## RESULTS

### The EMC92 signature

2

GEPs obtained from newly diagnosed MM patients were analyzed in relation to survival data, in order to generate a classifier to distinguish high-risk from standard-risk disease. We used the HOVON-65/GMMG-HD4 data as a training set.<sup>7</sup> After filtering for probe set intensity, using internal Affymetrix control probe sets, 27680 probe sets were analyzed in a univariate Cox regression analysis with progression free survival (PFS) as survival endpoint. This resulted in 1093 probe sets associated with PFS with a false discovery rate of < 10% (online supplemental document B). Based on these 1093 probe sets, a supervised principal components analysis based model was built in which simulated annealing was applied to generate the optimal model settings in a 20-fold cross-validation. The final predictive model consisted of 92 probe sets with specific weighting coefficients. The sum of normalized intensity values multiplied by this weighting is the output of the signature. This model was termed the EMC92 signature. A positive weighting coefficient indicates that increased expression contributes to a higher value for the EMC92 signature value and thus a higher risk for poor survival. The majority of the probe sets are annotated genes ( $n = 85$ , with one of the genes represented by two probe sets). The remaining probe sets are open reading frames ( $n = 3$ ), expressed sequence tags ( $n = 2$ ) and one additional probe set without annotation. Several known cancer genes are among these genes, of which *FGFR3* (weighting coefficient = 0.06), *STAT1* (weighting coefficient = 0.05) and *BIRC5* (weighting coefficient = 0.02) were described in detail in relation to myeloma (online Table S1).<sup>29-31</sup> To define a high-risk population, the cut-off threshold for the continuous signature score was set to a value of 0.827 based on the proportion of patients in the training set that had an overall survival of less than two years (63 out of 290 patients (21.7%); online Figure S2).

Four independent validation datasets were available: UAMS-TT2, UAMS-TT3, MRC-IX and APEX. Gene expression datasets UAMS-TT2 and TT3 consisted of 351 and 142 transplant-eligible patients whereas the MRC-IX dataset contained both transplant-eligible and non-transplant-eligible MM patients ( $n = 247$ ). In the



APEX dataset, GEPs of 264 relapse patients were collected. The results of the EMC92 signature in the validation sets are shown in Figure 1 and online Table S2. In the UAMS-TT2 dataset, the EMC92 signature identified a high-risk population of 19.4% with a hazard-ratio of 3.4, 95% confidence interval (95%CI)=[2.2 – 5.3] ( $p= 5.7 \times 10^{-8}$ ). In the UAMS-TT3, 16.2% of patients were identified as high-risk with a hazard-ratio of 5.2, 95%CI [2.5 – 11], ( $p= 1.8 \times 10^{-5}$ ). In the MRC-IX dataset, 20.2% of patients were identified as high-risk with a hazard-ratio of 2.4, 95%CI [1.7 – 3.4], ( $p= 3.6 \times 10^{-6}$ ). The high-risk signature was able to identify patients with significantly shorter survival in both the transplant-eligible and non-transplant-eligible patients included in the MRC-IX study. In non-transplant-eligible patients, 23.9% high-risk patients were identified with a hazard-ratio of 2.4, 95%CI [1.5 – 3.9], ( $p= 4.3 \times 10^{-4}$ ), whereas 16.8% of transplant-eligible patients were high-risk with a hazard-ratio of 2.5, 95%CI [1.4 – 4.5], ( $p= 1.5 \times 10^{-3}$ ; Figures 1d and e). The signature was not restricted to newly diagnosed patients as 16.3% of patients included in the APEX relapse dataset were designated high-risk with a hazard-ratio of 3.0, 95%CI [2.1 – 4.4], ( $p= 1.26 \times 10^{-8}$ ; Figures 1f and 2e).

To assess the relation between EMC92 signature outcome and treatment, we evaluated whether there is evidence for differences in survival between treatment arms in the high-risk group or standard-risk group. Within the high-risk patients of the HOVON-65/GMMG-HD4 trial, the survival of bortezomib treated patients was longer than patients treated with conventional chemotherapy (VAD) (30 months compared to 19 months), albeit not significant ( $p= 0.06$ ; number of bortezomib treated patients: 26 vs. 37 in the VAD arm). Within the high-risk patients of MRC-IX, no difference was observed between the treatment arms ( $p= 0.5$ : MRC-IX non-transplant eligible: CTDA  $n = 14$  vs. MP  $n = 12$ ) and  $p= 1.0$  (MRC-IX transplant eligible; CTD  $n = 16$  vs. CVAD  $n = 7$ ). For the standard-risk patients no differences in survival between treatment arms were found in either trial.

Multivariate analysis was performed in the training set and in the APEX and MRC-IX validation sets, for which information on a large number of variables were available. This showed that in addition to the EMC92 signature, del(17p) was an independent predictor in HOVON-65/GMMG-HD4. Furthermore, in both

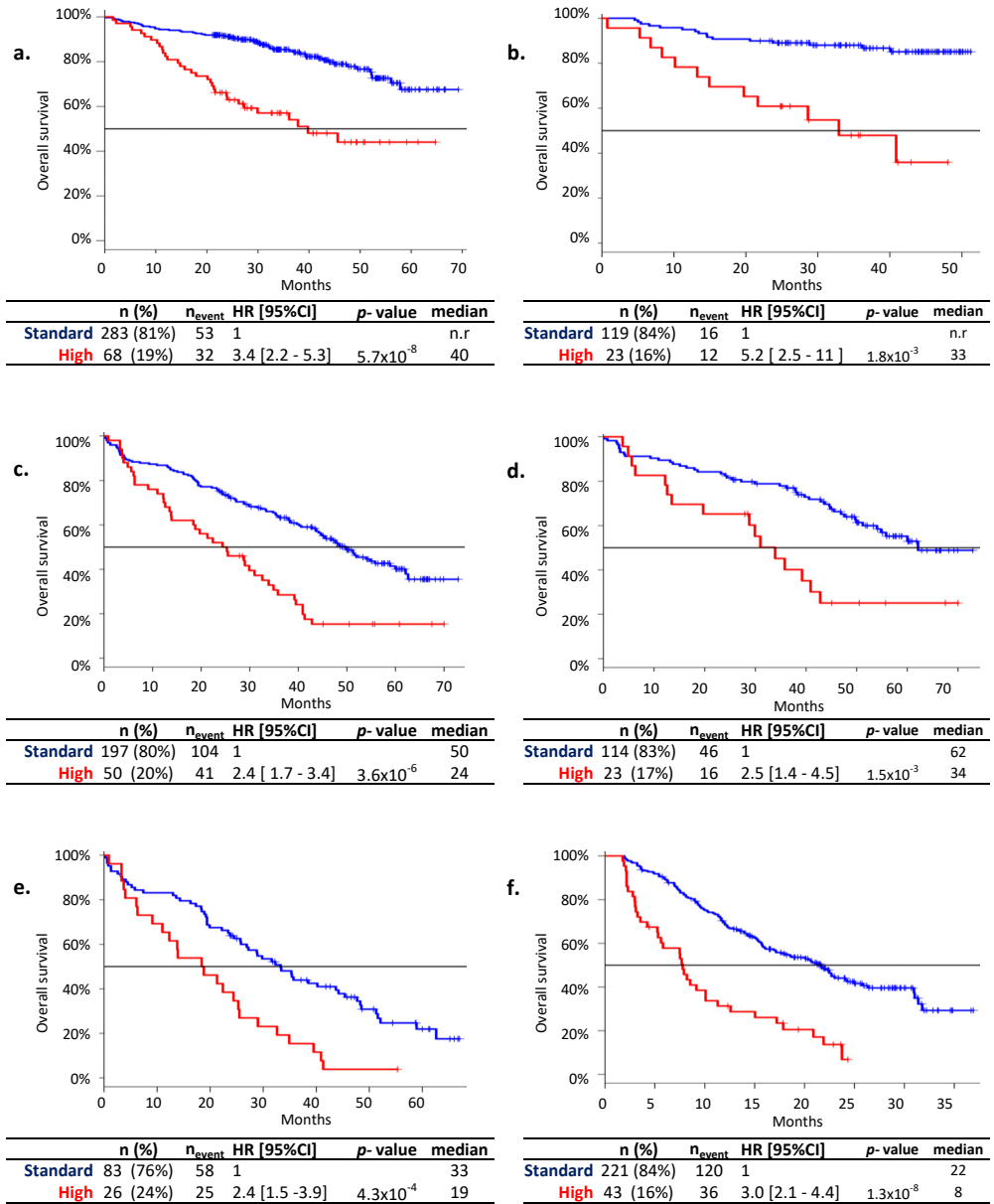


**Figure 1. Kaplan-Meier overall survival curves for EMC92 signature defined high-risk patients versus standard-risk patients in five validation sets.** The cut-off value is fixed at 0.827 based on the proportion of patients with OS < 2 years in the HOVON-65/GMMG-HD4 set. In the MRC-IX one patient had an unknown treatment status and was disregarded in Figures d and e. **a)** UAMS Total Therapy 2. **b)** UAMS Total Therapy 3. **c)** MRC-IX. **d)** MRC-IX transplant-eligible patients. **e)** MRC-IX non-transplant-eligible. **f)** APEX. N, number of patients; Events, number of events; HR, hazard ratio; *p*-value for equality to standard-risk group; Median, median survival time; n.r. median not reached.

HOVON-65/GMMG-HD4 and in the APEX multivariate analysis, a component of the ISS was an additional independent prognostic predictor ( $\beta$ 2-microglobulin for the HOVON65/GMMG-HD4 set and serum albumin for the APEX data set). Trial specific covariates were seen in each multivariate analysis such as sub-study in the APEX dataset and the MP treatment arm in the MRC-IX set. In conclusion, in all three datasets of newly diagnosed and relapse MM patients the EMC92 signature performed as the strongest predictor for survival after inclusion of available covariates (Table 1). For univariate associations to survival see online Tables S3.1-S3.3.

Using the nearest neighbor classification method, all patients in the validation sets were classified into molecular clusters based on the HOVON-65/GMMG-HD4 classification.<sup>7</sup> A clear enrichment of the MF, MS, PR clusters and decreased proportion of the HY cluster was found in the pooled high-risk populations of all validation sets (online Table S4).

To define the biological relevance of the EMC92 signature and the 1093 probe sets found by initial univariate ranking, pathway analysis of the 92 and the 1093 probe sets was performed. Significant functions for the EMC92 signature included multiple 'cell cycle' pathways ( $p= 1.8 \times 10^{-3} - 4.9 \times 10^{-2}$ ; online Table S5), including genes such as *BIRC5*, *TOP2A* and *CENPE*. The 1093 probe sets indicated functions such as 'protein synthesis' ( $p= 9.5 \times 10^{-31} - 1.5 \times 10^{-12}$ ), 'cancer' ( $p= 4.8 \times 10^{-12} - 4.9 \times 10^{-2}$ ) and 'cell cycle' ( $p= 3.7 \times 10^{-9} - 4.9 \times 10^{-2}$ ; online Table S6). Next, we compared the chromosomal locations of the probe sets within the EMC92 signature to the expected proportion represented on the Affymetrix chip (online Table S7). None of the chromosomes demonstrated a significant enrichment in the EMC92 signature, while all somatic chromosomes are represented. Within the set of 1093 probe sets, which formed the basis of the EMC92 signature and were identified by univariate survival analyses, chromosomes 1 and 4 were found to be significantly overrepresented. Further analysis of chromosome 1 demonstrated a clear enrichment of the long arm of chromosome 1 in this set of genes (online Table S8).

**Table 1. Multivariate analysis.** Shown are the EMC92 with a cut-off value of 0.827 in a) the HOVON-65/GMMG-HD4, b) APEX and c) MRC-IX. Covariates that were non-missing in more than 90% of the patients were included. Variants were selected into the model by a backward stepwise approach ( $p \leq 0.05$ ).

a. HOVON65/GMMG-HD4 (n=290)		
	HR [ 95%CI ]	p
EMC92 [1/0]	3.4 [2.2 – 5.4]	$5.1 \times 10^{-8}$
B2m $\geq 3.5$ mg/L	2.4 [1.5 – 3.4]	$4.1 \times 10^{-4}$
del(17p) [1/0]	2.2 [1.4 – 3.7]	$1.6 \times 10^{-3}$
WHO $\geq 1$	2.1 [1.3 – 3.3]	$2.1 \times 10^{-3}$
<b>Likelihood ratio test:</b> 95.8 on 4 df, $p < 2 \times 10^{-16}$ , $n = 257$ , number of events = 93; 33 observations deleted due to missing data.		
<b>Available covariates:</b> del(17p)[1/0], del(13p)[1/0], gain(1q)[1/0], age[yr], age[ $\geq 60$ yr], bortezomib treated[1/0], ISS=2[1/0], ISS=3[1/0], female[1/0], creatinine[mg/dL], creatinine[ $< 20$ mg/dL], B2m[mg/L], B2m $\geq 3.5$ mg/L, B2m $\geq 5.5$ mg/L, serum albumin[g/L], serum albumin $\leq 3.5$ g/L, LDH[ $>ULN$ ], IgA[1/0], IgG[1/0], light chain disease[1/0], $\kappa$ light chain[1/0], diffuse osteoporosis[1/0], hemoglobin[mmol/L], hemoglobin[ $< 6.5$ mmol/L], hemoglobin[ $< 5.3$ mmol/L], calcium[mmol/L], calcium[ $> 2.65$ mmol/L], WHO[ $\geq 1$ ], WHO[ $\geq 2$ ], WHO[ $\geq 3$ ], WHO[ $= 4$ ]		
b. APEX (n=264)		
	HR [ 95%CI ]	p
EMC92-gene [1/0]	2.4 [1.6 – 3.6]	$1.5 \times 10^{-5}$
serum albumin [g/L]	0.95 [0.93 – 0.98]	$1.2 \times 10^{-4}$
age [ $\geq 60$ yr]	1.7 [1.2 – 2.4]	$1.6 \times 10^{-3}$
IgG [1/0]	0.64 [0.46 – 0.90]	$1.0 \times 10^{-2}$
studyAPEX [1/0]	0.58 [0.41 – 0.82]	$1.8 \times 10^{-3}$
<b>Likelihood ratio test:</b> 64.5 on 5 df, $p = 1.43 \times 10^{-12}$ , $n = 250$ , number of events = 150; 14 observations deleted due to missing data		
<b>Available covariates:</b> age [yr], age $\geq 60$ yr, age $\geq 65$ yr, bortezomib treated [1/0], female [1/0], black [1/0], white [1/0], IgA [1/0], IgG [1/0], light chain [1/0], studyCREST [1/0], studySUMMIT [1/0], studyAPEX [1/0], studyAPEXprogressive [1/0], serum albumin [g/L], serum albumin $\leq 3.5$ g/L, priorlines		
c. MRC-IX (n=247)		
	HR [95%CI]	p
EMC92-gene [1/0]	2.5 [1.7 – 3.6]	$3.4 \times 10^{-6}$
age [yr]	1.0 [1.0 – 1.1]	$3.0 \times 10^{-5}$
hemoglobin [mg/L]	0.86 [0.79 – 0.95]	$1.8 \times 10^{-3}$
MP treatment [1/0]	1.6 [1.1 – 2.4]	$1.8 \times 10^{-2}$
<b>Likelihood ratio test:</b> 74.8 on 4 df, $p = 2.1 \times 10^{-15}$ , $n = 246$ , number of events = 145; 1 observation deleted due to missing data.		
<b>Available covariates:</b> del(13q)[1/0], IgH split[1/0], hyperdiploid[1/0], t(4;14)[1/0], t(11;14)[1/0], t(14;16)[1/0], t(14;12)[1/0], t(6;14)[1/0], del(17p)[1/0], gain(1q) [1/0], female[1/0], bone disease[1/0], albumin[g/L], albumin $\leq 3.5$ g/L, hemoglobin[mg/L], hemoglobin[ $< 8.5$ mg/L], hemoglobin[ $< 10.5$ mg/L], calcium[mmol/L], calcium[ $> 2.65$ mmol/L], creatinine[mg/dL], creatinine[ $< 20$ mg/dL], WHO[ $\geq 1$ ], WHO[ $\geq 2$ ], WHO[ $\geq 3$ ], WHO[ $= 4$ ], age[yr], age $\geq 60$ yr, age $\geq 65$ yr, intensive treatment[1/0], CVAD treatment[1/0], CTD treatment[1/0], MP treatment[1/0], CTDA treatment[1/0]		

## Comparison to published gene signatures

We set out to evaluate the performance of the EMC92 signature in relation to available GEP based prognostic signatures for OS in multiple myeloma. To this end, the following signatures were evaluated: UAMS70, UAMS17, UAMS80, IFM15, gene proliferation index (GPI50), MRCIX6 and, MILLENNIUM100.<sup>9-14</sup>

These signatures were evaluated as continuous variables as well as using the cut-off values as published (Figures 2a-e, online Figure S2 and supplemental documents A and B). Overall, the performance of the EMC92 signature is robust, consistent and compares favorably to previously published signatures. Specifically, the EMC92, UAMS, IFM15, MRC-IX and GPI50 signatures demonstrated significance in all validation sets tested both for the dichotomized and the continuous values of the signatures. The MILLENNIUM100 signature had significant performance in the dichotomized model in one out of four independent studies. Thus, performance was less robust for the MILLENNIUM100 signature. Although the proliferation index GPI50 was found to be significant in all validation sets tested, the proportion of high-risk patients was much lower compared to the proportion found using either the EMC92 or the UAMS80 signatures. Ranked, weighted high-risk proportions are GPI: 10.0%, UAMS17: 12.4%, UAMS70: 13.0%, MRCIX6: 13.3%, EMC92: 19.1% and UAMS80: 23.4%. To determine which signature best explained the observed survival, pair-wise comparisons were performed. For every comparison the EMC92 is the strongest predictor for OS tested in an independent environment (Figure 3 and online Table S9).

There is a varying degree of overlapping probe sets between all signatures. Overlapping genes are shown in online Figure S3. Seven out of fifty probe sets present in the GPI50 overlap with the EMC92 signature (*BIRC5*, *FANCI*, *ESPL1*, *MCM6*, *NCAPG*, *SPAG5* and *ZWINT*). One of the six MRC-IX genes (*ITM2B*) is also seen in the EMC92. Overlap between EMC92 and the remaining signatures is limited (EMC92 vs. UAMS17/70: *BIRC5* and *LTBP1*; EMC92 vs. MILLENNIUM100: *MAGEA6* and *TMEM97* and EMC92 vs. IFM15: *FAM49A*).

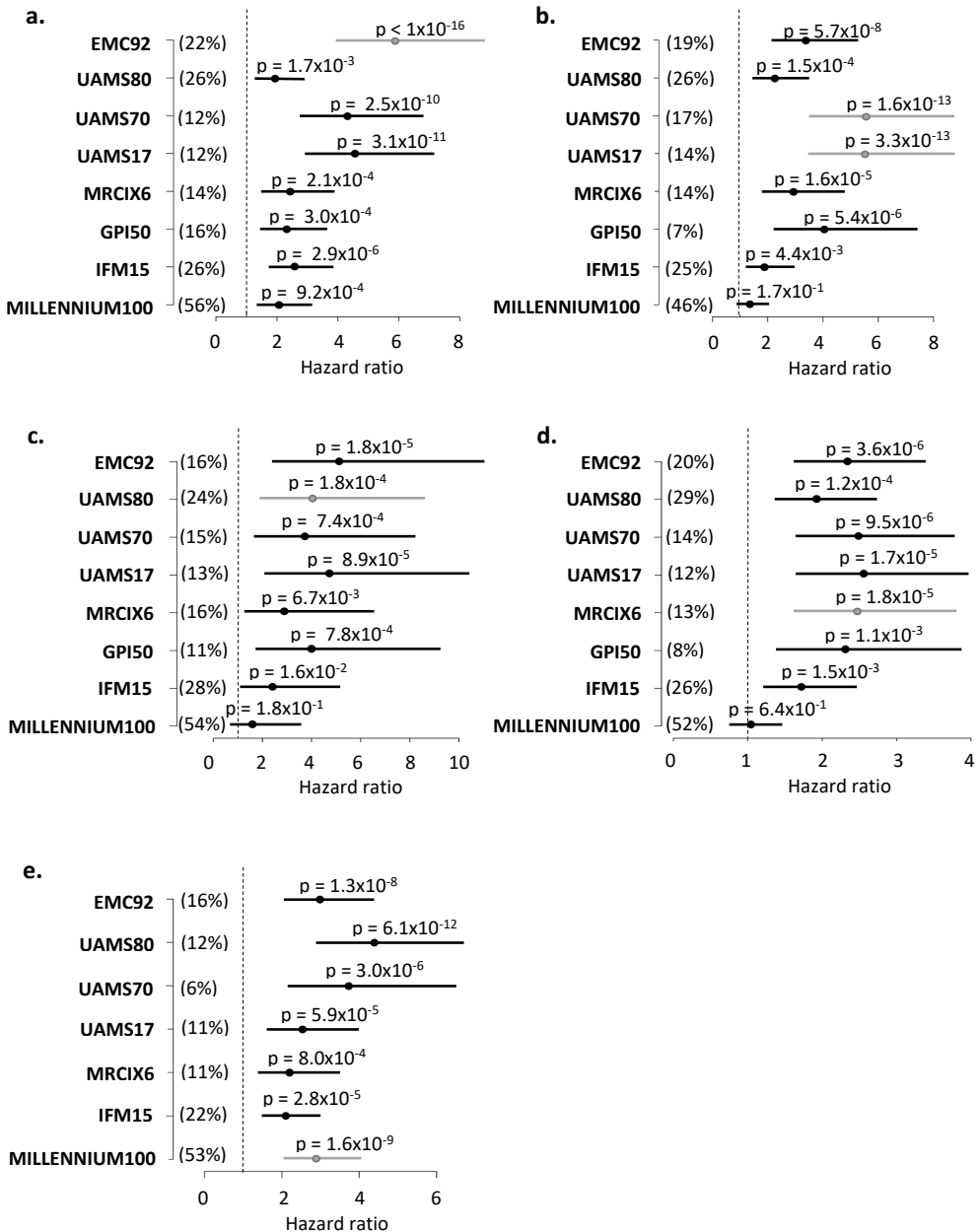


**Figure 2. Performance per signature in available datasets.** For every signature the hazard ratio (high-risk versus standard-risk) is shown with 95% confidence interval. Grey lines indicate results on training set. **a)** HOVON-65/GMMG-HD4, **b)** UAMS-TT2, **c)** UAMS-TT3, **d)** MRC-IX, **e)** APEX.  $p$ :  $p$ -value for equal survival in high and standard-risk groups; percentage: proportion of high-risk defined patients.

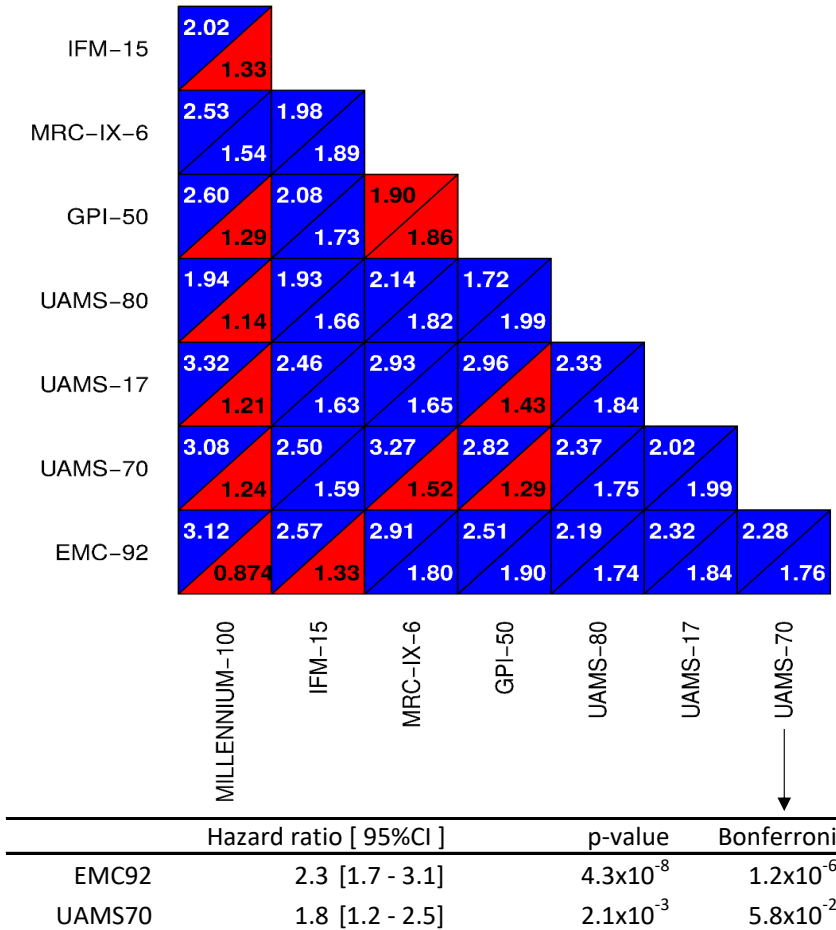


**Figure 3. Pair-wise comparison for all signatures.** To find the signature best fitting the underlying datasets, Cox regression models (high-risk versus standard-risk) were made for all pair-wise signatures. These models are based on pooled independent datasets (i.e. excluding training sets) and stratified for study. The two paired hazard ratios associated with the signatures derived per model are shown in the two cells within the square panels. Only hazard ratios within one panel can be compared because these are based on the same dataset. Blue cells indicate significant hazard ratios (Bonferroni-Holm corrected p-value); red cells denote non-significant findings. For the bottom right panel (i.e. UAMS70 vs. EMC92 signatures) the underlying model is given. All other models can be found in online Table S9.

## Combined risk classifiers

The performance of the EMC92 signature was in line with the UAMS signatures, although they were derived from quite different patient populations. The inter-

section of high-risk patients between the EMC92 and UAMS70 signatures was approximately 8% of the total population on the pooled datasets that were independent of both our training set and the UAMS70 training set (i.e. MRC-IX, TT3 and APEX; online Table S11). Approximately 13% of patients were classified as high-risk by either one of these signatures. The intersecting high-risk group had the highest hazard-ratio as compared to the intersecting standard-risk group (HR=3.9, 95%CI [2.8 – 5.4],  $p= 3.6 \times 10^{-15}$ ). Patients classified as high-risk by either signature, showed an intermediate risk, i.e. with an HR of 2.4, 95%CI [1.8 – 3.3], for the EMC92 signature ( $p= 5.1 \times 10^{-8}$ ) and an HR of 2.2, 95%CI [1.2 – 4.1], for the UAMS70 signature ( $p= 1.1 \times 10^{-2}$ ; online Table S12). To test whether there is evidence for better performance if outcomes of two dichotomous predictors are merged, we took the models made in the pair-wise comparison (online Table S9) and tested these in a likelihood-ratio test against a single signature outcome model. Merging the EMC92 with UAMS80 ( $p= 2.2 \times 10^{-3}$ ), UAMS17 ( $p= 9.4 \times 10^{-3}$ ), GPI50 ( $p= 3.0 \times 10^{-2}$ ), MRCIX6 ( $p= 1.6 \times 10^{-2}$ ) and UAMS70 ( $p= 4.0 \times 10^{-2}$ ) demonstrated a better fit to the data than any of the single models (online Table S10).

## EMC92 signature and FISH

To compare the high-risk populations composition as defined by the EMC92 and the UAMS70 signatures, cytogenetic aberration frequencies in both populations were determined using an independent set for which cytogenetic variables were known, i.e. MRC-IX (Figure 4 and online Table S13). As expected, poor prognostic cytogenetic aberrations gain(1q), del(17p), t(4;14), t(14;16), t(14;20) and del(13q) were enriched in the high-risk populations (Figure 5), whereas the standard-risk cytogenetic aberrations such as t(11;14) were diminished in the high-risk populations. In contrast, only 15% (6 out of 39) of MRC-IX cases with high-risk status as determined by the EMC92 signature showed absence of any poor prognostic cytogenetic aberrations, as opposed to 44% (74 out of 168) in standard-risk cases ( $p= 1.8 \times 10^{-3}$ ). Similarly, of the UAMS70 defined high-risk patients 4% (1 out of 23) did not have any poor prognostic cytogenetics, whereas of the UAMS70 defined standard-risk patients this proportion was 43% (79 out of 183) ( $p= 5.3 \times 10^{-3}$ ).



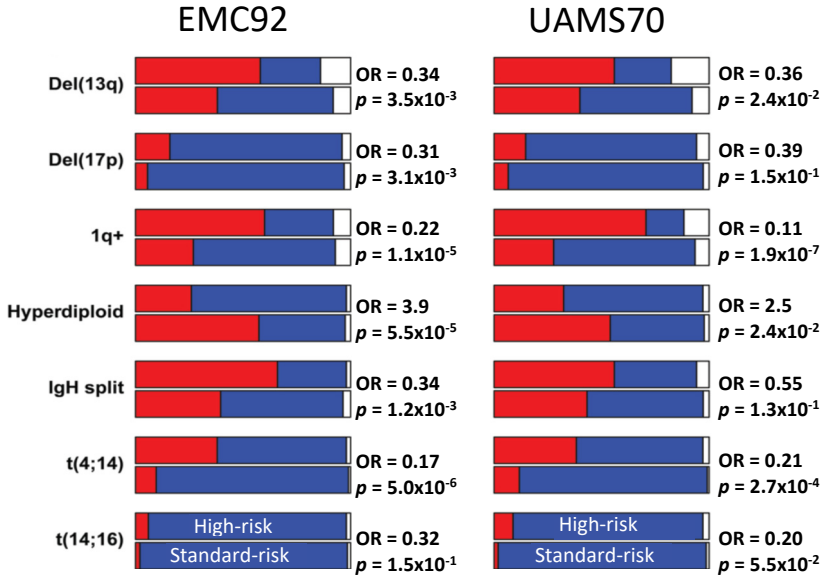


**Figure 4. Distributions of high-risk and standard-risk patients per FISH marker in the MRC-IX dataset.** Distribution of FISH markers within the high-risk (top panels) and standard-risk (bottom panels) groups for the EMC92 and UAMS70 signatures. The EMC92 and UAMS70 identified 50 and 42 patients out of 247 as high-risk, respectively. OR, Odds ratio; *p*, Fisher exact *p*-value; red, presence of an aberration; blue, absence of an aberration; white, missing data. Details are given in online Table S13.

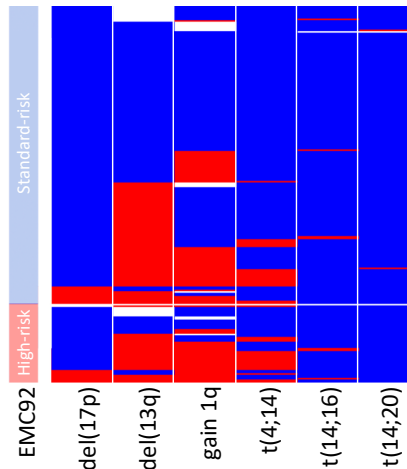


**Figure 5. Poor prognostic cytogenetic aberrations in comparison to the EMC92 signature in MRC-IX patients.** Each horizontal line represents one patient. The first column denotes the distinction between high-risk (in red,  $n = 50$ ) and standard-risk (in blue,  $n = 197$ ). Columns 2 to 7 represent cytogenetic aberrations as shown. Red, presence of an aberration; blue, absence and white, missing data. More than half of the EMC92 standard-risk patients are affected by one or more poor FISH markers.

---

## DISCUSSION

Here we report on the generation and validation of the EMC92 signature, which was based on the HOVON65/GMMG-HD4 clinical trial. Conventional prognostic markers such as ISS stage and adverse cytogenetics have been augmented by signatures based on gene expression in order to increase accuracy in outcome prediction in MM. More accurate prognosis may lead to the development of treatment schedules which are specifically aimed at improving survival of high-risk MM patients. Prognostic signatures for MM include the UAMS70, the UAMS17, the UAMS80, the IFM15, the gene proliferation index (GPI50), the MRCIX6 and the MILLENNIUM100 signatures.

For clinical relevance, a signature must have both the ability to separate risk groups as clearly as possible and to predict stable groups of relevant size. The EMC92 signature meets both criteria. In all validation sets a high-risk group of patients can be significantly determined and the proportion of high-risk patients is stable across the validation sets. The validation sets represent different drug regimens, including thalidomide (MRC-IX, TT2) and bortezomib (APEX, TT3). Also the signature is relevant to both transplant eligible (e.g. TT3) and non-transplant eligible patients (subset of MRC-IX) as well as newly diagnosed (e.g. TT2) and relapsed patients (APEX).

In contrast, the predictions of the MRCIX6, GPI50, IFM15 and MILLENNIUM-100 were not as convincing as those of the EMC92 and UAMS signatures. Especially the predictions of the MILLENNIUM100 signature in the validation sets fail to reach significance in independent data sets such as MRC-IX, TT2 and TT3. The differences in gene expression platform may have contributed to this in part. Indeed, the IFM signature is based on a custom cDNA-based gene expression platform, rather than the Affymetrix GeneChips, which have become common for MM GEP studies.<sup>32</sup> The cDNA platforms have been reported to be difficult to compare with the Affymetrix oligonucleotide platform.<sup>12</sup> Although the MILLENNIUM100 signature was generated using Affymetrix GeneChips, the use of an earlier version of this platform may have contributed to the limited performance of this signature.<sup>11</sup> The performance of the EMC92 signature is comparable to the UAMS derived signatures, MRCIX6 and the GPI50, as measured by the significance of

prediction in validation sets. For the UAMS70 and GPI50 the proportion high-risk patients appears more variable, which may hinder clinical interpretation, especially when the high-risk proportion is less than 10%. Importantly, pair-wise comparisons of all the signatures evaluated in this paper demonstrated that the EMC92 has the best fit to the observed survival times in independent sets. Strikingly, we found that performance can be improved by simply combining signatures (e.g. EMC92 with UAMS80). However, this analysis is only an indication of the possibilities of combining signatures, and future work involving more complex combined signatures is in progress.

It is important to note that the genes within the signature reflect optimal performance of the signature rather than a biological definition of survival in MM. The initially selected 1093 probe sets which were found to be associated with PFS in univariate testing, are more likely to give a good representation of myeloma biology, as indicated for instance by the protein synthesis related pathways. Although an extended biological discussion is outside the scope of this paper, a number of interesting genes are included in the signature. *BIRC5* was found in 4 signatures evaluated in this paper: EMC92, UAMS17, UAMS70 and the GPI50. This gene is a member of the inhibitor of apoptosis gene family, which encodes negative regulatory proteins that prevent apoptotic cell death, and up-regulation has been described to be associated with lower EFS and OS in newly diagnosed MM patients.<sup>11,12,31</sup> Other important myeloma genes include *FGFR3* and *STAT1*. *FGFR3* is deregulated as a result of translocation t(4;14), which is an adverse prognostic cytogenetic event.<sup>30</sup> *FGFR3* - a transmembrane receptor tyrosine kinase - is involved in the regulation of cell growth and proliferation.<sup>30</sup> *STAT1* - an important component of the JAK/STAT signaling - is involved in multiple pathways including apoptosis induced by interferon signaling.<sup>29</sup>

A clear enrichment of the long arm of chromosome 1 was observed in the 1093 probe sets in this study. Previously the importance of chromosome 1 was reported for the UAMS70 signature. Genes on 1q in the UAMS70 signature include *CKS1B* and *PSMD4*, both of which were not in the EMC92 signature, although *CKS1B* was found to be associated with PFS in our set and thus in the 1093 set.<sup>9,10</sup> The EMC92 signature did contain 9 genes on 1q of which *S100A6* has been described in relation to 1q21 amplification in MM and other cancer

---

types.<sup>34</sup> This may also be part of the explanation why, despite the use of the same GEP platform, the overlap between different signatures is limited. Indeed, multiple genes are found within the 1q21 amplicon with downstream factors possibly over-expressed as a result of this. Which gene will be linked most significantly to survival in a specific set is most likely due to factors such as variability in datasets, to which population differences and differences in used techniques may contribute. Other reasons may be found in the difference in treatment strategies used, in which other genes could be responsible for adverse prognosis.

To characterize the high-risk group in depth, we have demonstrated that in the MRC-IX study, high-risk patients are enriched for poor cytogenetic aberrations gain(1q), del(17p), t(4;14), t(14;16), t(14;20) and del(13q). Still more than half of the patients in the standard-risk group showed one or more poor prognostic cytogenetic markers indicating that the occurrence of a single poor-risk marker does not have very strong prognostic value.

Clinical use of a gene signature (UAMS70) has recently been incorporated in the mSMART risk stratification, which additionally includes FISH, metaphase cytogenetics, and plasma cell labeling index. The mSMART risk stratification is the first risk stratification system adjusting treatment regimens according to risk status, although this has not been validated in prospective clinical trials.<sup>15,35</sup> Ultimately, clinical use of any signature must be proven to be of use in prospective clinical trials, which allow treatment choice based on risk assessment. This will result in clinical guidelines to improve treatment of patients with a poor PFS and OS on novel therapies. For practical application of the EMC92 signature it is essential to stress that this signature has not been designed for classification of a single patient. However, collection of a set of more than ~25 patients will result in reliable prediction, and each additional patient can be predicted as soon as it is tested.

In conclusion, we developed a risk signature highly discriminative for patients with high-risk versus standard-risk MM, irrespective of treatment regime, age and relapse setting. Use of this signature in the clinical setting may lead to a more informed treatment choice and potentially better outcome for the patient.

## REFERENCES

1. Avet-Loiseau H. Ultra high-risk myeloma. *Am. Soc. Hematol. Educ. Program.* . 2010; :489–493.
2. Palumbo A & Anderson K. Multiple myeloma. *N. Engl. J. Med.* . 2011; **17**(364):1046–1060.
3. Munshi NC, Anderson KC, Bergsagel PL, *et al.* Consensus recommendations for risk stratification in multiple myeloma: report of the International Myeloma Workshop Consensus Panel 2. *Blood* . 2011; **117**(18):4696–700.
4. Neben K, Jauch A, Bertsch U, *et al.* Combining information regarding chromosomal aberrations t(4;14) and del(17p13) with the International Staging System classification allows stratification of myeloma patients undergoing autologous stem cell transplantation. *Haematologica* . 2010; **95**(7):1150–7.
5. Bergsagel PL, Kuehl WM, Zhan F, Sawyer J, Barlogie B, & Shaughnessy J J. Cyclin D dysregulation: an early and unifying pathogenic event in multiple myeloma. *Blood* . 2005; **106**(1):296–303.
6. Zhan F, Huang Y, Colla S, *et al.* The molecular classification of multiple myeloma. *Blood* . 2006; **108**(6):2020–2028.
7. Broyl A, Hose D, Lokhorst H, *et al.* Gene expression profiling for molecular classification of multiple myeloma in newly diagnosed patients. *Blood* . 2010; **116**(14):2543–53.
8. Chng WJ, Kuehl WM, Bergsagel PL, & Fonseca R. Translocation t(4;14) retains prognostic significance even in the setting of high-risk molecular signature. *Leukemia* . 2008; **22**(2):459–61.
9. Shaughnessy J J D, Zhan F, Burington BE, *et al.* A validated gene expression model of high-risk multiple myeloma is defined by deregulated expression of genes mapping to chromosome 1. *Blood* . 2007; **109**(6):2276–2284.
10. Shaughnessy J J D, Qu P, Usmani S, *et al.* Pharmacogenomics of bortezomib test-dosing identifies hyperexpression of proteasome genes, especially PSMD4, as novel high-risk feature in myeloma treated with total therapy 3. *Blood* . 2011; **118**:3512–3524.
11. Mulligan G, Mitsiades C, Bryant B, *et al.* Gene expression profiling and correlation with outcome in clinical trials of the proteasome inhibitor bortezomib. *Blood* . 2007; **109**(8):3177–3188.
12. Decaux O, Lode L, Magrangeas F, *et al.* Prediction of survival in multiple myeloma based on gene expression profiles reveals cell cycle and chromosomal instability signatures in high-risk patients and hyperdiploid signatures in low-risk patients: a study of the Intergroupe Franco-phone du Myelome. *J Clin Oncol* . 2008; **26**(29):4798–4805.
13. Dickens NJ, Walker BA, Leone PE, *et al.* Homozygous deletion mapping in myeloma samples identifies genes and an expression signature relevant to pathogenesis and outcome. *Clin Cancer Res* . 2010; **16**(6):1856–1864.
14. Hose D, Reme T, Hielscher T, *et al.* Proliferation is a central independent prognostic factor and target for personalized and risk-adapted treatment in multiple myeloma. *Haematologica* . 2011; **96**(1):87–95.
15. Dispenzieri A, Rajkumar SV, Gertz MA, *et al.* Treatment of newly diagnosed multiple myeloma

- based on Mayo Stratification of Myeloma and Risk-adapted Therapy (mSMART): consensus statement. *Mayo Clin Proc* . 2007; **82**(3):323–41.
16. Sonneveld P, Schmidt-Wolf I, van der Holt B, *et al*. HOVON-65/GMMG-HD4 Randomized Phase III Trial Comparing Bortezomib, Doxorubicin, Dexamethasone (PAD) Vs VAD Followed by High-Dose Melphalan (HDM) and Maintenance with Bortezomib or Thalidomide In Patients with Newly Diagnosed Multiple Myeloma (MM). *Blood* . 2010; **116**(21):40–40.
  17. Pineda-Roman M, Zangari M, Haessler J, *et al*. Sustained complete remissions in multiple myeloma linked to bortezomib in total therapy 3: comparison with total therapy 2. *Br J Haematol* . 2008; **140**(6):625–634.
  18. Barlogie B, Pineda-Roman M, van Rhee F, *et al*. Thalidomide arm of Total Therapy 2 improves complete remission duration and survival in myeloma patients with metaphase cytogenetic abnormalities. *Blood* . 2008; **112**(8):3115–3121.
  19. Morgan GJ, Davies FE, Gregory WM, *et al*. Thalidomide Maintenance Significantly Improves Progression-Free Survival (PFS) and Overall Survival (OS) of Myeloma Patients When Effective Relapse Treatments Are Used: MRC Myeloma IX Results. *Blood* . 2010; **116**(21):623–623.
  20. Morgan GJ, Davies FE, Owen RG, *et al*. Thalidomide Combinations Improve Response Rates; Results from the MRC IX Study. *Blood* . 2007; **110**(11):3593–3593.
  21. Jagannath S, Barlogie B, Berenson J, *et al*. A phase 2 study of two doses of bortezomib in relapsed or refractory myeloma. *Br Journal Haematol* . 2004; **127**(2):165–172.
  22. Richardson PG, Sonneveld P, Schuster MW, *et al*. Bortezomib or high-dose dexamethasone for relapsed multiple myeloma. *N Engl J Med* . 2005; **352**(24):2487–2498.
  23. Richardson PG, Barlogie B, Berenson J, *et al*. A phase 2 study of bortezomib in relapsed, refractory myeloma. *N Engl J Med* . 2003; **348**(26):2609–2617.
  24. Gentleman RC, Carey VJ, Bates DM, *et al*. Bioconductor: open software development for computational biology and bioinformatics. *Genome Biol* . 2004; **5**(10):R80.
  25. Johnson WE, Li C, & Rabinovic A. Adjusting batch effects in microarray expression data using empirical Bayes methods. *Biostatistics* . 2007; **8**(1):118–27.
  26. Therneau & Lumley T. survival: Survival analysis, including penalised likelihood. *R package version 2.36-2* . 2010; .
  27. Bair E, Hastie T, Paul D, & Tibshirani R. Prediction by Supervised Principal Components. *J Amer Statistical Assoc* . 2006; **101**(473):119–137.
  28. Benjamini Y & Hochberg Y. Controlling the False Discovery Rate: A Practical and Powerful Approach to Multiple Testing. *J Roy Stat Soc B Met* . 1995; **57**(1):289–300.
  29. Arulampalam V, Kolosenko I, Hjortsberg L, Bjorklund AC, Grandner D, & Tamm KP. Activation of STAT1 is required for interferon-alpha-mediated cell death. *Exp Cell Res* . 2011; **317**(1):9–19.
  30. Chesi M, Nardini E, Brents LA, *et al*. Frequent translocation t(4;14)(p16.3;q32.3) in multiple myeloma is associated with increased expression and activating mutations of fibroblast growth factor receptor 3. *Nat Genet* . 1997; **16**(3):260–4.
  31. Hideshima T, Catley L, Raje N, *et al*. Inhibition of Akt induces significant downregulation of survivin and cytotoxicity in human multiple myeloma cells. *Br J Haematol* . 2007; **138**(6):783–91.

32. Mah N, Thelin A, Lu T, *et al.* A comparison of oligonucleotide and cDNA-based microarray systems. *Physiol Genomics* . 2004; **16**(3):361–70.
33. Trudel S, Ely S, Farooqi Y, *et al.* Inhibition of fibroblast growth factor receptor 3 induces differentiation and apoptosis in t(4;14) myeloma. *Blood* . 2004; **103**(9):3521–8.
34. Inoue J, Otsuki T, Hirasawa A, *et al.* Overexpression of PDZK1 within the 1q12-q22 amplicon is likely to be associated with drug-resistance phenotype in multiple myeloma. *Am J Pathol* . 2004; **165**(1):71–81.
35. Kumar SK, Mikhael JR, Buadi FK, *et al.* Management of newly diagnosed symptomatic multiple myeloma: updated Mayo Stratification of Myeloma and Risk-Adapted Therapy (mSMART) consensus guidelines. *Mayo Clin Proc* . 2009; **84**(12):1095–110.





# CHAPTER

# 3

## Prediction of High- and Low-Risk Multiple Myeloma Based on Gene Expression and the International Staging System

Rowan Kuiper, Mark van Duin, Martin H. van Vliet, Annemiek Broijl, Bronno van der Holt, Laila el Jarari, Erik van Beers, George Mulligan, Hervé Avet-Loiseau, Walter M. Gregory, Gareth Morgan, Hartmut Goldschmidt, Henk M. Lokhorst & Pieter Sonneveld

---

## ABSTRACT

Patients with multiple myeloma have variable survival, and require reliable prognostic and predictive scoring systems. Currently, clinical and biological risk markers are used independently. Here, ISS, FISH markers and gene expression (GEP) classifiers were combined to identify novel risk classifications in a discovery/validation setting.

We used the datasets of HOVON-65/GMMG-HD4, UAMS-TT2, UAMS-TT3, MRC-IX, APEX and Intergroupe Francophone du Myelome (IFM-G) (total number of patients: 4750). A total of 20 risk markers were evaluated including t(4;14) and deletion of 17p (FISH), EMC92 and UAMS70 (GEP classifiers) and ISS.

The novel risk classifications demonstrated that ISS is a valuable partner to GEP classifiers and FISH. Ranking all novel as well as existing risk classifications showed that the EMC92-ISS combination is the strongest predictor for overall survival, resulting in a four group risk classification. The median survival was 24 months for the highest risk group, 47 and 61 months for the intermediate risk groups and median not reached after 96 months for the lowest risk group.

The EMC92-ISS classification is a novel prognostic tool, based on biological and clinical parameters, which is superior to current markers and offers a robust clinically relevant 4-group model.

## INTRODUCTION

In multiple myeloma (MM) patients, malignant plasma cells accumulate in the bone marrow, leading to a wide range of clinical symptoms which include bone disease, hypercalcemia, renal impairment and anemia.<sup>1</sup> The prognosis is variable, with survival for newly diagnosed patients ranging from less than two to more than twenty years.<sup>2</sup> Adequate prognostication of disease outcome is important in order to make treatment choices and to allocate high-risk patients to alternative treatment options. Clinical trials that address specific treatment of high-risk patients include TT4, TT5 and MUK9 (TT4: Total Therapy 4, NCT00734877; TT5: Total Therapy 5, NCT02128230; MUK9, OPTIMUM trial, Myeloma UK Clinical Trial Network).

Heterogeneous treatment outcome can in part be explained by different biological subgroups in MM, which are characterized by primary translocations involving genes such as MMSET (t(4;14)), and c-MAF (t(14;16)).<sup>3,4</sup> These subgroups can be identified using gene expression profiling.<sup>5,6</sup> In addition, gene expression profiling has been utilized to establish classifiers for prognostication. The EMC92 is a robust risk marker for the identification of high-risk MM, and was validated in independent clinical trials showing a solid and independent performance in comparison to other MM GEP classifiers such as UAMS70.<sup>7-13</sup> Clinical prognostic systems for MM, are primarily based on beta2-microglobulin (B2m), albumin, lactate dehydrogenase, C-reactive protein, calcium and creatinine.<sup>14,15</sup> The International Staging System (ISS) is based on B2m and albumin, with stage I representing limited disease, stage II intermediate and stage III the most unfavorable disease.<sup>16</sup> Today it is used as the standard clinical risk classification for MM.

FISH based cytogenetics and gene expression profiling are biology based prognostic markers.<sup>17</sup> ISS was combined with high-risk cytogenetic markers t(4;14) and deletion of 17p (del(17p)) to establish novel prognostic risk classifications as proposed by Neben and Avet-Loiseau.<sup>18,19</sup> Recently, serum lactate dehydrogenase (LDH) was added as a component to this marker combination.<sup>20</sup> Other prognostic systems include combinations of cytogenetic markers, such as the combination of del(17p), translocation t(4;14) and gain of 1q (gain(1q)).<sup>21</sup>

---

The goal of this study was to evaluate all published risk markers used in MM and to compare combinations of FISH, ISS and GEP based prognostic systems. By applying a study design with independent discovery and validation sets, we demonstrated that ISS can be combined with gene expression signatures into powerful classifiers for MM.

## MATERIALS AND METHODS

### Clinical data

The clinical data from the the Dutch-Belgium Hemato-Oncology Group (HOVON) and German-speaking Myeloma Multicenter Group (GMMG) (HO65/HD4), Medical Research Council-IX (MRC-IX), University of Arkansas for Medical Sciences Total Therapy (UAMS-TT2 and TT3), Intergroupe Francophone du Myelome (IFM-G; all newly diagnosed patients) and APEX (relapse patients) trials were used.<sup>7-9,19,22,23</sup> The IFM-G cohort is a clinical database of patients not separately published and was included in the ISS development.<sup>16</sup> Treatment regimens of the trials from which these datasets were derived are summarized in Table 1. Overall survival (OS) or progression-free survival (PFS) and at least one prognostic marker were available for all patients (Table 1; Figure S1). All patients signed an informed consent in accordance with the Declaration of Helsinki and all protocols were approved by institutional review boards.

### Gene expression profiling (GEP)

All GEP data are Affymetrix HG U133 Plus 2.0 platform based, except for the APEX study (Affymetrix U133 A/B platform). HO65/HD4 GEP was performed in our lab as described previously ( $n = 327$ ; GEO series GSE19784).<sup>6,7,21</sup> Other GEP sets were: TT2 ( $n = 345$ ; GSE24080)<sup>8</sup>, TT3 ( $n = 238$ ; E-TABM-1138 and GSE24080)<sup>24</sup>, MRC-IX ( $n = 247$ ; GSE15695)<sup>22</sup> and APEX ( $n = 264$ ; GSE9782).<sup>23</sup> Due to unavailable survival data, the Heidelberg-Montpellier (HM) dataset ( $n = 206$ ; E-MTAB-362), was used only to determine the probe set means and variances for the training set of the HM19 classifier.<sup>12</sup>

### Standard prognostic markers

Availability of risk markers and patients per dataset is shown in Table 1 and Figure S1. The International staging system (ISS) was determined by combining serum levels of  $\beta$ 2M and albumin.<sup>16</sup> Cytogenetics by Fluorescence in situ hybridization (FISH) was used with a 10% cut-off level except for a 20% cut-off used for numerical abnormalities in the MRC-IX trial.<sup>19,25-27</sup> Gain of chromo-

**Table 1. Distribution of risk markers and treatments per dataset.** The numbers of patients per data set are given with in brackets the number or percentage of positive patients according to the markers' risk classification.

	HO65/HD4	MRC-IX	
		Intensive	Non-intensive
N	827	701	491
median age [IQR][yrs]	57 (51 - 61)	58 (54 - 63)	74 (70-77)
Treatment [n]	PAD (413)	CTD(351)	CTDa(257)
Control	VAD(414)	CVAD(350)	MP(234)
High-dose alkylator	YES	YES	NO
EMC92 [n (% high)]	*	138 (17%)	109 (24%)
UAMS17	327 (12%)	138 (9%)	109 (16%)
UAMS70	327 (9%)	138 (7%)	109 (10%)
UAMS80	327 (8%)	138 (8%)	109 (9%)
MRCIX6	327 (5%)	*	*
IFM15	327 (25%)	138 (25%)	109 (28%)
HM19 (low/medium/high%)	327 (34/51/15%)	138 (45/48/7%)	109 (39/53/8)
GPI50	327 (34/51/15%)	138 (52/41/7%)	109 (52/38/10)
ISS [n (1/2/3%)]	756 (38/37/25)	636 (25/39/36)	449 (13/41/45)
t(4;14) [n (% positive)]	429 (12%)	619 (12%)	434 (10%)
t(11;14)	437 (16%)	617 (15%)	434 (12%)
t(14;16)	360 (2%)	612 (3%)	434 (3%)
t(14;20)	255 (0%)	612 (2%)	429 (1%)
IgH split	327 (48%)	609 (44%)	429 (40%)
gain 1q	344 (32%)	531 (37%)	371 (41%)
del(13q)	686 (41%)	612 (46%)	428 (43%)
del(17p)	351 (11%)	591 (8%)	423 (9%)
gain 9	454 (57%)	480 (60%)	351 (66%)
HR.FISH.A [n(%)]	354 (46%)	535 (48%)	368 (48%)
HR.FISH.B/ISS [n(1/2/3%)]	334 (60/22/18)	*	

\*, training set for these markers. Only the proportion and number that are not used for building the marker, if any, are shown.

\*\*, intersection of patients with available data between datasets is shown in Figure S1.

\*\*\*, the HR.FISH.A compound risk classification is based on a patient having either del(17p), t(4;14) or gain of 1q. If only gain of 1q is known (in TT2 patients), these are the only patients classified with certainty as high-risk. The remaining patients cannot be classified, since the status of t(4;14) and del(17p) are unknown. If the missing bias is strong enough (see methods), that marker is excluded from the combination analyses.

TT2	TT3	APEX	IFM-G	POOLED
351	238	264	1878	4750**
57 (49-64)	60 (53-66)	61 (54-67)	57 (51-61)	57 (51-62)
TD(175)	VTD(238)	BOR(188)	VD(740)	BOR(1579)/THAL(783)
MD(176)	No controls	DEX(76)	VAD(1138)	BOR(1628)/THAL(760)
YES	YES	YES	YES	
345 (19%)	238 (15%)	264 (16%)		1094 (18%)
*	238 (14%)	264 (12%)		1076 (12%)
*	238 (12%)	264 (8%)		1076 (9%)
345 (9%)	*	264 (7%)		1183 (8%)
345 (7%)	238 (5%)	264 (3%)		1174 (5%)
345 (24%)	238 (24%)			1157 (25%)
345 (50/47/8)	238 (47/47/7)	264 (41/50/8)		1420 (44/48/8)
345 (63/31/7)	238 (58/34/8)			1159 (51/39/10)
	208 (50/28/21)	202 (34/33/33)	1475 (34/39/28)	4074 (34/37/30)
			1635 (14%)	3180 (13%)
				1488 (15%)
			456 (4%)	1862 (3%)
				1296 (1%)
				1410 (44%)
	248 (47%)		891 (37%)	2385 (38%)
			1807 (48%)	3522 (46%)
			1651 (15%)	3016 (12%)
				1285 (60%)
	116 (100%***)		1022 (64%)	2395 (57%)
			516 (55/29/17)	850 (57/26/17)

**PAD:** bortezomib, doxorubicin, dexamethasone; **VAD:** vincristine, doxorubicin, dexamethasone; **CVAD:** cyclophosphamide, vincristine, doxorubicin, dexamethasone; **MP:** melphalan, prednisone; **CTD(a):** (attenuated) cyclophosphamide, thalidomide, dexamethasone; **VTD:** bortezomib, thalidomide, dexamethasone; **(V)MD:** (bortezomib,) melphalan, dexamethasone; **VD:** vincristine, dexamethasone; **BOR:** bortezomib; **THAL:** thalidomide.

some 9 (gain(9)) - one of the hyperdiploid chromosomes and most frequently available marker for this purpose - was used as a proxy for hyperdiploidy.<sup>28</sup> FISH probes used in MRC-IX and HO65/HD4 were described before.<sup>25,29</sup> Cytogenetic data obtained by methods other than FISH were excluded. High risk FISH was defined as having either del(17p) or t(4;14) or gain(1q), denoted here as HR.FISH.A.<sup>21</sup> The risk classification described by Avet-Loiseau *et al.* is denoted here as HR.FISH.B/ISS.<sup>19</sup> This risk classification distinguishes grade-I (ISS=1 or 2 with FISH markers t(4;14) and del(17p) both negative), grade-II (not grade-I or III) and grade-III (ISS=2 or 3 with FISH markers t(4;14) or del(17p) positive). In case of an arbitrary situation due to missing data for one of the markers, the observation was excluded.

### Gene expression classifiers

The following MM gene expression classifiers were used: EMC92<sup>7</sup>, UAMS17<sup>8</sup>, UAMS70<sup>8</sup>, UAMS80<sup>9</sup>, IFM15<sup>10</sup>, MRCIX6<sup>13</sup> (all two risk group classifiers) and HM19<sup>12</sup>, GPI50<sup>11</sup> (both three risk group classifiers). Normalization and cut-offs were calculated as described previously (see online supplemental methods for a brief description).

### Statistical analyses

In Figure 1, a flowchart of the analyses is given. The association of risk markers with survival was assessed using a Cox survival model (R 'survival' package, version 2.38-1).<sup>30-32</sup> To account for heterogeneous survival between studies, models were stratified per trial cohort. The trial cohorts were HO65/HD4, MRC-IX intensive, MRC-IX non-intensive, UAMS-TT2, UAMS-TT3, IFM-G and APEX. Datasets used for generating risk markers were systematically excluded in validation analyses in order to avoid training bias. For instance, HO65/HD4 patients were excluded in analyses involving the EMC92 classifier (Table 1). The method for finding novel combination markers (compound markers) is illustrated in online Figure S2b and extensively described in the online supplemental methods. Briefly, since missing data may confound the analyses, combinations with increased risk for confounding were excluded (Table S1; online supplemental methods). Subsequently, the data were randomly split into a discovery and validation set. The



discovery set was used for finding meaningful combinations of markers as well as the most optimal way to split patients into subgroups, using these combinations. Stringent validation was performed in the designated validation set to confirm their prognostic strength. Finally, all new combinations and existing markers were ranked, with a low rank score indicating a high performing risk marker.

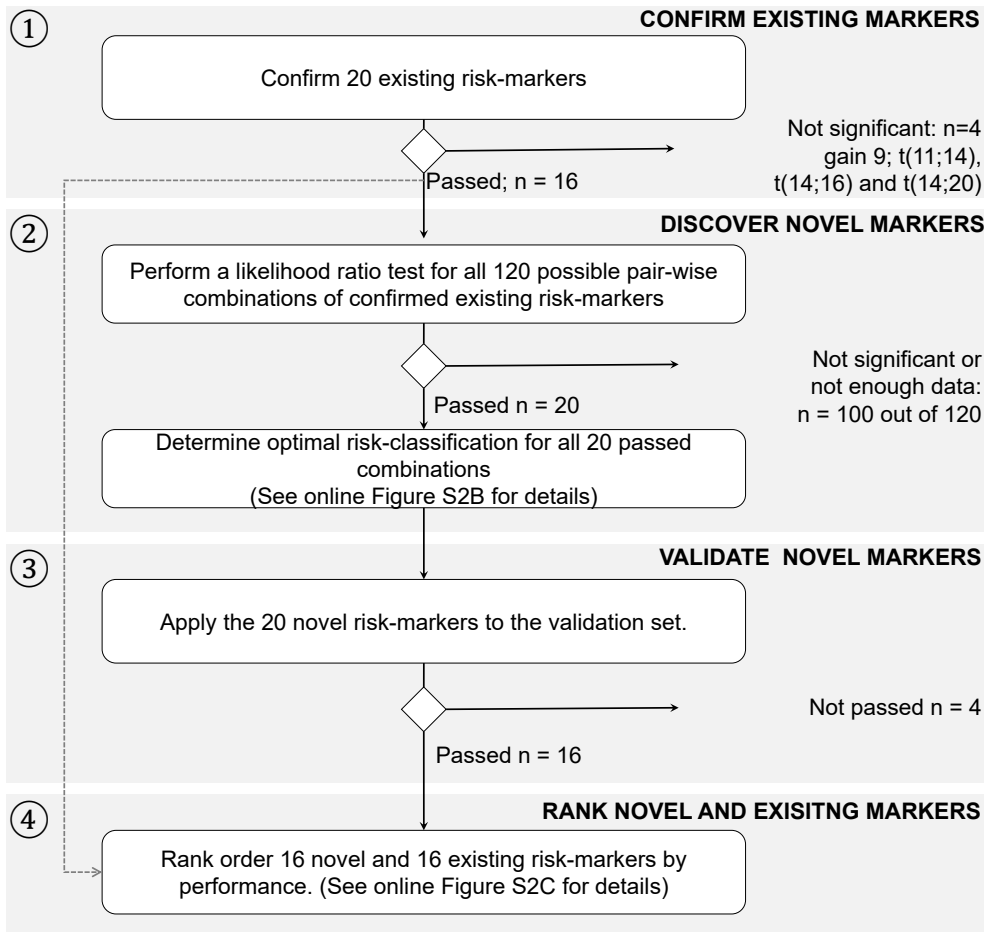


**Figure 1. Flowchart of analyses.** The analyses are organized as follows: **1)** confirmation of existing risk markers, **2)** systematically finding novel risk markers with improved prognostic strength by combining existing risk markers and **3)** validating them; **4)** ranking of confirmed existing- and validated novel risk markers. See Figure S2a-c for more details.

---

# RESULTS

## Confirmation of existing risk markers

3 The value of 20 existing risk markers was evaluated in a data set of 4750 patients. The markers and used cohorts are given in Table 1. The prognostic value was evaluated correcting for the differences in survival between cohorts (Figure 2, online Figures S3-S5 and Table S2). For all markers at least 2 cohorts were available. All gene expression (GEP) classifiers demonstrated a highly significant performance for OS. Hazard ratios for GEP classifiers ranged from 2.0 [95%CI [1.6 – 2.4]; IFM15) up to 3.3 (2.6 – 4.3] [UAMS70). Furthermore, hazard ratios for GEP classifiers were consistently higher than any of the other risk markers, including all FISH markers and ISS. This suggests better risk separation for GEP classifiers compared to FISH markers. GEP classifiers generally performed better for OS than for PFS (Figures S3A-B, S4 and S5; Table S2) with PFS hazard ratios between 1.8 [1.5 – 2.1] (IFM15) up to 2.3 [1.9 – 2.7] (EMC92). The percentage of high-risk patients varied between classifiers: 18% (EMC92), 12% (UAMS17), 10% (GPI50), 9% (UAMS70), 8% (UAMS80 and HM19; Table 1).

FISH markers with prognostic strength can be distinguished from markers with no or disputable value. For OS, markers t(4;14), del(17p), gain(1q) and del(13q) performed well with hazard ratios ranging between 1.7, 95%CI [1.5 – 1.8] for del(13q) up to 2.3 [2.0 – 2.6] for del(17p). The markers gain9, t(11;14), t(14;16) and t(14;20) were clearly not significant or had high variance due to lack of predictive value or small number of positive cases. These markers were excluded from further analyses. A similar pattern was found for PFS, but the strength of the markers was generally lower with PFS hazard ratios ranging from 1.4 [1.3 – 1.5] (del(13q)) up to 1.8 [1.6 – 2.0](t(4;14)).

ISS was confirmed as a valuable and highly significant prognostic marker. A hazard ratio of 1.6 95%CI [1.4 – 1.8] (ISS = 2) and 2.3 [2.1 – 2.6] (ISS = 3) was found for OS and 1.4 [1.3 – 1.6] (ISS = 2) and 1.7 [1.6 – 1.9] (ISS = 3) for PFS. Other previously published compound risk markers, denoted here as HR.FISH.A<sup>21</sup> (either t(4;14) or del(17p) or gain(1q)) and a combined FISH/ISS marker (HR.FISH.B-/ISS)<sup>19</sup> showed good performance. The hazard ratio was 2.3 [2.0 – 2.5] (HR.FISH.A).

For the three group HR.FISH.B/ISS risk classification, hazard ratios of 1.8 [1.4 – 2.4] (intermediate risk) and 3.6 [2.7 – 4.7] (high-risk) were found.

To correct for heterogeneity between studies, all analyses were corrected for the survival differences between trials as a result of differences in treatment, disease stage and patient populations. To evaluate the effect of this correction, all analyses were repeated per cohort and highly similar results were obtained, suggesting that these risk markers perform similarly across different cohorts (online supplemental results).

### Pair-wise combinations of risk markers

The next analysis was performed to explore combinations of risk markers. As indicated above, 16 of 20 evaluated markers had significant associations with OS and/or PFS. Based on these 16, all possible pair-wise combinations were generated. Twenty combinations were significant in the discovery set of which 16 remained significant in the independent validation set (Figure 2, online Figure S8a-b and Table S2-S3). In 10 of 16 combinations, ISS was combined with either GEP classifiers ( $n = 5$ ) or FISH markers ( $n = 5$ ), illustrating the strong additive power of ISS to these markers. Combinations of GEP ( $n = 3$ ) and FISH markers were observed ( $n = 3$ ), but no combinations of FISH with GEP. Two combinations divided patients in 3 groups, ten in 4 groups and four into 5 groups.

### Ranking of existing and novel markers

The markers described above, i.e. 16 existing plus 16 validated new risk markers, were ranked on the basis of performance, as described in the Supplemental methods. ISS-GEP combinations consistently ranked at the top with the EMC92-ISS compound risk marker having the best median rank score ( $RS$ ) (Figure 3;  $RS = 0.05$ ). Other high scoring markers included ISS-UAMS17 ( $RS = 0.11$ ), ISS-HM19 ( $RS = 0.13$ ) and ISS-UAMS70 ( $RS = 0.19$ ). The HR.FISH.B/ISS compound marker ranked in 5<sup>th</sup> place ( $RS = 0.20$ ) and ISS ranked in 23<sup>rd</sup> place (out of 32;  $RS = 0.61$ ). In general, compound markers tended to score better than single markers. The best single marker was EMC92 in 7<sup>th</sup> position ( $RS = 0.26$ ).

EMC92-ISS classifies patients into four groups with proportions of 38%, 24%, 22% and 17% for the lowest to the highest risk group, respectively (Figure 4A-B).

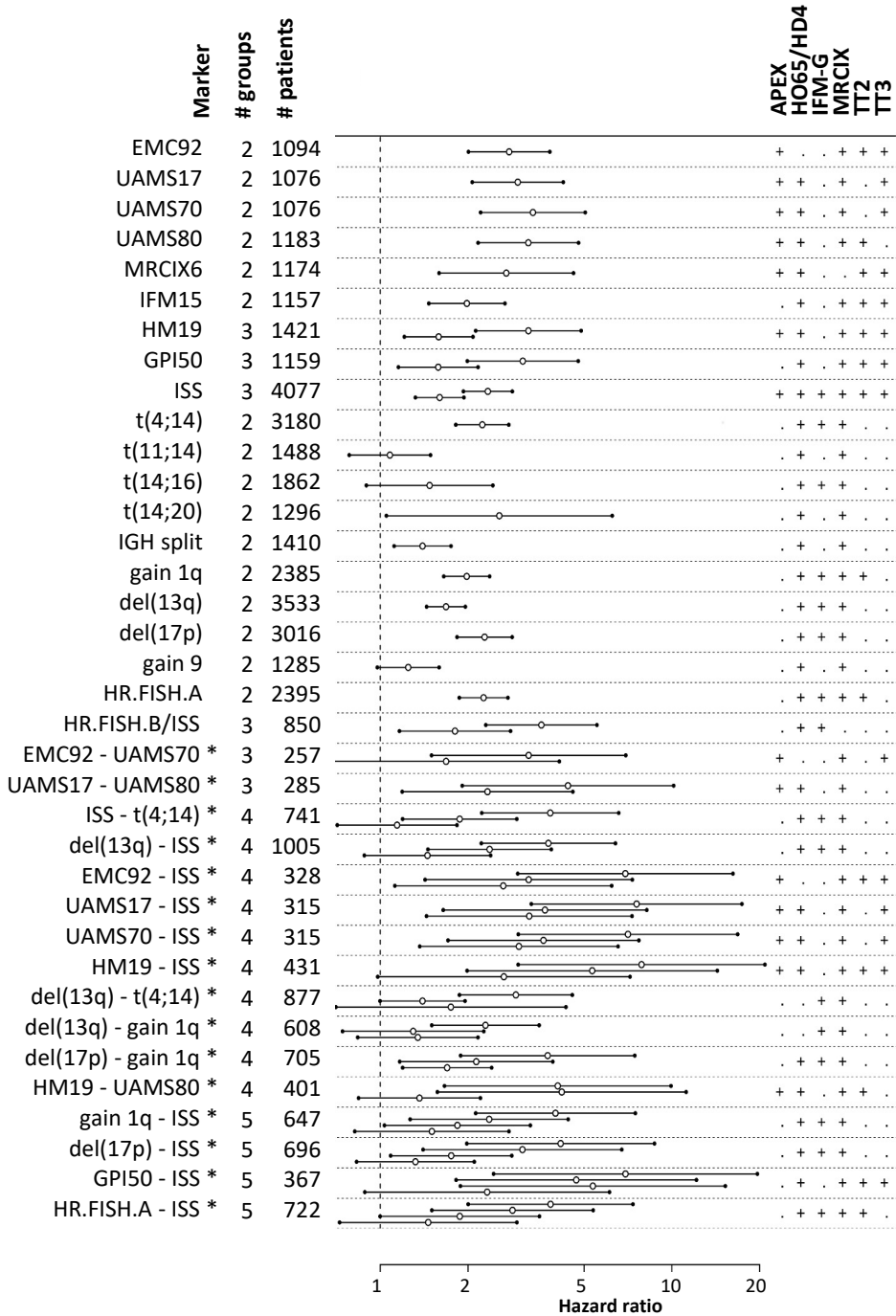


**Figure 2. Risk markers in relation to overall survival.** Both existing markers and validated novel combinations are shown. For novel combinations, the results shown represent the validation. For confirmation of existing markers no discovery/validation split is required and results shown are based on all available data. In the left panel, existing markers and novel combinations (denoted by an asterisk) are listed. For each marker, the number of risk groups (#groups) and number of available patients is given (# patients). Markers are sorted by the number of risk groups. In the center panel, the hazard ratios are shown (open circle), with Bonferroni adjusted 95% confidence intervals (indicated by two lines and closed circles). For coherent notation, hazard ratios are expressed relative to the lowest risk group. Every additional risk group results in an extra hazard ratio. For instance, for the novel combination EMC92 – ISS, 4 risk groups result in 3 hazard ratios, as indicated in the text and Table S2A (intermediate low risk relative to low risk: hazard ratio (HR) 2.6, 95%CI [1.6 - 4.5] intermediate high-risk relative to low risk: HR: 3.2, 95%CI [1.9 - 5.4] and high-risk relative to low risk: HR 6.9, 95%CI [4.1 - 12]). In the right panel, a plus sign indicates whether a data set could be used for the analysis of a specific marker or combination (for details of available data, see Table 1 and Figure S1). For the EMC92-ISS combination, the following datasets could be used: APEX, MRC-IX, TT2 and TT3.

The hazard ratios relative to the lowest risk group were 2.6 [1.6 – 4.5] (intermediate low), 3.2 [1.9 – 5.4] (intermediate high) and 6.9 [4.1 – 11.7] (high). Median survival times were 24 months (high), 47 (intermediate high) and 61 months (intermediate low) for the three highest risk groups, with median survival not reached after 96 months for the lowest risk group. To gain insight into the performance of this marker over time, we determined the proportions of surviving patients in each risk group and analyzed the EMC92-ISS at different time points. This marker is clearly applicable to younger as well as older and relapsed patients, and holds its value during follow up (Table 2 and online Figure S10).

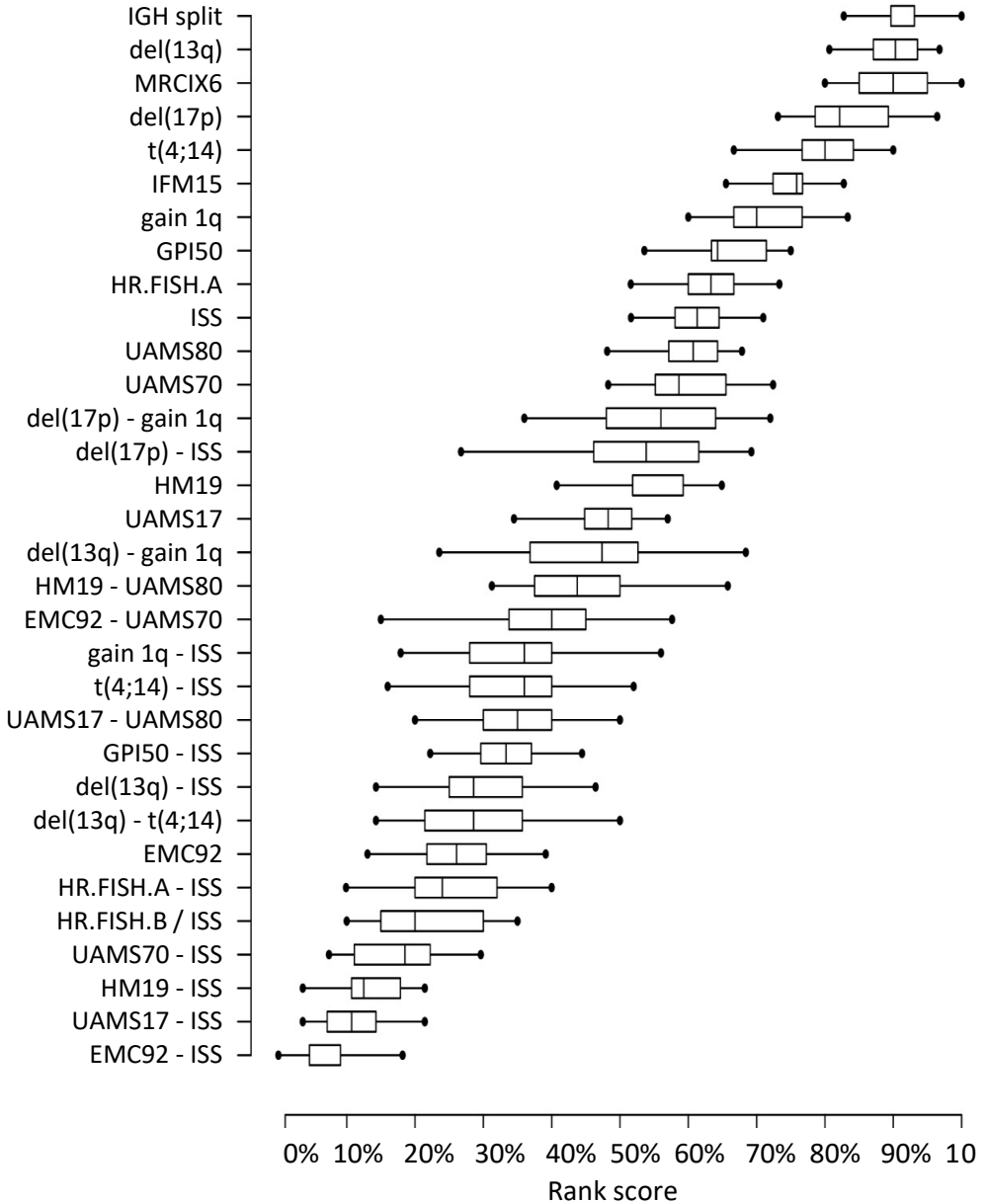
The composition of the four groups in terms of ISS, EMC92 and FISH markers is shown in Table 3. Interestingly, within the EMC92-ISS lowest risk group, 75% of patients – with truly favorable prognosis (Table S4) – were positive for either t(4;14), del(17p) or gain(1q). In the other risk categories 32%, 42% and 86% of patients were positive (intermediate low-, intermediate high- and high-risk, respectively) indicating that EMC92-ISS and FISH only partly represent overlapping patient sets.

**Table 2. Proportion of surviving patients at multiple time points per EMC92-ISS risk group in a Kaplan Meier analysis on the validation data (from top to bottom: 6, 12, 24 and 72 months respectively).** In the left column patient groups are pooled ( $n = 328$ ). Subsequent columns show percentages for newly diagnosed patients younger than 65 years ( $n = 174$ ), newly diagnosed older than 65 years ( $n = 90$ ) and relapsed patients ( $n = 64$ ) respectively. For the relapse category the 72 months' time point is not available.

6 months		Pooled	<65yr.	≥65yr.	Relapse
	Low-risk	98%	97%	96%	95%
	Intermediate low-risk	96%	95%	91%	85%
	Intermediate high-risk	86%	93%	73%	79%
	High-risk	84%	88%	56%	57%
	<b>Total survival</b>	92%	94%	81%	83%
12 months		Pooled	<65yr.	≥65yr.	Relapse
	Low-risk	97%	97%	96%	89%
	Intermediate low-risk	87%	93%	91%	54%
	Intermediate high-risk	74%	93%	73%	42%
	High-risk	67%	72%	56%	57%
	<b>Total survival</b>	84%	91%	81%	60%
24 months		Pooled	<65yr.	≥65yr.	Relapse
	Low-risk	92%	97%	92%	55%
	Intermediate low-risk	76%	88%	73%	23%
	Intermediate high-risk	57%	77%	58%	24%
	High-risk	46%	56%	31%	0%
	<b>Total survival</b>	72%	84%	67%	30%
72 months		Pooled	<65yr.	≥65yr.	Relapse
	Low-risk	77%	86%	96%	–
	Intermediate low-risk	43%	59%	32%	–
	Intermediate high-risk	27%	39%	28%	–
	High-risk	22%	33%	0%	–
	<b>Total survival</b>	48%	62%	36%	–

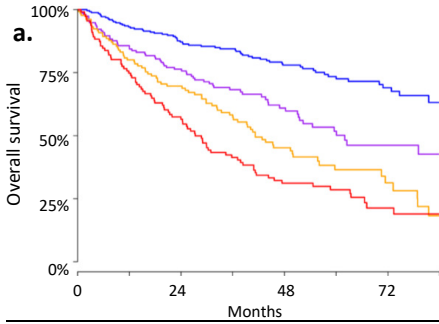
**Table 3. Distribution of markers in each of the four EMC92-ISS based risk groups.** Shown are the numbers in the data for which the EMC92-ISS risk classification could be determined.  $n$ , number of patients in the EMC92-ISS based risk group for which the specified marker was available. Positive, the percentage of patients positive for the specified marker; HR, the percentage of patients indicated as high-risk according to the specified marker. For the classifications based on del(13q), 1q gain and HR.FISH.A, a clear correlation was found to the EMC92-ISS classifications. For instance, 93% of EMC92-ISS high-risk patients are positive for HR.FISH.A compared to 44% - 55% of the intermediates and 75% of the low-risk patients.

EMC92 - ISS	EMC92		ISS				del(17p)		del(13q)		gain 1q		HR.FISH.A	
	HR	n	1	2	3	n	pos.	n	pos.	n	pos.	n	HR	n
<b>Low</b>	0%	365	100%	0%	0%	365	8%	39	44%	39	34%	154	75%	76
<b>Interm. low</b>	0%	231	0%	100%	0%	231	5%	60	37%	60	34%	92	44%	70
<b>Interm. high</b>	0%	211	0%	0%	100%	211	8%	66	44%	66	41%	101	55%	84
<b>High</b>	100%	166	30%	32%	39%	166	16%	38	74%	39	76%	90	93%	76



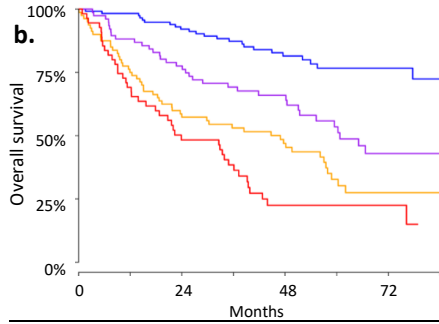
3

**Figure 3. Ranking of confirmed existing risk markers and validated novel risk markers, in relation to overall survival on the validation data.** The markers are vertically ordered by rank score, which reflects the observed proportion of risk markers with a better performance. Each box shows the interquartile range of the rank score per marker.



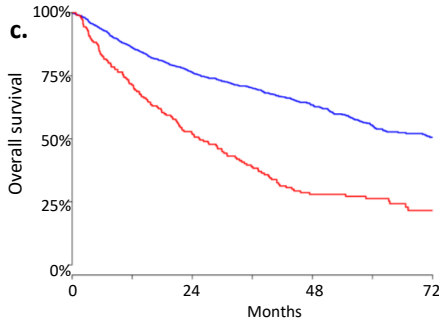
	prop.	HR [95%CI]	p-value
<b>EMC92 SR + ISS I</b>	39%	1	
<b>EMC92 SR + ISS II</b>	24%	1.6 [1.1 - 2.2]	0.016
<b>EMC92 SR + ISS III</b>	20%	2.3 [1.6 - 3.2]	$3.9 \times 10^{-6}$
<b>EMC92 high-risk</b>	17%	4.5 [3.2 - 6.3]	$\leq 1 \times 10^{-15}$

Likelihood ratio test:  $p \leq 1 \times 10^{-15}$ ; n = 645; n.events = 286



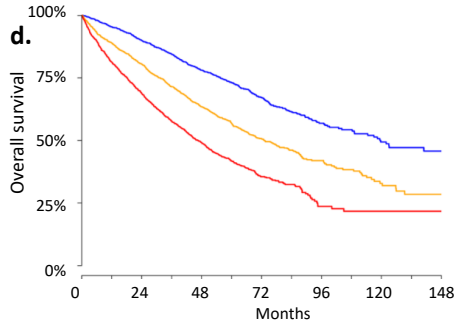
	prop.	HR [95%CI]	p-value
<b>EMC92 SR + ISS I</b>	35%	1	
<b>EMC92 SR + ISS II</b>	23%	2.6 [1.6 - 4.5]	$3 \times 10^{-4}$
<b>EMC92 SR + ISS III</b>	24%	3.2 [1.9 - 5.4]	$5.9 \times 10^{-6}$
<b>EMC92 high-risk</b>	17%	6.9 [4.1 - 12]	$5.9 \times 10^{-13}$

Likelihood ratio test:  $p = 2.7 \times 10^{-12}$ ; n = 328; n.events = 149



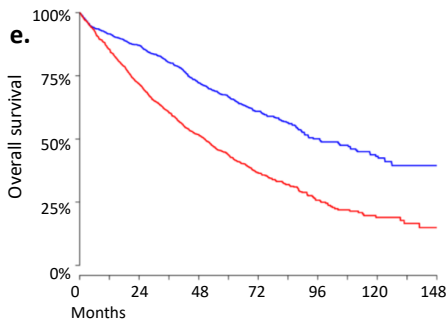
	prop.	HR [95%CI]	p-value
<b>EMC92 SR</b>	82%	1	
<b>EMC92 high-risk</b>	18%	2.8 [2.3 - 3.4]	$\leq 1 \times 10^{-15}$

Likelihood ratio test:  $p \leq 1 \times 10^{-15}$ ; n = 1094; n.events = 504



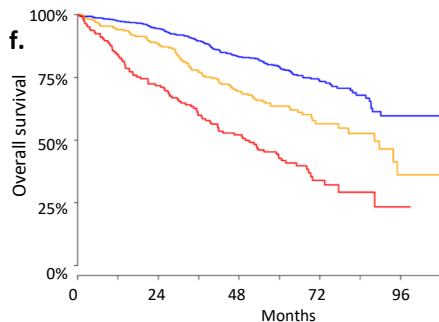
	prop.	HR [95%CI]	p-value
<b>ISS I</b>	34%	1	
<b>ISS II</b>	37%	1.6 [1.4 - 1.8]	$1 \times 10^{-14}$
<b>ISS III</b>	30%	2.3 [2.1 - 2.6]	$\leq 1 \times 10^{-15}$

Likelihood ratio test:  $p \leq 1 \times 10^{-15}$ ; n = 4077; n.events = 1925



	prop.	HR [95%CI]	p-value
<b>HR.FISH.A negative</b>	43%	1	
<b>HR.FISH.A positive</b>	57%	2.3 [2.0 - 2.5]	$\leq 1 \times 10^{-15}$

Likelihood ratio test:  $p \leq 1 \times 10^{-15}$ ; n = 2395; n.events = 1309



	prop.	HR [95%CI]	p-value
<b>HR.FISH.B/ISS Low</b>	57%	1	
<b>HR.FISH.B/ISS Interm</b>	26%	1.8 [1.4 - 2.4]	$2.1 \times 10^{-5}$
<b>HR.FISH.B/ISS High</b>	17%	3.6 [2.7 - 4.7]	$\leq 1 \times 10^{-15}$

Likelihood ratio test:  $p \leq 1 \times 10^{-15}$ ; n = 850; n.events = 309



**Figure 4. Survival analysis of EMC92-ISS, FISH and ISS.** Given are Kaplan-Meier curves (not stratified) and Cox models (stratified; i.e. corrected for differences in survival in different cohorts). **a)** EMC92-ISS in the discovery set; **b)** EMC92-ISS in the validation set; **c)** EMC92 in all data; **d)** ISS in all data; **e)** HR.FISH.A in all data; **f)** HR.FISH.B/ISS in all data. In order of increasing risk: low-risk (blue); intermediate low-risk (purple); intermediate high-risk (orange); high-risk (red); SR = standard-risk; HR = high-risk. Below the Kaplan-Meier curves, results of the stratified Cox model are found. prop. = proportion of patients within the specified risk group. HR [95%CI] = hazard ratio relative to the lowest risk group with 95% confidence interval;  $p$ -value =  $p$ -value relative to the lowest risk group; The bottom line shows the result of the likelihood ratio goodness of fit test.

### Biological relevance of GEP classifiers

Genes within GEP classifiers are selected based on association with survival, rather than a direct link to biology. Still, a gene ontology enrichment analysis<sup>33</sup> can highlight biological processes important for a poor outcome (online Tables S5a-h). All GEP classifiers had enrichment of cell-cycle related genes. When all probe-sets in all classifiers were pooled 191 biological processes were found to be enriched (FDR < 0.05). Top processes included ‘nuclear division’, ‘mitosis’ and ‘cell division’, processes sharing the genes *BIRC5*, *BUB1* and *UBE2C*. Other prominent processes included ‘DNA metabolic process’, ‘DNA packaging’ and ‘DNA replication’ (genes such as *TOP2A* and *MCM2*).

---

## DISCUSSION

### 3

Important prognostic markers in MM are based on ISS, FISH markers and GEP classifiers.<sup>7-13,16,17</sup> Previously, we showed that combining various GEP classifiers resulted in a stronger prediction of the high-risk population.<sup>7</sup> Here we systematically evaluated additional, new combinations of prognostic markers. We limited the search for new compound risk markers to pair-wise combinations of existing markers. This choice is mainly driven by the lack of complete data sets which contain all risk markers (online Figure S1), which hinders the analyses of more complex risk models. The number of patients positive for specific markers was remarkably stable between cohorts, irrespective of the type of marker. This adds strength to the belief that these markers, and thus decisions based on them can be reliably replicated.

Three findings are of particular interest: first, ISS has a clear and independent value in combination with either GEP classifiers or FISH markers. GEP classifiers combined with ISS are the strongest risk classifications found here. By combining the EMC92 gene classifier with ISS, patients are effectively stratified into four risk groups including a distinctive low risk group of 38% and a high-risk group of 17%. This strong additive strength of ISS to GEP has been recognized before in a previous smaller study.<sup>34</sup> Also ISS was integrated with GEP and other factors, but this risk score did not take into account correlations between markers, and was generated without using a solid discovery/validation design.<sup>35</sup> In contrast, we have opted for a study design in which part of the data was reserved for validation.

Secondly, our study confirmed that FISH markers can be divided into those consistently associated with shorter OS as opposed to inconsistent markers. Consistent FISH markers included t(4;14), gain(1q), del(17p) and del(13q). Combinations of any of these markers with ISS constituted solid prognostic predictors reported previously, t(4;14) and del(17p) are currently regarded as the most important high-risk FISH markers.<sup>17</sup> Thirdly, by combining these FISH markers into the previously defined risk classifications HR.FISH.A and HR.FISH.B/ISS, a major improvement of prognostic strength is achieved. Interestingly, patients classified as high-risk according to the HR.FISH.A marker but that actually had favorable

survival, were correctly identified as low risk patients by the EMC92-ISS compound marker. In addition to validating EMC92-ISS, we have now also validated the HR.FISH.B/ISS risk classification for the first time in independent data by excluding training data from the analyses. Combining FISH and ISS is thus a valid choice for routine clinical practice, including the existing HR-FISH.B/ISS, as proposed by Avet-Loiseau *et al.*<sup>19</sup> Incorporating LDH and bone imaging was outside the scope of this study because these markers were not consistently available.<sup>20</sup>

Combining GEP with ISS may become an attractive option for prognostication. The EMC92-ISS classification is independent from therapy choice: the EMC92 was shown to function in bortezomib clinical trials as well as in thalidomide and more conventional regimens.<sup>7</sup> In contrast, bortezomib and other novel agents may abrogate the unfavourable impact of some FISH markers on PFS.<sup>29</sup> EMC92-ISS is useful since it can identify both high-risk and low risk MM. This is an advantage over FISH markers which only seem to identify high-risk patients. Moreover, the technical applicability of GEP and its costs are thought to be comparable to FISH.<sup>36</sup> The agreement between GEP classifiers in terms of pathways is of interest. Although the primary force for classifier discovery is association with survival, the genes within classifiers appear to converge on the cell cycle pathways. Indeed, proliferative capacity, assessed as the plasma cell labeling index or by Ki-67 staining, has long been recognized to be an important prognostic factor.<sup>37,38</sup>

The clinical applicability of stratification into four risk groups will be increasingly relevant in the era of novel treatment modalities being available. First, increased accuracy of prognosis can improve patient counseling.<sup>17</sup> Secondly, and more important, risk stratification may lead to adaptation of treatment according to risk status. This composite risk marker opens the way to better risk stratification in clinical trials and explore novel drugs in different risk groups.<sup>39,40</sup> This could effectively be a first step towards a more individual treatment, using patient specific markers as a directional key.

Based on the current study we conclude that the combination of EMC92 with ISS is a strong disease based prognosticator for survival in MM. This risk classification is a good candidate to stratify patients for treatment options in a clinical trial.

---

## REFERENCES

1. Rajkumar SV, Dimopoulos MA, Palumbo A, *et al.* International Myeloma Working Group updated criteria for the diagnosis of multiple myeloma. *Lancet Oncol* . 2014; **15**(12):e538–48.
2. Brenner H, Gondas A, & Pulte D. Recent major improvement in long-term survival of younger patients with multiple myeloma. *Blood* . 2008; **111**(5):2521–6.
3. Bergsagel PL, Chesi M, Nardini E, Brents LA, Kirby SL, & Kuehl WM. Promiscuous translocations into immunoglobulin heavy chain switch regions in multiple myeloma. *Proc Natl Acad Sci U S A* . 1996; **93**(24):13931–6.
4. Fonseca R, Blood E, Rue M, *et al.* Clinical and biologic implications of recurrent genomic aberrations in myeloma. *Blood* . 2003; **101**(11):4569–75.
5. Zhan F, Huang Y, Colla S, *et al.* The molecular classification of multiple myeloma. *Blood* . 2006; **108**(6):2020–2028.
6. Broyl A, Hose D, Lokhorst H, *et al.* Gene expression profiling for molecular classification of multiple myeloma in newly diagnosed patients. *Blood* . 2010; **116**(14):2543–53.
7. Kuiper R, Broyl A, de Knecht Y, *et al.* A gene expression signature for high-risk multiple myeloma. *This thesis and Leukemia* . 2012; **26**(11):2406–13.
8. Shaughnessy J J D, Zhan F, Burington BE, *et al.* A validated gene expression model of high-risk multiple myeloma is defined by deregulated expression of genes mapping to chromosome 1. *Blood* . 2007; **109**(6):2276–2284.
9. Shaughnessy J J D, Qu P, Usmani S, *et al.* Pharmacogenomics of bortezomib test-dosing identifies hyperexpression of proteasome genes, especially PSMD4, as novel high-risk feature in myeloma treated with total therapy 3. *Blood* . 2011; **118**:3512–3524.
10. Decaux O, Lode L, Magrangeas F, *et al.* Prediction of survival in multiple myeloma based on gene expression profiles reveals cell cycle and chromosomal instability signatures in high-risk patients and hyperdiploid signatures in low-risk patients: a study of the Intergroupe Francophone du Myelome. *J Clin Oncol* . 2008; **26**(29):4798–4805.
11. Hose D, Reme T, Hielscher T, *et al.* Proliferation is a central independent prognostic factor and target for personalized and risk-adapted treatment in multiple myeloma. *Haematologica* . 2011; **96**(1):87–95.
12. Reme T, Hose D, Theillet C, & Klein B. Modeling risk stratification in human cancer. *Bioinformatics* . 2013; **29**(9):1149–57.
13. Dickens NJ, Walker BA, Leone PE, *et al.* Homozygous deletion mapping in myeloma samples identifies genes and an expression signature relevant to pathogenesis and outcome. *Clin Cancer Res* . 2010; **16**(6):1856–1864.
14. Greipp PR, Lust JA, O'Fallon WM, Katzmann JA, Witzig TE, & Kyle RA. Plasma cell labeling index and beta 2-microglobulin predict survival independent of thymidine kinase and C-reactive protein in multiple myeloma. *Blood* . 1993; **81**(12):3382–7.
15. Kyle RA, Gertz MA, Witzig TE, *et al.* Review of 1027 patients with newly diagnosed multiple myeloma. *Mayo Clin Proc* . 2003; **78**(1):21–33.

16. Greipp PR, San Miguel J, Durie BG, *et al.* International staging system for multiple myeloma. *J Clin Oncol* . 2005; **23**(15):3412–20.
17. Chng WJ, Dispenzieri A, Chim CS, *et al.* IMWG consensus on risk stratification in multiple myeloma. *Leukemia* . 2014; **28**(2):269–77.
18. Neben K, Jauch A, Bertsch U, *et al.* Combining information regarding chromosomal aberrations t(4;14) and del(17p13) with the International Staging System classification allows stratification of myeloma patients undergoing autologous stem cell transplantation. *Haematologica* . 2010; **95**(7):1150–7.
19. Avet-Loiseau H, Durie BG, Cavo M, *et al.* Combining fluorescent in situ hybridization data with ISS staging improves risk assessment in myeloma: an International Myeloma Working Group collaborative project. *Leukemia* . 2013; **27**(3):711–7.
20. Moreau P, Cavo M, Sonneveld P, *et al.* Combination of International Scoring System 3, High Lactate Dehydrogenase, and t(4;14) and/or del(17p) Identifies Patients With Multiple Myeloma (MM) Treated With Front-Line Autologous Stem-Cell Transplantation at High Risk of Early MM Progression-Related Death. *J Clin Oncol* . 2014; **32**(20):2173–80.
21. Broyl A, Kuiper R, van Duin M, *et al.* High cereblon expression is associated with better survival in patients with newly diagnosed multiple myeloma treated with thalidomide maintenance. *This thesis and Blood* . 2013; **121**(4):624–7.
22. Morgan GJ, Davies FE, Gregory WM, *et al.* Long-term follow-up of MRC Myeloma IX trial: Survival outcomes with bisphosphonate and thalidomide treatment. *Clin Cancer Res* . 2013; **19**(21):6030–8.
23. Mulligan G, Mitsiades C, Bryant B, *et al.* Gene expression profiling and correlation with outcome in clinical trials of the proteasome inhibitor bortezomib. *Blood* . 2007; **109**(8):3177–3188.
24. Nair B, van Rhee F, Shaughnessy J J D, *et al.* Superior results of Total Therapy 3 (2003-33) in gene expression profiling-defined low-risk multiple myeloma confirmed in subsequent trial 2006-66 with VRD maintenance. *Blood* . 2010; **115**(21):4168–73.
25. Ross FM, Ibrahim AH, Vilain-Holmes A, *et al.* Age has a profound effect on the incidence and significance of chromosome abnormalities in myeloma. *Leukemia* . 2005; **19**(9):1634–42.
26. Walker BA, Leone PE, Chiecchio L, *et al.* A compendium of myeloma-associated chromosomal copy number abnormalities and their prognostic value. *Blood* . 2010; **116**(15):e56–65.
27. Ross FM, Avet-Loiseau H, Ameye G, *et al.* Report from the European Myeloma Network on interphase FISH in multiple myeloma and related disorders. *Haematologica* . 2012; **97**(8):1272–7.
28. Wuilleme S, Robillard N, Lode L, *et al.* Ploidy, as detected by fluorescence in situ hybridization, defines different subgroups in multiple myeloma. *Leukemia* . 2005; **19**(2):275–8.
29. Sonneveld P, Schmidt-Wolf IG, van der Holt B, *et al.* Bortezomib induction and maintenance treatment in patients with newly diagnosed multiple myeloma: results of the randomized phase III HOVON-65/ GMMG-HD4 trial. *J Clin Oncol* . 2012; **30**(24):2946–55.
30. Cox DR & Oakes D. *Analysis of Survival Data.* Taylor & Francis. 1984.
31. Bland JM & Altman DG. Multiple significance tests: the Bonferroni method. *BMJ* . 1995; **310**(6973):170.

- 
32. Therneau TM & Grambsch PM. Modeling survival data : extending the Cox model. Springer, New York. 2000.
  33. Ashburner M, Ball CA, Blake JA, *et al.* Gene ontology: tool for the unification of biology. The Gene Ontology Consortium. *Nat Genet* . 2000; **25**(1):25–9.
  34. Waheed S, Shaughnessy J J D, van Rhee F, *et al.* International staging system and metaphase cytogenetic abnormalities in the era of gene expression profiling data in multiple myeloma treated with total therapy 2 and 3 protocols. *Cancer* . 2011; **117**(5):1001–9.
  35. Meissner T, Seckinger A, Reme T, *et al.* Gene expression profiling in multiple myeloma—reporting of entities, risk, and targets in clinical routine. *Clin Cancer Res* . 2011; **17**(23):7240–7.
  36. Hose D, Seckinger A, Jauch A, *et al.* The role of fluorescence in situ hybridization and gene expression profiling in myeloma risk stratification. *Srp Arh Celok Lek* . 2011; **139 Suppl 2**:84–9.
  37. Steensma DP, Gertz MA, Greipp PR, *et al.* A high bone marrow plasma cell labeling index in stable plateau-phase multiple myeloma is a marker for early disease progression and death. *Blood* . 2001; **97**(8):2522–3.
  38. Gastinne T, Leleu X, Duhamel A, *et al.* Plasma cell growth fraction using Ki-67 antigen expression identifies a subgroup of multiple myeloma patients displaying short survival within the ISS stage I. *Eur J Haematol* . 2007; **79**(4):297–304.
  39. Ludwig H, Sonneveld P, Davies F, *et al.* European Perspective on Multiple Myeloma Treatment Strategies in 2014. *Oncologist* . 2014; **19**(9):829–844.
  40. Crawley C, Iacobelli S, Bjorkstrand B, Apperley JF, Niederwieser D, & Gahrton G. Reduced-intensity conditioning for myeloma: lower nonrelapse mortality but higher relapse rates compared with myeloablative conditioning. *Blood* . 2007; **109**(8):3588–94.

**Gene expression classifier SKY92 identifies high-risk multiple myeloma in elderly patients of the HOVON-87/NMSG-18 study**

Rowan Kuiper, Sonja Zweegman, Mark van Duin, Martin H. van Vliet, Annemiek Broijl, Mark-David Levin, Leonie de Best, Erik H. van Beers, Belinda Dumee, Michael Vermeulen, Jasper Koenders, Bronno van der Holt, Heleen Visser-Wisselaar, Markus Hansson, Annette W.G. van der Velden, H. Berna Beverloo, Marian Stevens-Kroef, Anders Waage & Pieter Sonneveld

---

## ABSTRACT

The SKY92 prognostic classifier (published as the EMC92 classifier) is based on gene expression profiles of younger, transplant eligible multiple myeloma (MM) patients who were included in the HOVON-65/GMMG-HD4 trial. Here, this classifier is validated in elderly, non-transplant eligible patients of the HOVON-87/NMSG-18 trial (EudraCT number 2007-004007-34; median age=73;  $n = 178$ ).

In this trial melphalan, prednisone, thalidomide plus thalidomide maintenance (MPT-T) was compared with MPR-R (R: lenalidomide). Patients were risk stratified using the SKY92 gene classifier, FISH markers and revised ISS.

4

At the time of analysis, the median follow up was 34 months. Twenty-five out of 178 patients were SKY92 high-risk (14%) and demonstrated a significantly shorter progression free survival (PFS) compared to SKY92 standard-risk patients (median PFS: 12 months vs 23 months with a hazard ratio of 2.3, 95%*CI* = [1.5 – 3.7],  $p < .001$ ). Similarly, overall survival (OS) was inferior in SKY92 high-risk patients compared to SKY92 standard-risk (21 months vs 53 months with a hazard ratio of 3.0, 95%*CI* = [1.7 – 5.3],  $p < .001$ ). The 3-year OS rates were 27% (SKY92 high-risk), 47% (high-risk FISH) and 33% (revised-ISS-III). The multivariate Cox regression analysis included SKY92, revised-ISS, deletion of 13q, gain of 1q, t(11;14) and age. SKY92, revised-ISS, deletion of 13q and t(11;14) were found to be independently associated with PFS, and SKY92, revised-ISS and deletion of 13q remained independently associated with OS.

These data validate the SKY92 classifier as a robust and independent marker to identify high-risk patients in non-transplant eligible MM patients, and underline the value of cytogenetic prognostic markers.



## INTRODUCTION

Multiple myeloma (MM) is a cancer of plasma cells which mostly affects elderly people. The median age is 69 years at diagnosis, with 35-40% of patients older than 75.<sup>1-3</sup> From randomized clinical trials as well as from population based registries it is clear that elderly patients also benefit from novel agents such as proteasome inhibitors and immunomodulatory agents (IMiDs). However, the outcome is heterogeneous, being explained by both disease characteristics, such as high-risk cytogenetic disease, as well as side effects being more pronounced in a population that is characterized by a higher incidence of comorbidities. Therefore also in the elderly patients, upfront identification of high-risk disease is of utmost importance.

The International Staging System (ISS), based on serum levels of albumin and  $\beta$ 2-microglobulin, represents the most widely used method of identifying high-risk MM patients, so far.<sup>4</sup> Clinical variables such as frailty and renal impairment also identify subsets of patients with worse outcome.<sup>5,6</sup> Other prognostic factors include cytogenetic aberrations and gene expression classifiers. Translocations  $t(4;14)(p16;q32)$  and  $t(14;16)(q32;q23)$  and copy number changes such as deletion of 17p ( $del(17p13)$ ) are associated with a poor prognosis.<sup>7-11</sup> Of these, translocations such as  $t(4;14)$  were reported to be less common in elderly patients.<sup>12,13</sup> The value of high-risk cytogenetic markers is confirmed by the revised ISS (R-ISS), which combines serum levels of albumin and  $\beta$ 2-microglobulin (i.e. ISS) with serum levels of lactate dehydrogenase levels (LDH) and the cytogenetic markers  $del(17p)$ ,  $t(4;14)$  and  $t(14;16)$ .<sup>14</sup>

Gene expression classifiers include the EMC92 prognostic classifier, which was developed in our group.<sup>15-17</sup> Based on 290 gene expression profiles obtained from patients included in the HOVON-65/GMMG-HD4 trial, a prognostic model of 92 probe sets was generated. This model performed well in an initial round of validation sets (including UAMS Total Therapy cohorts 2 and 3 and Myeloma Research Council IX (MRC-IX)).<sup>18-21</sup> Subsequently, the model was validated in several sets including UAMS Total Therapy 6 trial and the Multiple Myeloma Genomics Initiative (MMGI),<sup>22,23</sup> after which it was standardized for use in the clinical practice as the SKY92 classifier. The EMC92/SKY92 model identifies on aver-

---

age 18% of patients as high-risk. Importantly, none of these cohorts were aimed specifically at the treatment of elderly MM patients; in the entire population of discovery and validation patients the median age was 62 years old with less than 16% of patients older than 70.

Therefore, the aim of this study was to assess the prognostic value of the SKY92 gene classifier in a homogeneous patient cohort of elderly, newly diagnosed MM patients. For this purpose, we used a subset of the HOVON-87/NMSG-18 trial for which purified bone marrow plasma cells were available (HOVON: Dutch-Belgium Cooperative Trial Group for Hematology Oncology; NMSG: the Nordic Myeloma Study Group).<sup>24</sup> The median age of patients included in this trial was 73 years. In addition, the value of other markers such as cytogenetic markers and R-ISS were available for comparison to the value of the SKY92. In this dataset of elderly MM patients, the SKY92 had a clear value as a prognostic marker, additional to other prognostic markers in a multivariate analysis.

## MATERIALS AND METHODS

### Patient characteristics

This analysis concerned patients who were included in the HOVON-87/NMSG-18 trial (HO87/NM18; online Figure S1) which was registered at [www.trialregister.nl](http://www.trialregister.nl) as NTR1630 (EudraCT number 2007-004007-34).<sup>24</sup> The trial was conducted in accordance with the declaration of Helsinki. It was approved by the institutional review board of all participating hospitals and written informed consent was obtained from all patients. Patient eligibility for the HO87/NM18 study was reported previously.<sup>24</sup> In brief, the HO87/NM18 was a randomized prospective phase III trial including patients with previously untreated symptomatic MM that were older than 65 years of age or younger than 65 years but not eligible for high-dose chemotherapy and peripheral stem cell transplantation (median age 73 years; total number of eligible patients in the trial: 637; with 3% of patients 65 or younger). Patients were randomized upfront for treatment (randomly assigned 1:1, stratified for hospital and ISS stage) with nine 4-weekly cycles of 28 days of either melphalan-prednisone-thalidomide followed by thalidomide maintenance (MPT-T;  $n = 318$ ), or melphalan-prednisone-lenalidomide followed by maintenance with lenalidomide (MPR-R;  $n = 319$ ) (online Figure S1). Bone marrow aspirates were obtained for the purpose of biobanking as part of the clinical protocol (protocol of HO87/NM18 on [www.hovon.nl](http://www.hovon.nl)). For 178 out of 637 patients (of which only 1 was younger than 65 yrs.), gene expression analysis was performed (online Figure S2). The main factors resulting in exclusion of patients were: no bone marrow sent to the biobank (42% of HOVON patients) and insufficient enrichment of plasma cells (19% of HOVON patients). 29% of HOVON patients were usable, compared to 28% overall (see online Supplemental data).

### SKY92 gene classification

The MMprofiler™CE IVD assay (SkylineDx, Rotterdam, The Netherlands) was used to obtain SKY92 scores, classifying a patient as high-risk or standard-risk. The SKY92 was originally published as the EMC92 classifier.<sup>15</sup> RNA sample workup was performed according to the MMprofiler's instructions for use at the

---

SkylineDx reference lab, Rotterdam, The Netherlands (online Figure S2). The resulting Affymetrix HG-U133 Plus2 gene expression profiles have been submitted to GEO under accession *GSE87900*.

## Interphase fluorescent in situ hybridization

Interphase fluorescent in situ hybridization (FISH) was performed on CD138+ enriched plasma cells using standard techniques according to the European Myeloma Network guidelines, with positive cut-off levels at 10% for fusion or break-apart probes and 20% for numerical abnormalities.<sup>25</sup> The standard analysis included loss of the *TP53* locus on chromosome 17, chromosome 13q14, gain of chromosome 1q and translocations t(4;14), t(11;14) and t(14;16). For details see online Supplemental data.

4

## International staging system, LDH, high-risk FISH, revised ISS and SKY92-ISS

The risk stratification according to the ISS was determined by combining serum levels of albumin and B2m (ISS-I: B2m < 3.5 mg/L and albumin  $\geq$  3.5g/dL; ISS-II: not I or III; ISS-III: B2m  $\geq$  5.5 mg/L).<sup>4</sup> Lactate dehydrogenase (LDH) was measured in serum and was considered elevated if the concentration exceeded the upper limit of normal range as defined per lab. Three different risk classification models were applied and combinations thereof; high risk FISH, R-ISS, SKY92-ISS. The definition of high-risk FISH was detection of del(17p13), t(4;14) or t(14;16).<sup>14</sup> R-ISS combines ISS with LDH and high-risk FISH resulting in 3 risk groups: R-ISS-I if ISS-I and no elevated LDH, del(17p), t(4;14) and t(14;16); R-ISS-III if ISS-III and either elevated LDH, del(17p), t(4;14) or t(14;16); R-ISS-II if not R-ISS-I or not R-ISS-III. SKY92-ISS combines SKY92 with ISS resulting in 4 risk groups: high-risk if SKY92 HR; intermediate high-risk if SKY92 SR and ISS-III; intermediate low-risk if SKY92 SR and ISS-II; low-risk if SKY92 SR and ISS-I.<sup>26</sup>

The R-ISS was not mandated by the HO87/NM18 study protocol. However, data were available for most patients and retrospectively analyzed. The R-ISS status is set to missing in 14% of analyzed patients for which the status could not be determined unequivocally.

## Statistical analyses

All statistics have been performed in R (v3.3.1).<sup>27</sup> The association between survival and the SKY92 classifier was evaluated by Cox regression analysis using the survival package (v2.40-1).<sup>28,29</sup> Deviations from the proportionality assumption were checked using the *cox.zph* function. All models satisfied the proportionality assumption ( $p > .05$ ). Kaplan-Meier curves were generated for visualization. A Cox regression multivariate analysis was performed by bidirectional stepwise selection using a criterion of  $p < .05$  for the likelihood ratio test. Enrichment of FISH markers within the SKY92 standard- or high-risk group was tested by the two-sided Fisher exact test using the *exact2x2* package (v1.4.1).<sup>30</sup>

---

## RESULTS

At the time of analysis the median follow up was 34 months. Age, ISS and occurrence of cytogenetic aberrations were not different in the patient groups with and without gene expression profiling (Table 1). The SKY92 classifier identified 25 high-risk patients ( $25/178 = 14\%$ ). The median progression-free survival (PFS) of high-risk patients was 12 months compared to 23 months for standard-risk patients with a hazard ratio of ( $HR_{pfs} = 2.3$ ;  $p < .001$ ; Figure 1a). Similarly, the median overall survival (OS) of high-risk patients was inferior; 21 months compared to 53 months for standard-risk patients ( $HR_{os} = 3.0$ ;  $p < .001$ ; Figure 1b).

4

Previously we identified the combination of SKY92 and ISS as the most consistent prognostic tool based on an extensive computational analysis.<sup>26</sup> This combination defines patients as low-risk (SKY92 SR + ISS-I), intermediate low-risk (SKY92 SR + ISS-II), intermediate high-risk (SKY92 SR + ISS-III) or high-risk (SKY92 HR). Median PFS is comparable for the three lower risk groups (Figure 1c). In contrast, SKY92 combined with ISS-I identifies a patient group with superior OS, i.e. 86% of patients are alive after 36 months (Figure 1d).

Next, SKY92 was compared to the revised ISS and high-risk FISH. The availability of data between different markers and distribution of high-risk vs standard-risk patients is shown in Figure 2. This figure demonstrates that SKY92, FISH and R-ISS identify in part different patients as high-risk (see also below). Only 12 out of 155 patients with R-ISS-III (8%) were identified, compared to 121 patients with R-ISS-II (78%) and 22 patients with R-ISS-I (14%; Figures 1e-f). High-risk FISH, i.e. ( $t(4;14)$  and/or  $t(14;16)$  and/or  $del(17p)$ ), was identified in 30 out of 137 patients (22%; Figures 1g-h). The median PFS for high-risk patients was found to be comparable between different risk classifiers, SKY92: 12 months, R-ISS-III: 13 months and high-risk FISH: 14 months (Figures 1a,e,g). The median OS for these patient groups is more diverse, SKY92: 21 months, R-ISS-III: 25 months and high-risk FISH: 31 months (Figures 1b,f,h; online Tables S1 and 2 for survival rates).

In the multivariate analysis, SKY92, R-ISS,  $del(13q)$  and  $t(11;14)$  were independently associated with PFS. SKY92, R-ISS and  $del(13q)$  were independently associated with OS (Tables 2b and c). High-risk FISH markers were also asso-

**Table 1. Comparison between the HO87/NM18 study population and the gene expression subset analyzed in this project.**

		Not in analysis	In analysis	Total	
		N %	N %	N %	
Age	Median	73	72	73	$p = .21(a)$
	Q1	69	69	69	
	Q3	77	76	77	
	Range	60-91	60-84	60-91	
	Number	459	178	637	
Sex	Male	252 55%	94 53%	346 54%	$p = .63(b)$
	Female	207 45%	84 47%	291 46%	
ISS stage	ISS-I	115 25%	42 24%	157 25%	$p = .94(b)$
	ISS-II	219 48%	85 48%	304 48%	
	ISS-III	118 25%	47 26%	165 26%	
	Not available	7 2%	4 2%	11 2%	
FISH performed	No	142 31%	14 8%	156 24%	$p = < .001(c)$
	Yes	316 69%	164 92%	480 75%	
	Not done	1 <1%	0 0%	1 <1%	
gain 1q	No	147 65%	77 60%	224 63%	$p = < .36(c)$
	Yes	79 35%	52 40%	131 37%	
del(13q)	No	162 58%	82 53%	244 56%	$p = < .31(c)$
	Yes	117 42%	73 47%	190 44%	
del(17p)	No	257 90%	134 91%	391 90%	$p = < .87(c)$
	Yes	30 10%	14 9%	44 10%	
t(4;14)	No	282 92%	143 91%	425 91%	$p = < .61(c)$
	Yes	25 8%	15 9%	40 9%	

(a) Kruskal-Wallis test; (b)  $\chi^2$  test; (c) Fisher exact test

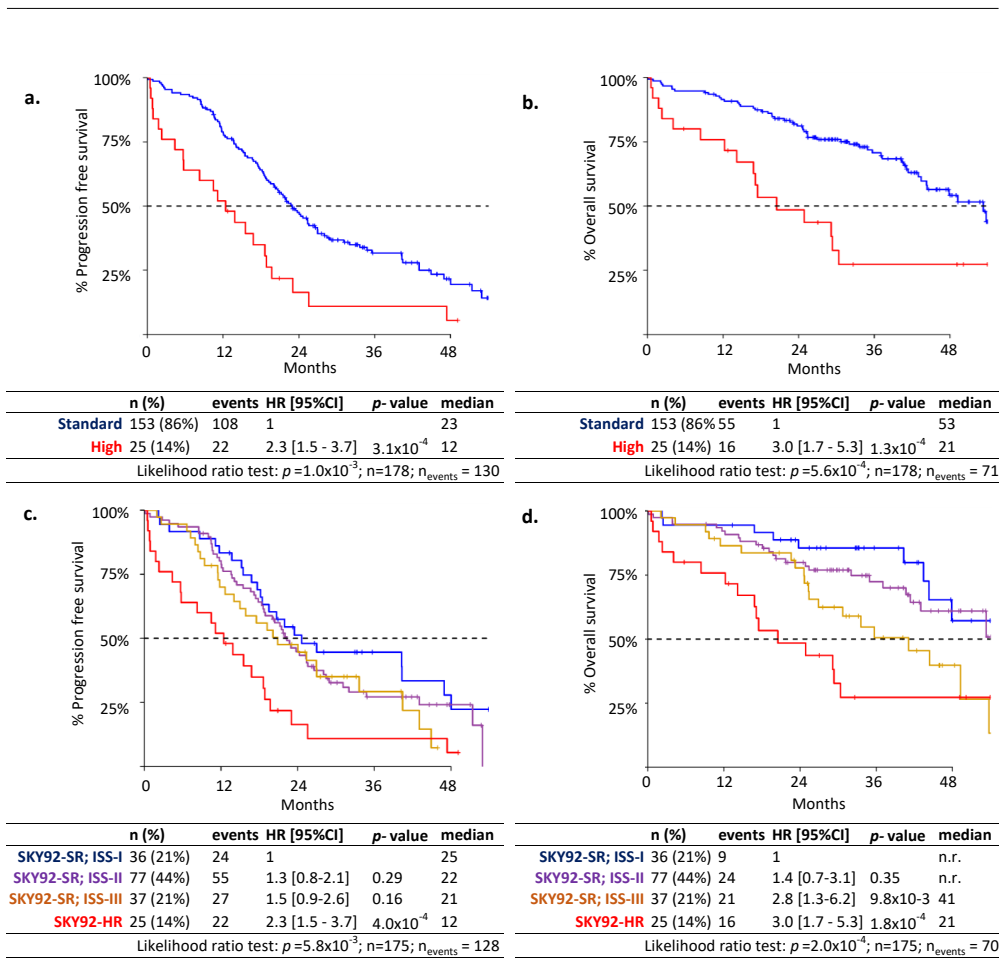
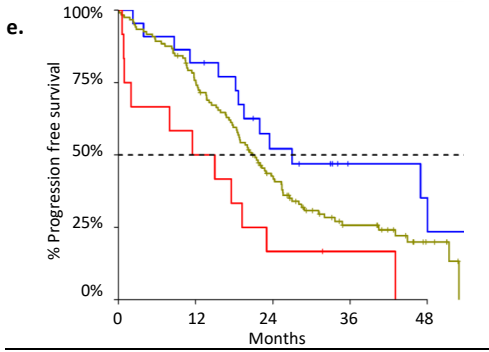


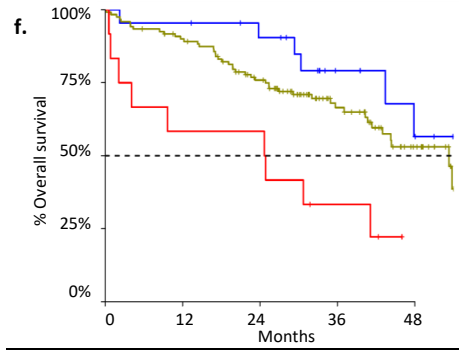
**Figure 1. Survival for the SKY92 PFS (a) and OS (b), SKY92-ISS PFS (c) and OS (d) R-ISS PFS (e) and OS (f) and high-risk FISH PFS (g) and OS (h).** Colors indicate the risk groups: low- or standard-risk (blue), intermediate-high-risk (orange), intermediate-risk (green), intermediate-low-risk (purple) and high-risk (red). Tables show the results of the Cox regression analysis with: n (%) = number and proportion of patients, events = number of events, HR [95%CI] = hazard ratio relative to lowest risk group of patients with 95% confidence interval, p-value = probability of observing the hazard ratio, median = median survival in months with n.r. = median not reached. In the last row, the likelihood ratio test for the model is given.





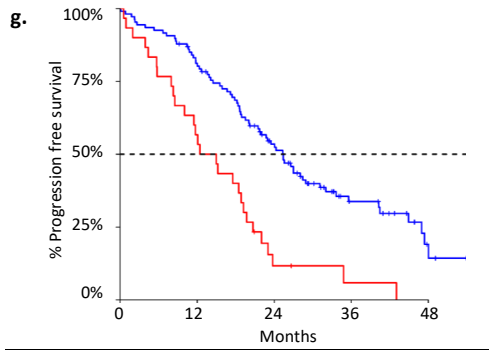
	n (%)	events	HR [95%CI]	p-value	median
R- ISS-I	22 (14%)	14	1		27
R- ISS-II	121 (78%)	88	1.6 [0.9-2.9]	0.11	21
R- ISS-III	12 (7.7%)	11	3.2 [1.4-7.2]	$5.1 \times 10^{-3}$	13

Likelihood ratio test:  $p=0.025$ ;  $n=155$ ;  $n_{\text{events}} = 113$



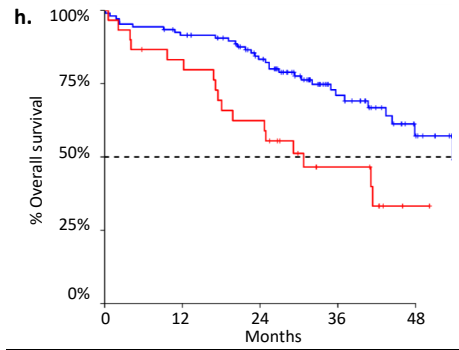
	n (%)	events	HR [95%CI]	p-value	median
R- ISS-I	22 (14%)	8	1		n.r.
R- ISS-II	121 (78%)	46	1.7 [0.7-4.1]	0.21	53
R- ISS-III	12 (7.7%)	9	5.0 [1.7-14.1]	$2.6 \times 10^{-3}$	25

Likelihood ratio test:  $p=9.8 \times 10^{-3}$ ;  $n=155$ ;  $n_{\text{events}} = 61$



	n (%)	events	HR [95%CI]	p-value	median
no HR-FISH	107 (78%)	71	1		25
HR FISH	30 (22%)	28	2.7 [1.7-4.3]	$1.4 \times 10^{-5}$	14

Likelihood ratio test:  $p=5.4 \times 10^{-5}$ ;  $n=137$ ;  $n_{\text{events}} = 99$



	n (%)	events	HR [95%CI]	p-value	median
no HR-FISH	107 (78%)	33	1		54
HR FISH	30 (22%)	17	2.5 [1.4-4.5]	$2.6 \times 10^{-3}$	31

Likelihood ratio test:  $p=4.4 \times 10^{-3}$ ;  $n=137$ ;  $n_{\text{events}} = 50$

4

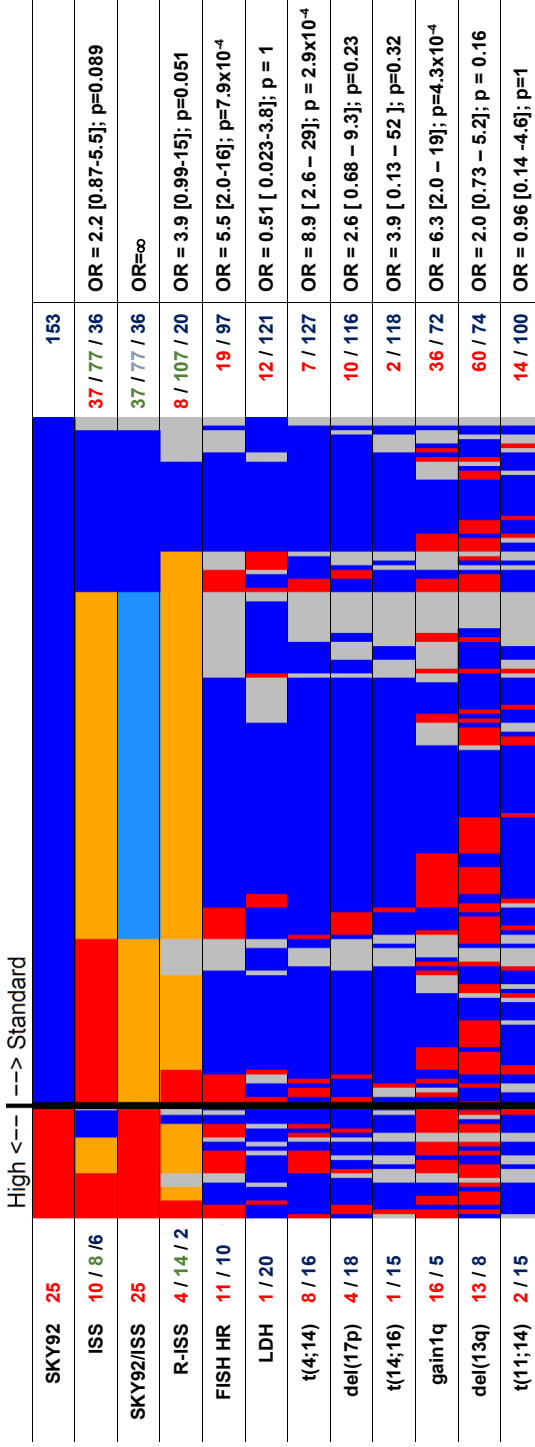


**Figure 2. Composition of markers compared to the SKY92 classification.** The plot shows the co-occurrence of markers (vertical) within each patient (horizontal). Patients are ordered by SKY92 risk status. Red indicates presence or highest risk of the marker, dark blue absence or lowest risk, light blue intermediate low, orange intermediate risk and grey if the marker status is unknown. The numbers on the sides correspond to the number of high/intermediate/low risk marker status (indicated by color) within the SKY92 high-risk group (left) or standard-risk group (right). On the right the odds ratios (OR) with 95% confidence interval as estimated in a Fisher exact test for enrichment of the marker in one of the SKY92 risk group is given; p: p-value corresponding to the odds ratio.

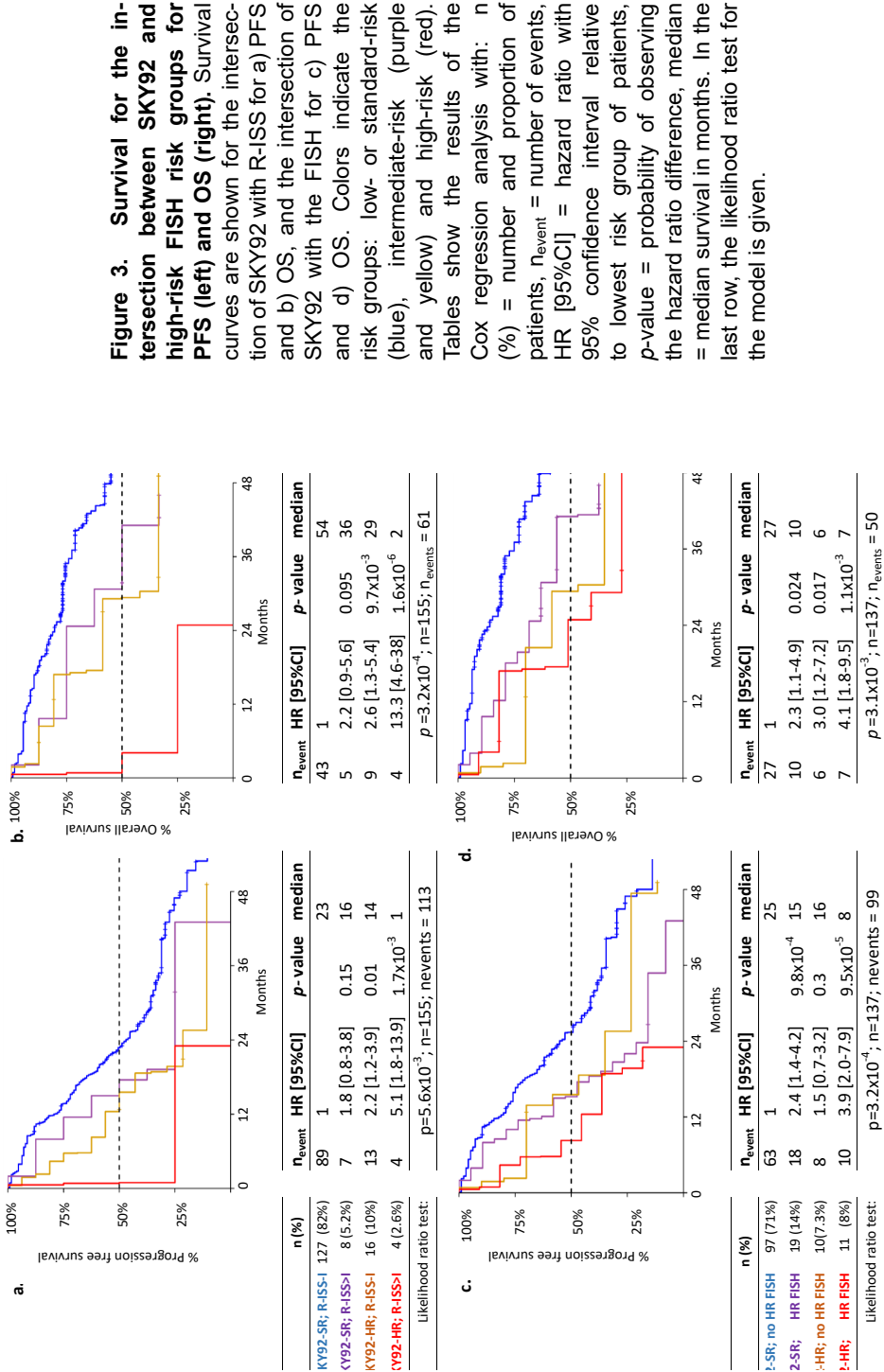


**Figure 3. Survival for the intersection between SKY92 and high-risk FISH risk groups for PFS (left) and OS (right).** Survival curves are shown for the intersection of SKY92 with R-ISS for a) PFS and b) OS, and the intersection of SKY92 with the FISH for c) PFS and d) OS. Colors indicate the risk groups: low- or standard-risk (blue), intermediate-risk (purple) and high-risk (red). Tables show the results of the Cox regression analysis with: n = number and proportion of patients, n<sub>event</sub> = number of events, HR [95%CI] = hazard ratio with 95% confidence interval relative to lowest risk group of patients, p-value = probability of observing the hazard ratio difference, median = median survival in months. In the last row, the likelihood ratio test for the model is given.

---

ciated with OS (see Table 2a), but did not have an independent effect in the final multivariate model, since high-risk FISH is incorporated in the R-ISS. As indicated by these results, SKY92, R-ISS and FISH markers can all be used independently for prognostication.

4 Finally, the combination of SKY92 with R-ISS and SKY92 with high-risk FISH was evaluated. Patients can be divided into four groups: double negative, i.e. standard-risk for both markers, positive-negative, negative-positive and double positive, i.e. high-risk for both markers. The results of these combinations are shown in Figure 3. For PFS and for OS, double negative patients demonstrated a favorable survival in both comparisons, whereas double positive patients had the poorest survival. Patients with a discordant risk classification for both markers showed an intermediate survival. Interestingly, the SKY92/R-ISS combination identifies a small subset of patients with extremely poor survival: only 2.6% were SKY92 high-risk and R-ISS III (Figure 3a-b). In this small group of double positive patients, the median PFS was only 1 month (HR = 5.1,  $p < 0.01$ ) with a median OS of 2 months (HR = 13,  $p < 0.0001$ ).

**Table 2. Univariate (a) and multivariate PFS (b) and OS (c) associations in the HOVON-87/NMSG-18 trial.** For the multivariate analyses a bidirectional stepwise selection procedure was applied excluding covariates with the highest *p*-values until all are significant. Initially included covariates were SKY92, R-ISS, gain1q, del(13q), t(11;14) and age. High-risk FISH, LDH and ISS were not included as they were already part of the R-ISS. SKY92-ISS could not be included because of collinearity. In bold: *p*<.05, pos: positive, neg: negative and NA: not available, HR: hazard ratios relative to the lowest risk category with 95% confidence intervals (CI), *p*: likelihood ratio *p*-value indicating the association of each covariate with OS or PFS.

a) Univariate

					PFS		OS	
		pos	neg	NA	HR	<i>p</i>	HR	<i>p</i>
					[95%CI]		[95%CI]	
SKY92 high-risk		25	153	0	2.4	$1.0 \times 10^{-3}$	3.0	$5.6 \times 10^{-4}$
ISS	I	42	132	4	1.0	0.26	1.0	$6.9 \times 10^{-3}$
	II	85	89	4	1.3		1.2	
	III	47	127	4	1.5		2.5	
SKY92-ISS	Low-risk	36	142	3	1.0	$5.8 \times 10^{-3}$	1.0	$2.0 \times 10^{-4}$
	Interm-low	77	101	3	1.3		1.4	
	Interm-high	37	141	3	1.5		2.8	
	High-risk	25	153	3	2.9		4.9	
R-ISS	I	22	133	23	1.0	0.024	1.0	$9.8 \times 10^{-3}$
	II	121	34	23	1.6		1.7	
	III	12	143	23	3.2		5.0	
LDH		13	141	24	1.3	.53	1.5	.32
High-risk FISH		30	107	41	2.7	$5.4 \times 10^{-5}$	2.5	$5.4 \times 10^{-3}$
gain1q		52	77	49	1.4	0.15	2.1	<b>0.015</b>
del(17p)		14	134	30	2.5	$9.4 \times 10^{-3}$	3.3	$3.1 \times 10^{-3}$
del(13q)		73	82	23	1.8	$2.0 \times 10^{-3}$	1.6	.07
t(4;14)		15	143	20	2.3	$7.1 \times 10^{-3}$	1.4	.46
t(11;14)		16	115	47	0.8	.61	1.2	.73
t(14;16)		3	133	42	3.3	.088	4.6	.091
Age		178	0	0	1.0	1.0	1.0	.53

b) Multivariate PFS

					PFS	
		pos	neg	NA	HR	<i>p</i>
					[95%CI]	
SKY92 high-risk		13	103	0	2.3	<b>.031</b>
R-ISS	I	18	98	0	1.0	<b>.024</b>
	II	89	27	0	1.7	
	III	9	107	0	4.0	
del(13q)		56	60	0	2.0	$3.6 \times 10^{-3}$
t(11;14)		11	105	0	0.33	<b>.015</b>

*n* = 116; number of events = 81; 5 degrees of freedom; *p* =  $3.1 \times 10^{-4}$

c) Multivariate OS

					OS	
		pos	neg	NA	HR	<i>p</i>
					[95%CI]	
SKY92 high-risk		17	122	0	2.9	$8.6 \times 10^{-3}$
R-ISS	I	20	119	0	1.0	$7.8 \times 10^{-3}$
	II	107	32	0	1.7	
	III	12	127	0	5.5	
del(13q)		67	72	0	1.9	<b>.024</b>

*n* = 139; number of events = 53; 4 degrees of freedom; *p* =  $3.6 \times 10^{-4}$

---

## DISCUSSION

In this study the SKY92 gene expression classifier was retrospectively validated in a group of homogeneously treated, elderly MM patients. The SKY92 classifier was previously validated in several cohorts comprising both newly diagnosed and relapsed patients, treated with a variety of therapies, including bortezomib and thalidomide.<sup>15,22,31,32</sup> Here we demonstrate that the SKY92 classifier with or without ISS, is also of prognostic value in elderly MM patients treated with IMiDs.

The incidence of high-risk patients in this population of elderly newly diagnosed MM patients as defined by SKY92 (14%) is comparable to what we found previously in other MM cohorts (15 – 20%). In contrast, the UAMS70, an alternative gene expression classifier, consistently identifies a smaller high-risk proportion compared to SKY92 (on average 12% vs 18%, respectively).<sup>18,33</sup> In the H087/NM18 patients, the proportion of high-risk UAMS70 patients was only 3%, suggesting that the UAMS70 classifier would have limited value in the H087/NM18 patient group.<sup>34</sup>

In a previous report from our group the SKY92 classifier was combined with ISS staging, resulting in a powerful classifier which distinguishes a low- and two intermediate-risk groups in addition to the SKY92 high-risk group.<sup>26</sup> In that report the lowest risk patients – defined by SKY92 standard-risk and ISS-I – had a median OS of more than 8 years. Strikingly, in the H087/NM18 study, 86% of patients in this lowest risk group is still alive after 3 years which is higher than observed for any other marker. The relatively short median follow up of less than three years means that the current study does not offer full insight into the lower risk groups. Still, this result confirms previously identified potential of this marker. In the multivariate analysis SKY92 was shown to be an independent prognostic factor, together with both clinical and cytogenetic markers. Also del(13q) is independently associated with both OS and PFS. This marker is currently not considered to be an important prognostic factor.<sup>35,36</sup> However, also in a previous analysis we performed, del(13q) was found to be a strong independent marker which may be of complementary value to prognostication.<sup>26</sup>

It must be noted that the multivariate analysis reported here consisted of t(4;14), t(11;14), t(14;16), gain1q, del(17p) and del(13q), which incorporated

additional FISH markers that were not included in the analysis on the total HO87/NM18 cohort by Zweegman *et al.*<sup>24</sup> Translocations t(11;14), t(14;16) and del(13q) were unique to the analysis reported here. Univariate hazard ratios for the overlapping markers had the same direction and magnitude in both studies, e.g. t(4;14)  $HR_{pfs} = 2.3 [1.3-4.0]$  in our study compared to  $HR_{pfs} = 2.2 [1.6-3.1]$  in the study of the entire trial population.

A potentially interesting but small group of patients (2.6%) was identified both R-ISS-III and SKY92 high-risk: out of four patients, three died within 5 months. Data from other cohorts is required to assess the value of this observation. Future analyses of the HOVON-123 (EudraCT:2013-000320-33) and HOVON-126 (EudraCT:2013-003266-14) may be of interest in this context. HOVON-123 and HOVON-126 are aimed at elderly MM patients, evaluating bortezomib and ixazomib in this patient population, respectively.

In a previous study, the SKY92 classifier was investigated in mostly elderly patients included in the non-intensive treatment arm of the MRC-IX trial, treated with either melphalan-prednisone or cyclophosphamide-thalidomide-dexamethasone.<sup>15,37</sup> Also in that cohort, SKY92 was able to identify high-risk MM patients. Comparable median OS values for the high-risk groups were found (high-risk MRC-IX: 19 months; high-risk HO87/NM18: 21 months), whereas the OS of the entire group (i.e. high- and standard-risk) was very different (MRC-IX: 29 months; HO87/NM18: 49 months).<sup>26</sup> In that study, a higher proportion of SKY92 high-risk patients was found (24%) compared to the proportion in the HO87/NM18 cohort (14%). The difference in proportion may be attributed to the proportion of ISS-III patients which is almost twice as high in the non-intensive MRC-IX cohort compared to the HO87/NM18 cohort (51% in MRC-IX and 27% in HO87/NM18), which in turn is likely caused by a difference in exclusion criteria between the studies. Surprisingly, within the SKY92 high-risk patients, the difference between the proportions of patients with ISS-III was less distinct in the MRC-IX and HO87/NM18 trial; 57 and 42% respectively. SKY92 high-risk groups demonstrate some additional similarities across these studies, including OS (19 months, high-risk MRC-IX non-intensive cohort and 21 months in high-risk HO87/NM18 patients) and the occurrence of FISH aberrations (FISH comparison: online Table S3). The similarity in OS is reminiscent of the similarity

---

in the median OS in three trials of transplant eligible newly diagnosed patients published previously, with median OS of 34, 40, and 33 months (MRC-IX, TT2 and TT3, respectively; see Kaplan Meier curves in Kuiper *et al.*<sup>15</sup>

Finally, it is evident that SKY92 defined high-risk patients are not the same as high-risk patients defined by FISH; there are high-risk FISH patients outside the SKY92 high-risk group and vice versa. Both the FISH high-risk only and SKY92 high-risk only patients have a poor OS with the patients positive for both having the highest risk. Studies aimed at incorporating risk stratification into trial design, whether this is by FISH or by gene classifier (e.g. MRC-XI or SWOG-S1211),<sup>31,38</sup> will ultimately result in evidence based recommendations for high-risk patients.

## 4

In conclusion, in addition to R-ISS and HR-FISH analysis, SKY92 is a robust classifier to identify high-risk patients in elderly MM patients. Combining SKY92 with R-ISS may result in a definition of a small group of patients with dismal prognosis; conversely, combining SKY92 with ISS results in identification of a group of patients of substantial size with favorable outlook.



## REFERENCES

1. SEER. National Cancer Institute; Surveillance, Epidemiology, and End Results Program. <http://seer.cancer.gov/> (June 17) . 2016; .
2. Zweegman S, Palumbo A, Bringhen S, & Sonneveld P. Age and aging in blood disorders: multiple myeloma. *Haematologica* . 2014; **99**(7):1133–7.
3. Palumbo A, Bringhen S, Ludwig H, *et al*. Personalized therapy in multiple myeloma according to patient age and vulnerability: a report of the European Myeloma Network (EMN). *Blood* . 2011; **118**(17):4519–29.
4. Greipp PR, San Miguel J, Durie BG, *et al*. International staging system for multiple myeloma. *J Clin Oncol* . 2005; **23**(15):3412–20.
5. Terpos E, Katodritou E, Roussou M, *et al*. High serum lactate dehydrogenase adds prognostic value to the international myeloma staging system even in the era of novel agents. *Eur J Haematol* . 2010; **85**(2):114–9.
6. Anagnostopoulos A, Gika D, Symeonidis A, *et al*. Multiple myeloma in elderly patients: prognostic factors and outcome. *Eur J Haematol* . 2005; **75**(5):370–5.
7. Lode L, Eveillard M, Trichet V, *et al*. Mutations in TP53 are exclusively associated with del(17p) in multiple myeloma. *Haematologica* . 2010; **95**(11):1973–6.
8. Shaughnessy J J D. Amplification and overexpression of CKS1B at chromosome band 1q21 is associated with reduced levels of p27Kip1 and an aggressive clinical course in multiple myeloma. *Hematology* . 2005; **10 Suppl 1**:117–26.
9. Teoh PJ, Chung TH, Sebastian S, *et al*. p53 haploinsufficiency and functional abnormalities in multiple myeloma. *Leukemia* . 2014; **28**(10):2066–74.
10. Teoh PJ & Chng WJ. p53 abnormalities and potential therapeutic targeting in multiple myeloma. *Biomed Res Int* . 2014; **2014**:717919.
11. Gertz MA, Lacy MQ, Dispenzieri A, *et al*. Clinical implications of t(11;14)(q13;q32), t(4;14)(p16.3;q32), and -17p13 in myeloma patients treated with high-dose therapy. *Blood* . 2005; **106**(8):2837–40.
12. Ross FM, Ibrahim AH, Vilain-Holmes A, *et al*. Age has a profound effect on the incidence and significance of chromosome abnormalities in myeloma. *Leukemia* . 2005; **19**(9):1634–42.
13. Avet-Loiseau H, Hulin C, Campion L, *et al*. Chromosomal abnormalities are major prognostic factors in elderly patients with multiple myeloma: the intergroupe francophone du myelome experience. *J Clin Oncol* . 2013; **31**(22):2806–9.
14. Palumbo A, Avet-Loiseau H, Oliva S, *et al*. Revised International Staging System for Multiple Myeloma: A Report From International Myeloma Working Group. *J Clin Oncol* . 2015; **33**(26):2863–9.
15. Kuiper R, Broyl A, de Knecht Y, *et al*. A gene expression signature for high-risk multiple myeloma. *This thesis and Leukemia* . 2012; **26**(11):2406–13.
16. Sonneveld P, Schmidt-Wolf IG, van der Holt B, *et al*. Bortezomib induction and maintenance treatment in patients with newly diagnosed multiple myeloma: results of the randomized phase III HOVON-65/ GMMG-HD4 trial. *J Clin Oncol* . 2012; **30**(24):2946–55.

- 
17. Broyl A, Hose D, Lokhorst H, *et al.* Gene expression profiling for molecular classification of multiple myeloma in newly diagnosed patients. *Blood* . 2010; **116**(14):2543–53.
  18. Shaughnessy J J D, Zhan F, Burington BE, *et al.* A validated gene expression model of high-risk multiple myeloma is defined by deregulated expression of genes mapping to chromosome 1. *Blood* . 2007; **109**(6):2276–2284.
  19. Pineda-Roman M, Zangari M, Haessler J, *et al.* Sustained complete remissions in multiple myeloma linked to bortezomib in total therapy 3: comparison with total therapy 2. *Br J Haematol* . 2008; **140**(6):625–634.
  20. Morgan GJ, Davies FE, Gregory WM, *et al.* Cyclophosphamide, thalidomide, and dexamethasone as induction therapy for newly diagnosed multiple myeloma patients destined for autologous stem-cell transplantation: MRC Myeloma IX randomized trial results. *Haematologica* . 2012; **97**(3):442–50.
  21. Mulligan G, Mitsiades C, Bryant B, *et al.* Gene expression profiling and correlation with outcome in clinical trials of the proteasome inhibitor bortezomib. *Blood* . 2007; **109**(8):3177–3188.
  22. van Beers E, van Vliet M, Kuiper R, *et al.* Prognostic validation of SKY92 and its combination with International Staging System in an independent cohort of Multiple Myeloma patients. *Clinical Lymphoma, Myeloma and Leukemia* . 2017; **17**(9):555–562.
  23. van Vliet M, Ubels J, de Best L, van Beers EH, & Sonneveld P. The combination of SKY92 and ISS provides a powerful tool to identify both high risk and low risk multiple myeloma cases, validation in two independent cohorts [abstract]. *Blood* . 2015; **126**(23):2970.
  24. Zweegman S, van der Holt B, Mellqvist UH, *et al.* Melphalan, prednisone, and lenalidomide versus melphalan, prednisone, and thalidomide in untreated multiple myeloma. *Blood* . 2016; **127**(9):1109–16.
  25. Ross FM, Avet-Loiseau H, Ameye G, *et al.* Report from the European Myeloma Network on interphase FISH in multiple myeloma and related disorders. *Haematologica* . 2012; **97**(8):1272–7.
  26. Kuiper R, van Duin M, van Vliet MH, *et al.* Prediction of high- and low-risk multiple myeloma based on gene expression and the International Staging System. *Blood* . 2015; **126**(17):1996–2004.
  27. R Core Team. R: A language and environment for statistical computing. *R Foundation for Statistical Computing, Vienna, Austria.* (<https://www.R-project.org/>) . 2016; .
  28. Cox DR & Oakes D. *Analysis of Survival Data.* Taylor & Francis. 1984.
  29. Therneau TM & Grambsch PM. *Modeling survival data : extending the Cox model.* Springer, New York. 2000.
  30. Fay MP. Confidence intervals that match Fisher’s exact or Blaker’s exact tests. *Biostatistics* . 2010; **11**(2):373–4.
  31. Sherborne A, Begum D, Price A, *et al.* Identifying Ultra-High Risk Myeloma By Integrated Molecular Genetic and Gene Expression Profiling [abstract]. *Blood* . 2016; **128**(22):4407.
  32. van Vliet MH, Jasielc J, Dytfeld D, *et al.* Prognostic and Predictive Gene Expression Profiling (GEP) Markers Confirmed in Carfilzomib, Lenalidomide, and Dexamethasone (KRd) Treated Newly Diagnosed Multiple Myeloma (NDMM) Patients. *Blood* . 2014; **124**(21):2141.

33. van Laar R, Flinchum R, Brown N, *et al.* Translating a gene expression signature for multiple myeloma prognosis into a robust high-throughput assay for clinical use. *BMC Med Genomics* . 2014; **7**:25.
34. Kuiper R. Application of gene classifiers. *geneClassifiers R package* . 2017; .
35. Fonseca R, Oken MM, & Greipp PR. The t(4;14)(p16.3;q32) is strongly associated with chromosome 13 abnormalities in both multiple myeloma and monoclonal gammopathy of undetermined significance. *Blood* . 2001; **98**(4):1271–2.
36. Kalf A & Spencer A. The t(4;14) translocation and FGFR3 overexpression in multiple myeloma: prognostic implications and current clinical strategies. *Blood Cancer J* . 2012; **2**(9):e89.
37. Dickens NJ, Walker BA, Leone PE, *et al.* Homozygous deletion mapping in myeloma samples identifies genes and an expression signature relevant to pathogenesis and outcome. *Clin Cancer Res* . 2010; **16**(6):1856–1864.
38. Usmani SZ, Sexton R, Ailawadhi S, *et al.* Phase I safety data of lenalidomide, bortezomib, dexamethasone, and elotuzumab as induction therapy for newly diagnosed symptomatic multiple myeloma: SWOG S1211. *Blood Cancer J* . 2015; **5**:e334.



# CHAPTER

# 5

## **Nopaco: A Non-Parametric test for concordance in unbalanced data**

Rowan Kuiper, Sjoerd M.H.Huisman, Remco Hoogenboezem,  
Pieter Sonneveld & Mark van Duin

Submitted

---

## ABSTRACT

No method currently exists to test for differences between two coefficients of concordance. Especially if they are based on non-similar underlying distributions. Here we have extended previous work on concordance coefficients, resulting in a non-parametric concordance coefficient (*nopaco*), applicable to real valued repeated measurements. Importantly, a coefficient can be determined for unbalanced data (i.e. data in which there are an unequal number of measurements between subjects) and may include tied values. Subsequently we have developed a method to compare the coefficients found. First we show how to determine the coefficient and its sampling properties. Next we describe methods to test whether true concordance is found, i.e. is the concordance better than random - including an algorithm to obtain exact p-values - and whether two concordance coefficients are significantly different from each other. These tests are demonstrated in two real life examples in which i) the concordances and differences between concordances are assessed for three gene models in an unbalanced set of gene expression profiles and ii) two state of the art models for risk assessment in multiple myeloma are compared based on concordance between replicate measurements. The concordance tests are available via the CRAN repository <https://CRAN.R-project.org/package=nopaco> as the *nopaco* R package.

## INTRODUCTION

Gene expression profiling (GEP) involves the genome-wide, parallel detection of mRNA levels, for instance in patient samples. GEP based classification models - aimed to predict the disease course of a specific patient and even to guide treatment choice - were developed for various cancer types. Our work focuses on multiple myeloma, a type of cancer in which malignant plasma cells accumulate in the bone marrow. Like any other laboratory measurement, GEP based classification models should report the same outcome if repeated under the same conditions. Due to the variability in observing, measuring and testing, this can be difficult to achieve.

For multiple myeloma patients several prognostic GEP classification models were developed, and were demonstrated to have a clear correlation to survival in independent datasets. Still, there is no absolute agreement between these models, i.e. different models predict partly overlapping, partly different patients with high-risk disease. The best performing models include EMC92 and UAMS70.<sup>1,2</sup> These models have comparable performance in terms of association to overall survival and as a result, consensus on the best model to use has not been reached. Whether these models with good performance report the same results in repeated measurements under unchanged conditions has not yet been assessed. This can be expressed in terms of concordance.

Several characteristics are used to categorize coefficients of concordance.<sup>3</sup> These include the number of measurements that can be simultaneously compared, sampling theory (e.g. parametric or non-parametric), exchangeability of measurements, and whether replicate measurements are considered to be random or fixed. In case of normally distributed continuous data, a suitable parametric method is the intra class correlation coefficient (ICC).<sup>4</sup> The ICC is an analysis of variance (ANOVA) approach to measure concordance between any number of replicate measurements. This can be a one way random effect model - in which no structural bias between measurements is assumed such that measurements are exchangeable - or a two way random effect model with possible structural bias between measurements. The two way model is largely equivalent to the parametric concordance correlation coefficient.<sup>5,6</sup> This coefficient was originally applica-

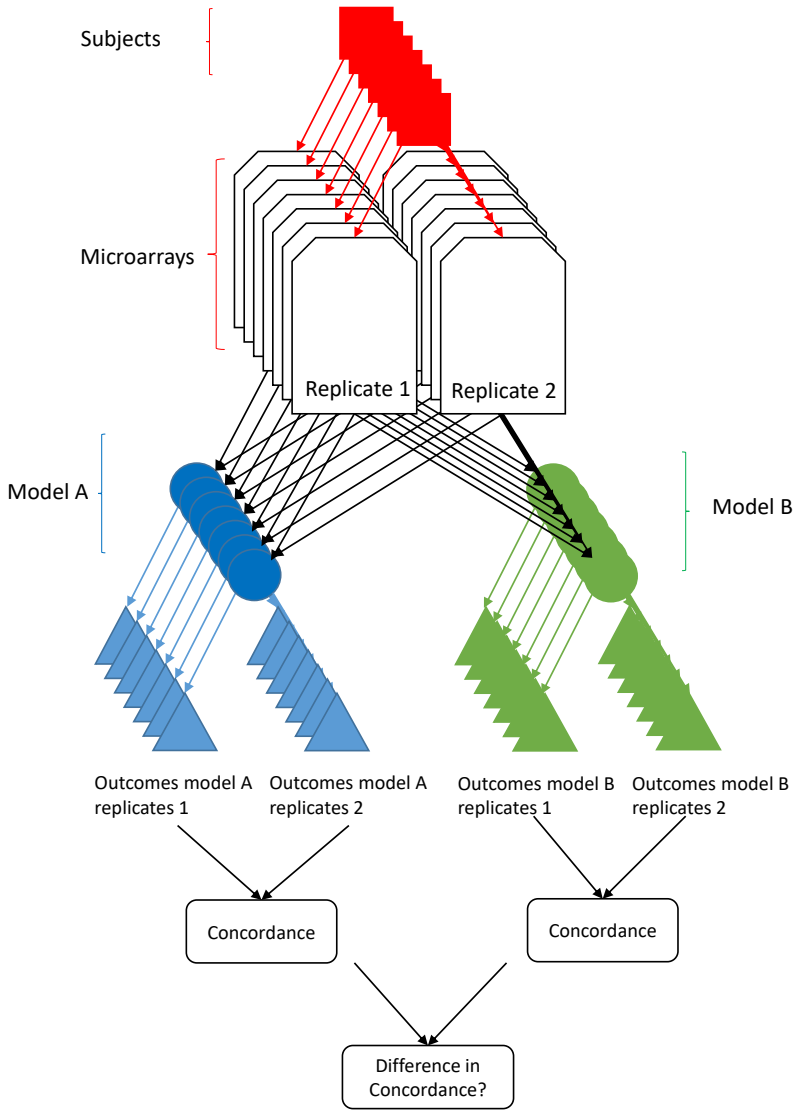


**Figure 1. Methodology visualized for a microarray setting.** Gene expression profiles of multiple subjects are obtained by microarray measurements. Although in this case two replicates for each subject are shown, any number of replicates or an unequal number of replicate measurements between subjects is allowed. Even subjects with single measurements contribute. These measurements serve as input for two different models (A and B) that estimate a quantity of interest (e.g. survival prediction). Concordances between the replicate outputs within both models are determined, and the presence of a difference between the two concordances is assessed.



ble to two replicate measurements only, but it was extended to allow for more replicates, the addition of confounding variables, categorical data, and distance functions that are more robust than the mean squared difference.<sup>7</sup>

The non-parametric analogue of the one way ICC - which is applicable to balanced designs - has been described by Rothery. Because non-parametric methods protect against inconsistencies arising from incompatible distributions, we have used this method as the basis for quantifying the difference between concordance coefficients. We have extended the coefficient for use in unbalanced or incomplete data with or without tied values, and described its sampling properties. Our non-parametric coefficient - termed *nopaco* - is particularly suitable for GEP for which it is difficult to obtain complete series of repeated measurements, due to cost and scarcity of the biological material. Because balanced design is not required, *nopaco* can integrate data with single measurements with series of repeated measurements. Furthermore, the hypothesis of random concordance can be tested in an exact test as well as the hypothesis of absence of differences between two concordance coefficients. *nopaco* is available as an R package '*nopaco*' (see CRAN; <https://CRAN.R-project.org/package=nopaco>).

# Non-parametric concordance coefficient for multi-observer continuous measurements

We will start below by describing the non-parametric concordance coefficient reported by Rothery for repeated measurements in balanced and unbalanced data.

Non-parametric concordance is defined in terms of triplets of measurements: a pair of measurements drawn from the same subject and a third measurement from an unrelated subject is discordant if the third measurement falls between the paired measurements. The concordance coefficient  $\bar{\psi}$  is then defined as the complement of the ratio between the number of discordant triplets  $\Delta$  in the data and the total number of triplets  $\omega$ :

$$\bar{\psi} = 1 - \frac{\Delta}{\omega}. \tag{5.1}$$

## 5

### Balanced data

In the following example, the concordance coefficient is calculated for a hypothetical balanced scenario of  $b = 3$  repeated measurements on  $n = 4$  subjects described by matrix  $Y$ . The input measurements in  $Y$  are transformed to ordered rank space in  $R$ , such that the distance between subsequently ranked measurements within each subject can be determined in  $Q$ :  $Y =$

$$Y = \begin{pmatrix} 50.2 & 45.1 & 12.3 \\ 542.2 & 19391.1 & 120.6 \\ 84.6 & 74.3 & 48.8 \\ 169.0 & 1368.7 & 126.0 \end{pmatrix} \mapsto$$

$$R = \begin{pmatrix} 1 & 2 & 4 \\ 7 & 10 & 12 \\ 3 & 5 & 6 \\ 8 & 9 & 11 \end{pmatrix} \mapsto Q = \begin{pmatrix} 0 & 1 \\ 2 & 1 \\ 1 & 0 \\ 0 & 1 \end{pmatrix}. \quad Q \text{ contains the information required to}$$

determine the number of discordant triplets  $\Delta = \mathbf{1}^T Q \phi_b = (1 \ 1 \ 1 \ 1) \times$

$$\begin{pmatrix} 0 & 1 \\ 2 & 1 \\ 1 & 0 \\ 0 & 1 \end{pmatrix} \times \begin{pmatrix} 4 \\ 4 \end{pmatrix} = 24. \text{ The total number of possible triplets } \omega = nb^2(b-1)(n-1) =$$

$$216 \text{ resulting in } \bar{\psi} = 1 - \frac{\Delta}{\omega} = 1 - \frac{24}{216} = \frac{8}{9}.$$

To explain the above algorithm, consider an experiment in which the gene expression profile of  $n > 1$  independent subjects are determined repeatedly in  $b > 1$  replicate measurements (Figure 1). The number of replicate profiles is assumed to be equal for all subjects (i.e. balanced) such that there are  $nb$  measured profiles. Each profile is used as input for a model which yields an output  $y_{i,j} \in \mathbf{Y} \in \mathbb{R}^{n \times b}$  for subject  $i = (1, \dots, n)$  in replicate  $j = (1, \dots, b)$ .

The concordance coefficient between the replicate model outcomes in matrix  $\mathbf{Y}$  depends on the number of discordant triplets  $\Delta$ . Whether a triplet is concordant or discordant (as defined above) only depends on the relative values within the triplet and is not affected by the ordering of the replicate measurements within a subject. Therefore  $\mathbf{Y}$  can be represented by an ordered rank matrix  $\mathbf{R}$ . Let  $1 \leq r_{i,1} \leq r_{i,2} \leq \dots \leq r_{i,b} \leq nb$ , in which element  $r_{ij} \in \mathbf{R}$  reflects the rank of the  $j$ 'th lowest measurement within subject  $i$ , relative to all measurements in  $\mathbf{Y}$ .

Note that the difference between the ranks in the columns minus one, corresponds to the number of occurrences  $q_{i,k}$  that satisfy  $r_{i,k} < r_{u,v} < r_{i,k+1}$  for  $u \neq i$ . So we define the matrix

$$\mathbf{Q} = \begin{pmatrix} q_{1,1} & \dots & q_{1,(b-1)} \\ \dots & \dots & \dots \\ q_{n,1} & \dots & q_{n,(b-1)} \end{pmatrix} = \begin{pmatrix} (r_{1,2} - r_{1,1} - 1) & \dots & (r_{1,b} - r_{1,(b-1)} - 1) \\ \dots & \dots & \dots \\ (r_{n,2} - r_{n,1} - 1) & \dots & (r_{n,b} - r_{n,(b-1)} - 1) \end{pmatrix}. \tag{5.2}$$

If  $r_{u,v}$  falls between the  $k$ 'th and  $(k + 1)$ 'th smallest values in a subject with  $b$  measurements, there are  $f(k, b) = 2k(b - k)$  possible ways to permute the order of measurements within the subject. The number of discordant triplets is then given by  $\Delta = \mathbf{1}^T \mathbf{Q} \phi_b$  in which  $\mathbf{1}$  is a vector of ones, and vector  $\phi_b = f(k, b)$  for  $k = (1, \dots, (b - 1))$ .

In the balanced case, the total number of triplets  $\omega$  is derived from the fact that there are  $b(b - 1)$  unique paired measurements within each of the  $n$  subjects (i.e.  $nb(b - 1)$ ) which are combined with  $b(n - 1)$  measurements from other subjects to form triplets. This gives the total number of triplets  $\omega = nb^2(b - 1)(n - 1)$ .

The maximum value of  $\bar{\psi} = 1$  occurs when the values within each subject are ranked consecutively. Following Rothery, the minimum value evaluates to  $\frac{2}{3} - \frac{1}{3b}$

---

and occurs when rankings within subjects are a distance of  $n$  apart.

## Unbalanced data

Here we generalize the concordance coefficient to apply it to unbalanced data, which can be a result of taking an unequal number of replicate measurements or of randomly missing data. A step-by-step example is given in online Appendix A.

Note that the definition of concordance easily extends toward unbalanced situations. In case of an unequal number of measurements between subjects, let  $\mathbf{B}$  be the set of all observed number of measurements per subject. Instead of a single matrix  $\mathbf{Q}$ , all subjects with  $b \in \mathbf{B}$  measurements will now be assigned to the matrix  $\mathbf{Q}_b$ . Each of these matrices have their own column vector  $\phi_b$  that has been fully defined above. The number of discordant triplets then is:  $\Delta = \sum_{\forall b \in \mathbf{B}} \mathbf{1}^T \mathbf{Q} \phi_b$

To find the total number of triplets, let  $b_i$  be the number of measurements within subject  $i$  and  $t = \sum_{i=1}^n b_i$  be the total number of measurements. Then subject  $i$  has  $b_i(b_i - 1)$  number of unique pairwise measurements. Each pair of measurements is compared against all  $t - b_i$  measurements not part of subject  $i$ . Therefore, the general formulation of the total number of triplets is  $\omega = \sum_{i=1}^n b_i (b_i - 1) (t - b_i)$ .

Note that in the unbalanced case even subjects with single measurements contribute to the concordance coefficient, provided there is at least a single subject with more than one measurement.

## Handling ties

The concordance coefficient is determined by comparing all measurements based on their rank. If all measurements differ, the ranks are well defined. Tied values by definition result in ranks of the same value. Although values randomly drawn from a continuous distribution are theoretically impossible, in practice they are likely to occur, for example due to a low measurement resolution, rounding numbers or winsorization. This type of tied values - which are intrinsically continuous in nature - can be resolved by considering that either measurement in a set of tied values is smaller or larger than the other with equal probability.

Consider the following input matrix  $\mathbf{Y} = \begin{bmatrix} 3 & 3 & 3 & 3 \\ 0 & 2 & 2 & 3 \\ 0 & 0 & 1 & 1 \end{bmatrix}$ , containing a limited set of measurement values  $y_{i,j} \in \{0, 1, 2, 3\}$  such that ties must occur. Due to ties there are  $3! \times 2! \times 2! \times 5! = 2880$  different but equally likely possible ways to rank the values in this matrix. The average rank of a measurement  $x \in \mathbf{Y}$  is determined as  $E[r_x] = \frac{1}{2} \left[ \sum_{i,j} I(y_{i,j} < x) + \sum_{i,j} I(y_{i,j} \leq x) \right]$ . However, in order to determine matrix  $\mathbf{Q}$ , the ranks are to be ordered within each subject such that instead of replacing tied values by their average rank, we have to consider the possible configurations of the ranked values when ordered into the ordered rank matrix.

As an example, consider the subject in the top row of  $\mathbf{Y}$  which contains  $k = 4$  tied values  $x = 3$  with  $v = 1$  tied value not in the subject. The average rank of these elements evaluates to  $E[r_{x=3}] = 10$ . However, after sorting the ranks within each subject, the last element has an ordered rank of  $r_{1,4} = 12$  in four out of five configurations, and one in which it evaluates to  $r_{1,4} = 11$  resulting in an expected order rank of  $E[r_{1,4}] = \frac{4 \times 12 + 1 \times 11}{5} = 11\frac{4}{5}$ . In general, the ordered rank of measurement  $y_{i,j}$  evaluates to  $E[r_{i,j}|k, v] = E[r_{i,j}] + \left(m - \frac{k+1}{2}\right) \left(1 + \frac{v}{k+1}\right)$  for  $m = (1, \dots, k)$  being the  $m^{th}$  tied value in subject  $i$ . This gives the ordered

rank matrix  $E[\mathbf{R}] = \begin{bmatrix} 8\frac{1}{5} & 9\frac{2}{5} & 10\frac{3}{5} & 11\frac{4}{5} \\ 2 & 6 & 7 & 10 \\ 1\frac{1}{3} & 2\frac{2}{3} & 4 & 5 \end{bmatrix}$  with corresponding matrix  $E[\mathbf{Q}] =$

$\begin{bmatrix} \frac{1}{5} & \frac{1}{5} & \frac{1}{5} \\ 3 & 0 & 2 \\ \frac{1}{3} & \frac{1}{3} & 0 \end{bmatrix}$  resulting in a concordance coefficient of  $\bar{\psi} = \frac{187}{216}$ .

## Sampling properties

### Mean and variance of $\bar{\psi}$ under random sampling conditions

The mean and variance of  $\bar{\psi}$  under random sampling conditions for the balanced case were described by Rothery as  $E[\bar{\psi}] = \frac{2}{3}$  and  $Var(\bar{\psi}) = \frac{4}{45} \frac{(t+1)}{\omega}$ . The mean also holds for the unbalanced case but the variance expands to  $Var(\bar{\psi}) =$

$$\frac{t+1}{45\omega^2} \left[ \left( \sum_{i=1}^n b_i (b_i - 1) (b_i + 3) (t - b_i) \right) - \left( \sum_{i=1}^n \sum_{j=1}^n (b_i - 1) b_i (b_j - 1) b_j \right) \right], \quad \text{for } i \neq j \text{ as is derived in online Appendix B.}$$

## Asymptotic normality

The coefficient  $\bar{\psi}$  can be written as the average over subject specific concordances:  $\sum_i^n \frac{\psi_i}{n}$ . A subject specific concordance coefficient expresses the probability that a randomly drawn measurement not from that subject will fit between a randomly drawn pair of measurements from that subject. Therefore, by definition there is a dependency between subjects such that  $Cov(\psi_i, \psi_j) \neq 0$  for any  $1 \leq i \neq j \leq n$ . However  $\lim_{n \rightarrow \infty} Cov(\psi_i, \psi_j) = 0$ . According to the central limit theorem, independent sample averages will asymptotically converge to a normal distribution irrespective of their original distributions such that the distribution of  $\bar{\psi}$  is asymptotically normal.

5

## Inference

### Testing the difference between two concordance coefficients

The hypothesis  $H_0 : \bar{\psi}(\mathbf{R}_1) - \bar{\psi}(\mathbf{R}_2) = 0$  which expresses equal concordance for the two equally sized rank matrices  $\mathbf{R}_1$  and  $\mathbf{R}_2$ , is compared against the alternative  $H_a : |\bar{\psi}(\mathbf{R}_1) - \bar{\psi}(\mathbf{R}_2)| > 0$ . Let  $\mathbf{X} = \begin{bmatrix} \mathbf{X}_1 & \mathbf{X}_2 \end{bmatrix} \sim N(\mu = 0, \Sigma_0)$  with standard normal marginal distributions and  $\Sigma_0 = \begin{pmatrix} \Sigma_{1,1} & \Sigma_{1,2} \\ \Sigma_{2,1} & \Sigma_{2,2} \end{pmatrix}$ . By assuming  $\mathbf{R}_1$  and  $\mathbf{R}_2$  were generated from  $\mathbf{X}_1$  and  $\mathbf{X}_2$  - in order for the null hypothesis to hold - each non diagonal element in  $\Sigma_{1,1}$  and  $\Sigma_{2,2}$  is expected to have similar Pearson correlation values  $\rho_1$  while all others including the elements within  $\Sigma_{1,2}$  and  $\Sigma_{2,1}$  are  $\rho_2$ .

In general, however, it cannot be assumed that a multivariate normal distribution underlies the rank matrices. Using the relationship between the population estimate of the Pearson correlation  $\rho$  and the concordance coefficient  $\bar{\psi} = 1 - \frac{1}{\pi} \arccos\left(\frac{1}{2}(1 + \rho)\right)$  an unbiased sample correlation matrix  $\hat{\Sigma}$  can be obtained.<sup>8</sup>

The covariance matrix of a multivariate standard normal distribution is known to have a Wishart distribution<sup>9</sup>:  $(n - 1) \hat{\Sigma} \sim W_b(\Sigma_0, n - 1)$  such that  $\Sigma_0$  is obtained by finding the values for  $\rho_1$  and  $\rho_2$  that maximize the likelihood of the Wishart distribution given the observed  $\hat{\Sigma}$ . As shown in online Appendix C, this evaluates to the average correlation over the corresponding elements in  $\hat{\Sigma}$ , such that  $\rho_1 = \frac{1}{2b(b-1)} \sum_i^b \sum_{j \neq i}^b (\hat{\sigma}_{i,j} + \hat{\sigma}_{(i+b),(j+b)})$  and  $\rho_2 = \frac{1}{2b^2} \sum_i^b \sum_j^b (\hat{\sigma}_{(i),(2b-j+1)} + \hat{\sigma}_{(2b-i+1),(j+b)})$ . Having set the value of  $\Sigma_0$  by its maximum likelihood estimate, many random instances of  $\mathbf{X}$  can be generated thereby obtaining an estimate of the joint distribution under the null hypothesis  $P(\bar{\psi}(\mathbf{X}_1), \bar{\psi}(\mathbf{X}_2))$  such that the  $p$ -value corresponding to  $H_0$  is reported as  $p(|\bar{\psi}(\mathbf{X}_1) - \bar{\psi}(\mathbf{X}_2)| > |\bar{\psi}_1 - \bar{\psi}_2|)$ . As the distribution for  $\bar{\psi}$  is asymptotically normal,  $\bar{\psi}_1 - \bar{\psi}_2$  is asymptotically normal. We approximate the distribution of  $H_0$  as  $H_0 \sim N(\mu = 0, \sigma^2 = s^2)$  with  $s^2$  being the observed variance for  $\bar{\psi}(\mathbf{X}_1) - \bar{\psi}(\mathbf{X}_2)$ . Confidence intervals are obtained by the above sampling approach using  $\hat{\Sigma}$  instead of  $\Sigma_0$ .

### Testing the hypothesis of a random concordance coefficient

If repeated measurement values are randomly paired, random concordance resulting in  $E[\bar{\psi}] = \frac{2}{3}$  will be observed. The appropriate test for absence of concordance has a null hypothesis  $H_0 : \bar{\psi} \leq \frac{2}{3}$  which is compared against the alternative  $H_a : \bar{\psi} > \frac{2}{3}$ . Although the distribution of  $\bar{\psi}$  has been described previously as a recursive expression which is applicable in the case of balanced data with two replicate measurements<sup>10</sup>, in general there is no simple expression. As a solution, we designed an algorithm which traces every possible path through a directed graph to obtain the exact probability mass function of the concordance coefficient under  $H_0$ . The algorithm is given in online Appendix D. The implementation in the *nopaco* package runs within 30 seconds on an Intel(R) Core™i7-4712HQ 2.3GHz CPU in case of a sample sizes of  $n < 150$  with  $b = 2$ ,  $n < 50$  with  $b = 3$ ,  $n < 25$  with  $b = 4$  or  $n < 11$  with  $b = 7$ . Still, for larger data sets approximations are probably more convenient. As the statistic is asymptotically normal, an option is to use the normal or the beta approximations as described by Rothery. However, these approximations tend to be anti-conservative (Figure

2). In contrast, an approximation referred to as the revised beta approximation (online Appendix E) gives  $p$ -value estimates which are close to exact for larger number of subjects and in contrast to the normal and beta approximations are mostly conservative (Figure 2).

## Power estimation

The power to accept the alternative one sided hypothesis for the *nopaco* coefficient ( $H_a : \bar{\psi} > \frac{2}{3}$ ) and the intraclass correlation ( $H_a : \rho > 0$ ) have been estimated in a multivariate normal and multivariate log normal setting for various values of  $b$  and  $n$ . (Figure 3 and Supplemental Tables). In case the data has a normal distribution the ICC has the largest power. However, after a log normal transformation of the data this power drops below the power of *nopaco*, which is invariant to monotonic non-linear transformations. For increasing values of  $n$  and  $b$ , the power increases in both settings for both methods.

## Real life examples

The main aim of model building is to accurately model a variable of interest such that it is applicable to unseen data. As stated above, generating concordant results is important for the application of a model in real life, an aspect which is often overlooked in model building. Indeed, some models may be more robust against sources of variation, e.g. in the pre-processing of samples, and these models are consequentially likely to demonstrate a higher concordance coefficient than others. In the examples below, data is obtained using MAS5.0 normalized gene expression (default settings; R Bioconductor 'affy' package version 1.50.0;<sup>11,12</sup>), measured using Affymetrix gene arrays.

### Comparison of models based on low, medium and high expression

First we will show an example of GEP profiles obtained from 264 multiple myeloma patients. Replicate gene expression measurements were available for most patients (range: 1-12; single measurement:  $n=10$ ; 3 replicates per patient ( $n=160$ ); 6 replicates per patient ( $n=59$ ) or other ( $n=35$ )). Each measurement



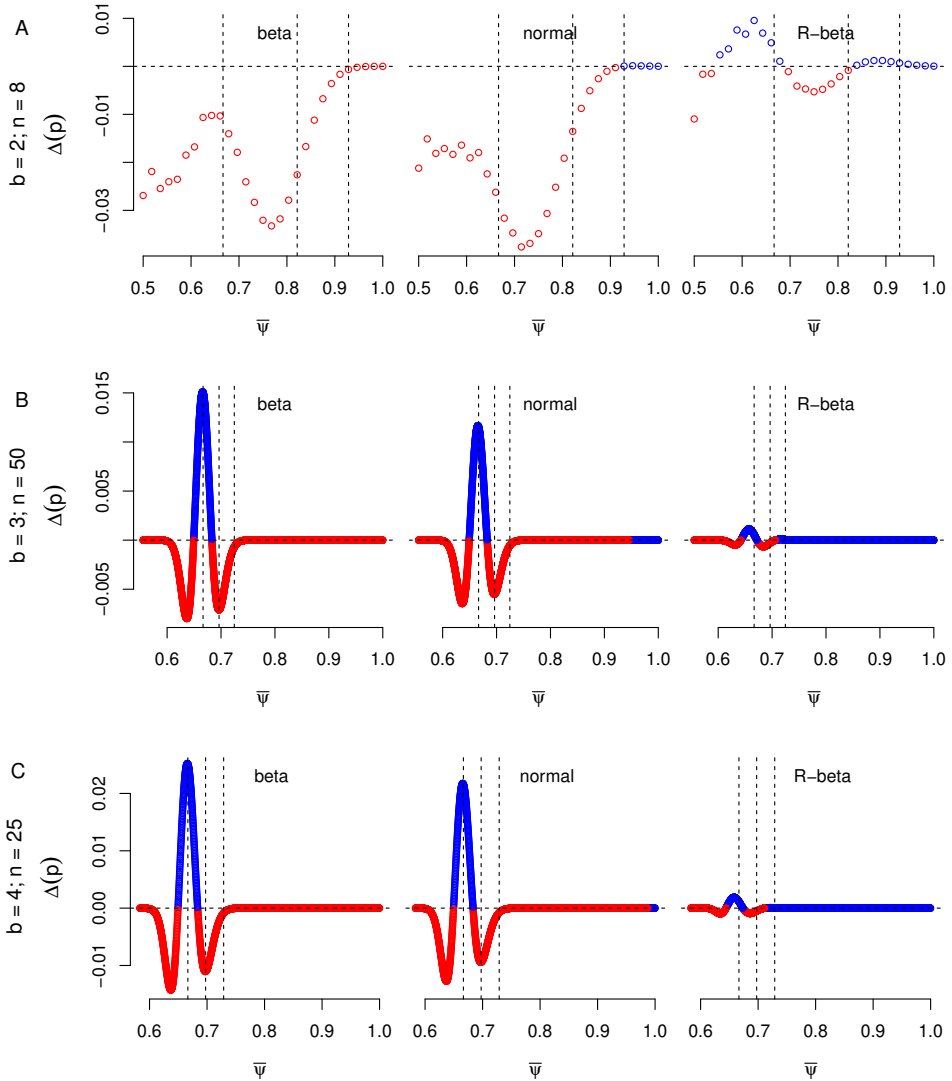


**Figure 2. Differences  $\Delta(p)$  in  $p$ -values between approximations and the exact approach over the complete range of all possible values of  $\bar{\psi}$ .** Approximations are by the beta distribution (left), normal distribution (center) and Revised-beta method (right). The plots in show the comparisons for a data set of size A)  $b = 2; n = 8$ , B)  $b = 3; n = 50$  and C)  $b = 4; n = 25$ . Blue segments indicate conservative estimates (i.e.  $\Delta(p) > 0$ ), red segments are anti-conservative  $p$ -value estimates (i.e.  $\Delta(p) < 0$ ). The left vertical dashed lines indicate  $\bar{\psi} = \frac{2}{3}$ , the two right-most vertical dashed lines indicate the value of  $\bar{\psi}$  at which  $p = 0.05$  and  $p = 0.005$  respectively according to the exact approach.

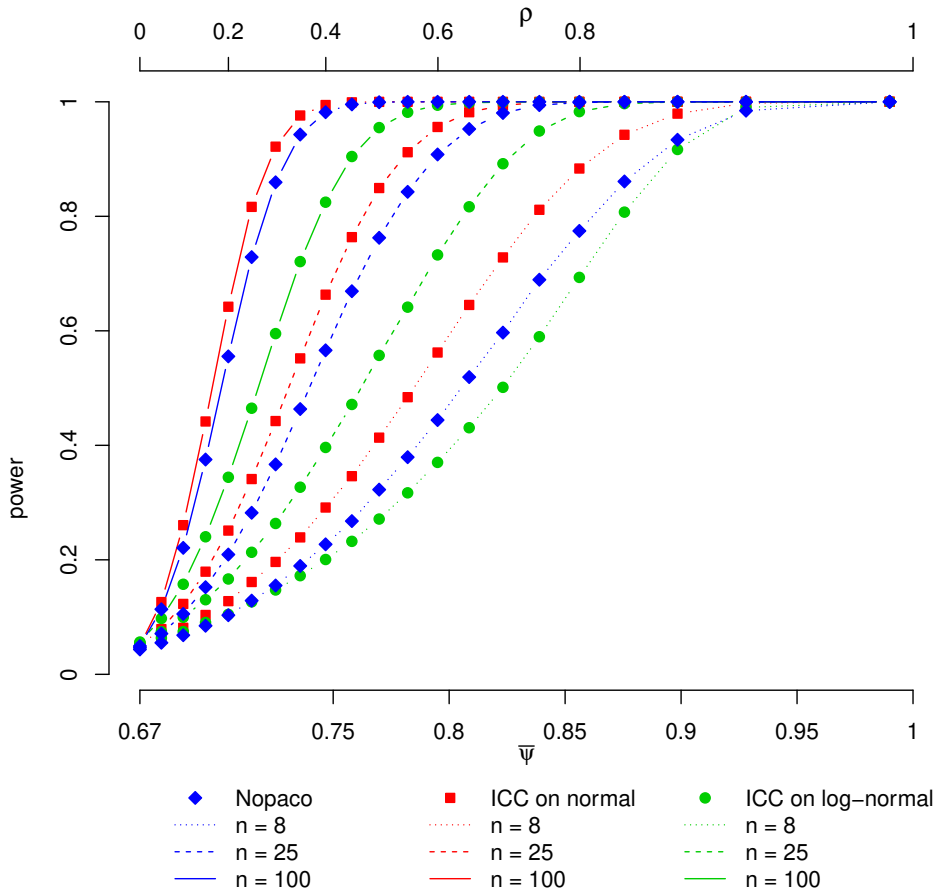


**Figure 3. Power analysis** Power for *nopaco* and the ICC in a multivariate normal and a multivariate log normal setting at  $b = 2$  for varying values of concordance ( $\bar{\psi}$ ), correlation ( $\rho$ ) and numbers of samples ( $n$ ).

was performed using an Affymetrix Human Genome U133A Array (22283 probe sets).

We define three models, in each case a score was generated by taking the sum of the expression values of 20 probe sets. These 20 probe sets are randomly selected and differ between the three models based on their average expression; either  $< 32$  (i.e. low expression), between 32 and 1024 (intermediate expression) or  $> 1024$  (high expression). These three models produce a score for each patients' replicate expression data. The concordance between the replicates are shown in Table 1.

**Table 1. Concordance  $\bar{\psi}$  between replicates for the models based on low, intermediate and highly expressed genes and the differences between their concordances  $\delta$  in 264 patients .**

Model	$\bar{\psi}$	95% lower bound	$p(\bar{\psi})$ exact	$\delta$	95% CI	$p(\delta)$
Low	0.799	0.781	$1.4 \times 10^{-53}$	-0.0407	[-0.0521 - -0.0069]	$5.7 \times 10^{-5}$
Intermediate	0.840	0.819	$2.8 \times 10^{-79}$	-0.0491	[-0.0754 - -0.0338]	$2.9 \times 10^{-6}$
High	0.889	0.866	$3.0 \times 10^{-114}$			

It is clear the models become more concordant when based on the higher expressed genes. This is in accordance with previous reports on microarray stability studies in which it was shown that lower expressed genes tended to have lower signal-to-noise ratios than higher expressed genes.<sup>13</sup>

### Precision and difference in precision between prognostic models

In multiple myeloma two alternative prognostic gene models have been described with comparable performance in survival analyses. These are the EMC92-score and the UAMS70-score which are based on 92 and 70 genes, respectively, of which the genes *LTBP1* and *BIRC5* are present in both models.<sup>1,2</sup> The prognostic scores are calculated using the R Bioconductor 'geneClassifiers' package. Briefly, CD138 enriched multiple myeloma samples were run on the Affymetrix HG-U133 Plus2 array, and resulting CEL files were normalized by MAS5.0 followed by log2 transformation. The score was calculated by taking the weighted summation of the expression values of specific genes (R Bioconductor 'geneClassifiers' package<sup>14</sup>).

Seven biological samples (either myeloma cell lines or heart RNA) were profiled 36 times under normal operational variations (e.g. varying reagent lots, operator, scanner). From these profiles, model-scores were obtained for both EMC92 and UAMS70 which are considered to reflect the full range of practically possible outcome values.

As shown in Figure 4, there is a linear relation between the two models which report their score on different scales. The concordance between the replicates is the same for both models ( $\bar{\psi} = 0.986$ ). Clearly no significant difference in concordance between the two models can be detected.

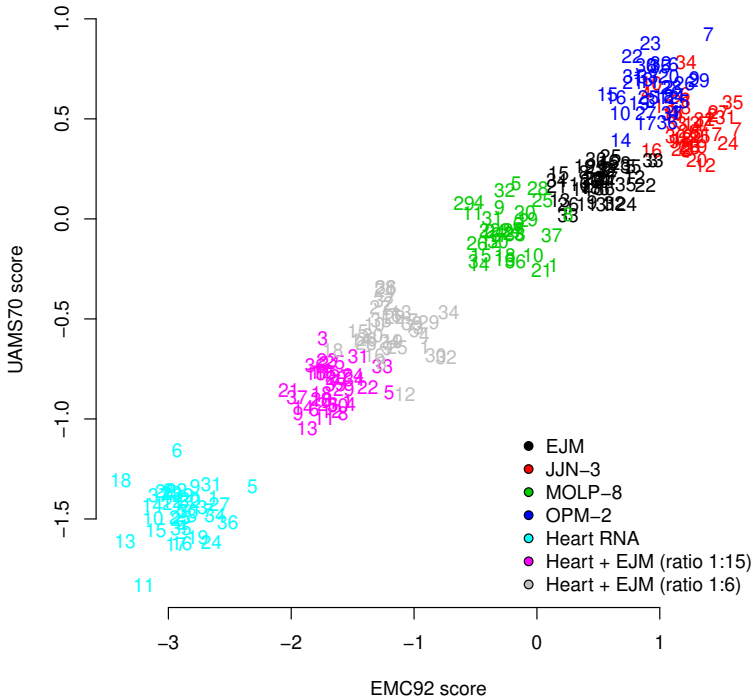


**Figure 4. Outcome of the EMC92 (horizontal) and UAMS70 (vertical) for each of the seven biological samples.** For each sample, 36 replicate measurements were performed as indicated by the numbers.

## Summary and discussion

In this study we describe *nopaco*, a method for calculating concordance by extending the concordance coefficient previously described by Rothery. This coefficient is defined as the complement of the probability that a randomly drawn measurement fits between a pair of measurements from another subject in the same population. Instead of balanced data - in which each subject has a similar number of replicate measurements - *nopaco* is applicable to unbalanced data as well, such that a failed replicate measurement does not automatically invalidate the experiment. In addition, subjects for which only single measurements are available, still contribute to the concordance estimate. This is an advantage par-

ticularly for experiments which are performed on limited patient material (like GEP).

In order to test the deviation from random sampling, Rothery recommended the use of a null distribution based on a normal, or preferably a beta approximation. Instead we were able to define an exact approach, and noticed the recommended methods often resulted in anti-conservative estimates, especially the beta variant. Therefore, for larger sized data - in which the exact approach becomes computationally infeasible - we described a more conservative revised beta approximation.

Being non-parametric, the power to detect a deviation from random sampling is slightly reduced compared to its parametric counterpart, the intra-class correlation coefficient. However, by relying on a non-parametric coefficient, an unbiased comparison can be made between any two coefficients, irrespective of the distribution of their underlying data. Therefore, differences between concordances as observed for any device or method which monitor similar phenomena can be determined (e.g. different blood pressure monitors, psychological tests, etc.).

In our case, the concordances for two gene models were determined and compared in two scenarios: 1) to demonstrate that gene models based on genes that are higher expressed produce more concordant results and 2) that the concordance between replicate measurement for two risk stratification models in multiple myeloma were found to be high. Moreover, there was no evidence that one of the two models was more concordant than the other.

In conclusion, *nopaco* is a non-parametric concordance coefficient that is applicable to unbalanced data with tied values that enables the unbiased assessment of the difference between two coefficients. The concordance coefficient is implemented in the R package *nopaco* which is publically available via the CRAN repository <https://CRAN.R-project.org/package=nopaco>.

---

## REFERENCES

1. Kuiper R, Broyl A, de Knegt Y, *et al.* A gene expression signature for high-risk multiple myeloma. *Leukemia* . 2012; **26**(11):2406–2413.
2. Shaughnessy JD, Zhan F, Burington BE, *et al.* A validated gene expression model of high-risk multiple myeloma is defined by deregulated expression of genes mapping to chromosome 1. *Blood* . 2007; **109**(6):2276–2284.
3. Müller R & Büttner P. A critical discussion of intraclass correlation coefficients. *Statistics in medicine* . 1992; **13**:2465–2476.
4. Shrout P & Fleiss J. Intraclass Correlations: Uses in Assessing Rater Reliability. *Psychological bulletin* . 1979; **86**:420–428.
5. Lin L. A Concordance Correlation Coefficient to Evaluate Reproducibility. *Biometrics* . 1989; **45**:255–268.
6. Carrasco J & Jover J. The concordance correlation coefficient estimated through variance components. *Biometrics* . 2003; **59**:849–858.
7. King TS & Chinchilli VM. A generalized concordance correlation coefficient for continuous and categorical data. *Statistics in medicine* . 2001; **20**(14):2131–2147.
8. Rothery P. A nonparametric measure of intraclass correlation. *Biometrika* . 1979; **66**(3):629–639.
9. Gupta AK & Nagar DK. Matrix variate distributions, volume 104. CRC Press. 1999.
10. Lukš A. A nonparametric test of zero intrapair correlation. *Aplikace matematiky* . 1983; **28**(2):91–102.
11. Gautier L, Cope L, Bolstad BM, & Irizarry RA. affy—analysis of Affymetrix GeneChip data at the probe level. *Bioinformatics* . 2004; **20**(3):307–315.
12. Huber W, Carey VJ, Gentleman R, *et al.* Orchestrating high-throughput genomic analysis with Bioconductor. *Nature methods* . 2015; **12**(2):115–121.
13. Kuo WP, Jenssen TK, Butte AJ, Ohno-Machado L, & Kohane IS. Analysis of matched mRNA measurements from two different microarray technologies. *Bioinformatics* . 2002; **18**(2):405–412.
14. Kuiper R. geneClassifiers: Application of gene classifiers. 2016. R package version 0.99.6.

## CHAPTER

# 6

### **High Cereblon Expression is Associated with Better Survival in Patients with Newly Diagnosed Multiple Myeloma Treated with Thalidomide Maintenance**

Annemiek Broyl, Rowan Kuiper, Mark van Duin, Bronno van der Holt, Laila el Jarari, Uta Bertsch, Sonja Zweegman, Arjan Buijs, Dirk Hose, Henk M. Lokhorst, Hartmut Goldschmidt & Pieter Sonneveld

*Blood* 2013; **121**(4):624-7

---

## ABSTRACT

Recently, cereblon (*CRBN*) expression was found to be essential for the activity of Thalidomide and lenalidomide. In the present study, we investigated whether the clinical efficacy of Thalidomide in multiple myeloma is associated with *CRBN* expression in myeloma cells. Patients with newly diagnosed multiple myeloma were included in the HOVON-65/GMMG-HD4 trial, in which postintensification treatment in 1 arm consisted of daily Thalidomide (50mg) for 2 years. Gene-expression profiling, determined at the start of the trial, was available for 96 patients who started Thalidomide maintenance. In this patient set, increase of *CRBN* gene expression was significantly associated with longer progression-free survival ( $p = .005$ ). In contrast, no association between *CRBN* expression and survival was observed in the arm with Bortezomib maintenance. We conclude that *CRBN* expression may be associated with the clinical efficacy of Thalidomide. This trial has been registered at the Netherlands Trial Register ([www.trialregister.nl](http://www.trialregister.nl)) as NTR213; at the European Union Drug Regulating Authorities Clinical Trials (EudraCT) as 2004-000944-26; and at the International Standard Randomized Controlled Trial Number (ISRCTN) as 64455289.



## INTRODUCTION

Introduction of Thalidomide, Bortezomib, and lenalidomide has greatly improved induction treatment for multiple myeloma (MM).<sup>1-4</sup> Attention is now shifting toward improving consolidation and maintenance therapy.<sup>5</sup> Thalidomide and lenalidomide represent immunomodulatory drugs (IMiDs) with variable efficacy during maintenance after high-dose therapy and in the nontransplantation setting.<sup>6-8</sup> So far, there are no biomarkers for prediction of outcome after Thalidomide and/or lenalidomide treatment. *CRBN* was recently identified as the target gene responsible for the teratogenic effects of Thalidomide.<sup>9</sup> *CRBN* levels were also shown to be critical for the antitumor activity of lenalidomide and Thalidomide in both in vitro model systems and in lenalidomide-resistant patients.<sup>10</sup> In the present study, we report that *CRBN* expression is associated with outcome of Thalidomide maintenance in newly diagnosed MM patients.

---

# MATERIALS AND METHODS

## Patients and procedures

In the HOVON-65/GMMG-HD4 trial, patients with newly diagnosed MM were randomly assigned to receive either VAD (Vincristine, Adriamycin, and Dexamethasone) induction, intensification with high-dose Melphalan (HDM), and autologous stem cell transplantation (ASCT) followed by maintenance therapy with Thalidomide or PAD (Bortezomib, Adriamycin, and Dexamethasone), HDM, and ASCT followed by maintenance with Bortezomib. The maximum duration of maintenance therapy in both arms was 2 years.<sup>11</sup> Patients randomized to VAD received maintenance with Thalidomide 50 mg daily for 2 years starting 4 weeks after HDM. This study was approved by the ethics committees of the Erasmus University MC, the University of Heidelberg, and the participating sites. All patients gave written informed consent and the trial was conducted according to the European Clinical Trial Directive 2005 and the Declaration of Helsinki.

## 6

## Response assessments and end points

Clinical characteristics were registered at diagnosis. Cytogenetic studies were performed as described previously.<sup>12</sup> For this subanalysis, progression-free survival (PFS) and overall survival (OS) were measured from start of the maintenance treatment. For PFS, progression was used as the end point and for OS, death from any cause. Patients alive at the date of last contact were censored. Evaluation of response is described in detail in supplemental Table S4.

## GEP and statistical analysis

The gene-expression profiling (GEP) dataset GSE19784 was used, which was derived from patients included in the HOVON-65/GMMG-HD4 trial.<sup>11,13</sup> *CRBN* expression was assessed using the intensity values of the probe sets *218142\_s\_at* and *222533\_at*, combined using the method of Dai *et al.*<sup>14</sup> Presence calls for *CRBN* expression were determined with the PANP algorithm using standard settings (see the PANP reference manual on the Bioconductor web site, <http://bioconductor.org/packages/panp/>).<sup>15</sup> Details of the quantitative RT-PCR

are given in online Figure S3. Multivariate Cox regression analysis was performed to assess the value of *CRBN* as a prognostic factor in relation to the International Staging System (ISS) and high-risk cytogenetics, as described previously.<sup>11</sup>

---

## RESULTS AND DISCUSSION

### Patients and response

A total of 833 patients were enrolled in the HOVON65/GMMG-HD4 trial. Of the patients randomized to the VAD arm, 77 of 347 (22%) went off protocol after HDM because of allo-SCT ( $n = 21$ , 6%), persisting toxicity ( $n = 11$ , 3%), or other reasons ( $n = 45$ , 13%), whereas 270 (78%) patients started Thalidomide maintenance treatment. Normal completion of Thalidomide maintenance was achieved in 73 of 270 (27%) patients. Eleven of 270 Thalidomide maintenance patients underwent allo-SCT and were not considered in this subanalysis. Of the remaining 259 patients, GEP and survival data were available for 96. Baseline characteristics between this subgroup ( $n = 96$ ) and the remainder ( $n = 163$ ) were comparable (online Table S1). Present calls were found for both *CRBN* probe sets in 95 of 96 Thalidomide maintenance cases, with one patient demonstrating a borderline present call (“M”) for one probe set and a present call for the other. A significant correlation was found between *CRBN* gene expression measured by microarray (National Center for Biotechnology Gene Expression Omnibus [NCBI-GEO] repository: GSE19784) and quantitative RT-PCR (Spearman  $\rho = 0.67$ ,  $p = .002$ ,  $n = 18$ ; online Figure S3). The EMC clustering represents our gene expression based classification of MM.<sup>16</sup> Of the clusters evaluated, the CTA cluster demonstrated a significantly higher *CRBN* expression compared with the other clusters (Bonferroni-Holm corrected  $p = .01$ , online Figure S2).<sup>16</sup>

In univariate Cox regression analysis, *CRBN* expression was significantly associated with PFS (hazard ratio = 0.68; 95% confidence interval, [0.52 – 0.89];  $p = .005$ ) and with OS (hazard ratio = 0.65; 95% confidence interval, [0.43 – 0.97];  $p = .04$ ; Table 1). Kaplan-Meier analysis was used solely for visualization with *CRBN* expression split in 2 or 4 groups using median or quartile intensities: patients with *CRBN* expression above the median demonstrated longer PFS compared with patients with *CRBN* levels below the median ( $p = .009$ ; Figure 1a-b quartile intensities and online Figure S4). In addition, an optimal *CRBN* cutoff was calculated (online Table S2). For this calculation, the PFS data that prohibit use of this cutoff in this dataset for any analyses related to PFS were used. In contrast,

**Table 1. Cox regression analyses.** HR indicates hazard ratio; and 95%CI, 95% confidence interval**a. Univariate PFS**

Covariate	HR [95%CI]	p
CRBN	0.68 [0.52 – 0.89]	0.005

**b. Univariate OS**

Covariate	HR [95%CI]	p
CRBN	0.65 [0.43 – 0.97]	0.04

**c. Multivariate PFS**

Covariate	HR [95%CI]	p
CRBN	0.66 [0.45 – 0.96]	0.03
ISS = 2	2.35 [1.2 – 4.8]	0.02
ISS = 3	2.55 [1.2 – 5.4]	0.01
High-risk FISH*	2.82 [1.59 – 5.00]	0.0004

**d. Multivariate OS**

Covariate	HR [95%CI]	p
CRBN	0.75 [0.42 – 1.3]	0.32
ISS = 2	4.66 [1.4 – 15.8]	0.01
ISS = 3	5.49 [1.7 – 18.1]	0.005
High-risk FISH*	3.65 [1.5 – 8.7]	0.003

\*High-risk FISH is defined as having del(17p) and/or 1q gain and/or t(4;14).

the median expression value was arbitrarily chosen and used for analysis in relation to response upgrade. Multivariate Cox regression analysis was performed on 81 patients for whom the following covariates were available: ISS, continuous *CRBN* levels, and high-risk FISH [del(17p) and/or 1q gain and/or t(4;14)]. Higher *CRBN* levels remained significantly related to longer PFS, but not OS, with a hazard ratio of 0.66 ( $p = .03$ ) and 0.75 ( $p = .3$ ), respectively (Table 1). No significant correlation was found between any of these covariates and *CRBN*, but lower *CRBN* expression was found in ISS=III compared with either ISS=I or ISS=II (Bonferroni corrected  $p = .10$  by Kruskal Wallis test). The *CRBN* gene is positioned on chromosome 3. Chromosome 3 trisomies are frequently found in patients with hyperdiploidy and, indeed, *CRBN* levels were significantly higher in hyperdiploid patients compared with nonhyperdiploid patients ( $p = .005$ ). However, in a multivariate Cox regression analysis, *CRBN* levels, but not hyperdiploidy, were found to be related to PFS ( $p = .006$  and  $p = .8$ , respectively; data not shown).

*CRBN* expression was not associated with an upgrade of response, considered to be improvement of response during Thalidomide maintenance ( $p = .3$ , online

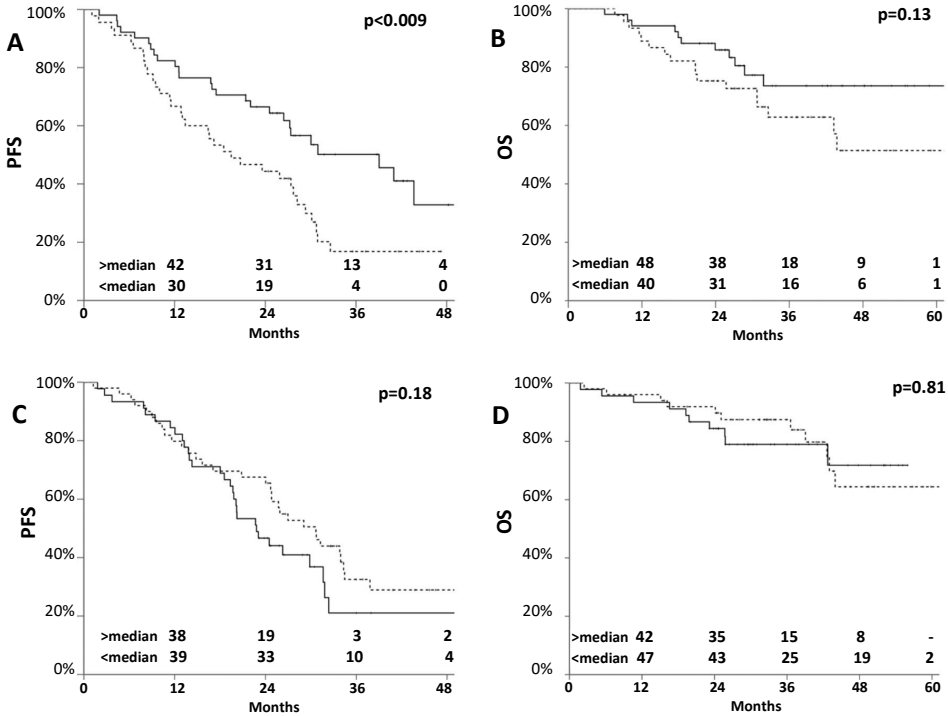


**Figure 1. *CRBN* expression in HOVON-65/GMMG-HD4** Shown is *CRBN* expression in relation to PFS and OS Kaplan-Meier curves of *CRBN* expression in relation to survival in Thalidomide treated patients (a-b) and in relation to Bortezomib treated patients (c-d). PFS is shown at left; OS on the right. Log-rank p-values are shown in the right corner of each panel. Broken lines indicate *CRBN* expression levels below the median and solid lines indicate expression levels above the median. Remaining patients at risk are shown above the x-axis (PFS at 1, 2, 3, and 4 years and OS at 1, 2, 3, 4, and 5 years). The median *CRBN* expression was determined on the combined data of both Thalidomide and Bortezomib treated patients: 45 of 96 patients were below the median in the Thalidomide subset, whereas 50 of 95 were below the median in the Bortezomib subset.

Table S4). To determine whether *CRBN* expression was specifically relevant for the outcome of Thalidomide treatment, we also examined the relationship between *CRBN* expression and survival in patients treated with Bortezomib maintenance. No association was observed between *CRBN* expression and PFS/OS after Bortezomib maintenance (Figure 1c-d). For validation of these results, the MRC-IX study was evaluated.<sup>17</sup> Only 30 patients with gene expression were available who received Thalidomide during maintenance but not during induction. This subset was too small to allow solid analysis of the relationship between *CRBN* expression and outcome after Thalidomide maintenance. Finally, *CRBN* forms an

E3 ubiquitin ligase complex with the proteins DDB1 and CUL4A.<sup>9</sup> This complex has been suggested to be involved in the regulation of  $\beta$ -catenin activity, which in turn affects downstream targets such as CCND1 and C-MYC. CRBN was also found to bind to AMPK $\alpha$ 1 (PRKAA1) and to the large conductance Ca<sup>2+</sup>-activated potassium channel KCNMA1.<sup>18</sup> In a multivariate model with *CRBN* levels, only *CCND1* and *CRBN* were found to be independently related to longer PFS (online Table S3). A relationship with PFS was not found for either *CCND1* or *CRBN* in the patients treated with Bortezomib in the maintenance phase.

In conclusion, in the present study, we observed that higher expression of CRBN was associated with increased PFS during maintenance treatment with Thalidomide, but not in patients with Bortezomib maintenance. This corresponds well to the report of reduced CRBN expression in > 85% of MM patients who were lenalidomide resistant.<sup>10</sup> Our observations warrant analysis of the predictive effect of CRBN expression in newly diagnosed and relapsed/refractory patients treated with IMiDs as part of induction and consolidation treatment.

---

## REFERENCES

1. Richardson PG, Sonneveld P, Schuster MW, *et al.* Bortezomib or high-dose dexamethasone for relapsed multiple myeloma. *N Engl J Med* . 2005; **352**(24):2487–2498.
2. Richardson PG, Barlogie B, Berenson J, *et al.* A phase 2 study of bortezomib in relapsed, refractory myeloma. *N Engl J Med* . 2003; **348**(26):2609–2617.
3. Dimopoulos M, Spencer A, Attal M, *et al.* Lenalidomide plus dexamethasone for relapsed or refractory multiple myeloma. *N Engl J Med* . 2007; **357**(21):2123–32.
4. Weber DM, Chen C, Niesvizky R, *et al.* Lenalidomide plus dexamethasone for relapsed multiple myeloma in North America. *N Engl J Med* . 2007; **357**(21):2133–42.
5. Palumbo A, Attal M, & Roussel M. Shifts in the therapeutic paradigm for patients newly diagnosed with multiple myeloma: maintenance therapy and overall survival. *Clin Cancer Res* . 2011; **17**(6):1253–63.
6. Palumbo A, Hajek R, Delforge M, *et al.* Continuous lenalidomide treatment for newly diagnosed multiple myeloma. *N Engl J Med* . 2012; **366**(19):1759–69.
7. Attal M, Lauwers-Cances V, Marit G, *et al.* Lenalidomide maintenance after stem-cell transplantation for multiple myeloma. *N Engl J Med* . 2012; **366**(19):1782–91.
8. Mahindra A, Laubach J, Raje N, Munshi N, Richardson PG, & Anderson K. Latest advances and current challenges in the treatment of multiple myeloma. *Nat Rev Clin Oncol* . 2012; **9**(3):135–43.
9. Ito T, Ando H, Suzuki T, *et al.* Identification of a primary target of thalidomide teratogenicity. *Science* . 2010; **327**(5971):1345–50.
10. Zhu YX, Braggio E, Shi CX, *et al.* Cereblon expression is required for the antimyeloma activity of lenalidomide and pomalidomide. *Blood* . 2011; **118**(18):4771–9.
11. Sonneveld P, Schmidt-Wolf IG, van der Holt B, *et al.* Bortezomib induction and maintenance treatment in patients with newly diagnosed multiple myeloma: results of the randomized phase III HOVON-65/ GMMG-HD4 trial. *J Clin Oncol* . 2012; **30**(24):2946–55.
12. Neben K, Lokhorst HM, Jauch A, *et al.* Administration of bortezomib before and after autologous stem cell transplantation improves outcome in multiple myeloma patients with deletion 17p. *Blood* . 2012; **119**(4):940–8.
13. Broyl A, Corthals SL, Jongen JL, *et al.* Mechanisms of peripheral neuropathy associated with bortezomib and vincristine in patients with newly diagnosed multiple myeloma: a prospective analysis of data from the HOVON-65/GMMG-HD4 trial. *Lancet Oncol* . 2010; **11**(11):1057–65.
14. Dai M, Wang P, Boyd AD, *et al.* Evolving gene/transcript definitions significantly alter the interpretation of GeneChip data. *Nucleic Acids Res* . 2005; **33**(20):e175.
15. Warren P, Taylor D, Martini P, Jackson J, & Bienkowska J. PANP - a New Method of Gene Detection on Oligonucleotide Expression Arrays. *Bioinformatics and Bioengineering, 2007. BIBE 2007. Proceedings of the 7th IEEE International Conference on* . 2007; :108–115.
16. Broyl A, Hose D, Lokhorst H, *et al.* Gene expression profiling for molecular classification of multiple myeloma in newly diagnosed patients. *Blood* . 2010; **116**(14):2543–53.



17. Morgan GJ, Gregory WM, Davies FE, *et al.* The role of maintenance thalidomide therapy in multiple myeloma: MRC Myeloma IX results and meta-analysis. *Blood* . 2012; **119**(1):7–15.
18. Chang XB & Stewart AK. What is the functional role of the thalidomide binding protein cereblon? *Int J Biochem Mol Biol* . 2011; **2**(3):287–94.



# CHAPTER

## **Genetic Factors Underlying the Risk of Bortezomib Induced Peripheral Neuropathy in Multiple Myeloma Patients**

Sophie L. Corthals, Rowan Kuiper, David C. Johnson,  
Pieter Sonneveld, Roman Hajek, Bronno van der Holt,  
Florence Magrangeas, Hartmut Goldschmidt,  
Gareth J. Morgan & Hervé Avet-Loiseau

---

## ABSTRACT

Bortezomib induced peripheral neuropathy is a dose-limiting side effect and a major concern in the treatment of multiple myeloma. To identify genetic risk factors associated with the development of this side effect in Bortezomib treated multiple myeloma patients, a pharmacogenetic association study was performed using a discovery set (IFM 2005-01;  $n = 238$ ) and a validation set (HOVON-65/GMMG-HD4 and a Czech dataset;  $n = 231$ ). After multiplicity correction, none of the 2149 single nucleotide polymorphisms tested revealed any significant association with Bortezomib induced peripheral neuropathy. However, 56 single nucleotide polymorphisms demonstrated an association with Bortezomib induced peripheral neuropathy with pointwise, uncorrected significance. Pathway analysis of these polymorphisms demonstrated involvement of neurological disease (FDR < 20%). Also a clear enrichment of major Bortezomib metabolizing genes was found. Univariate evaluation of these 56 polymorphisms in the validation set demonstrated one single nucleotide polymorphism with pointwise significance: *rs619824* in *CYP17A1*.

## INTRODUCTION

The introduction of Bortezomib (Millennium Pharmaceuticals, Cambridge, MA, USA), an inhibitor of the 26S proteasome, has greatly improved the management of multiple myeloma (MM).<sup>1</sup> The dose-limiting toxicity of Bortezomib is peripheral neuropathy, which frequently requires a dose reduction or treatment discontinuation.<sup>2-4</sup> Bortezomib induced peripheral neuropathy (BiPN) differs from pre-existing peripheral neuropathy associated with 10% of untreated MM patients. BiPN, described in detail by Delforge *et al.*,<sup>4</sup> is predominantly sensory, reversible in most cases, and characterized by distal paresthesias, numbness and neuropathic pain.

A multifactorial pathogenesis for BiPN seems likely, with suggested mechanisms including blockade of nerve-growth-factor-mediated neuronal survival through inhibition of the activation of nuclear factor  $\kappa$ B (NF $\kappa$ B),<sup>5</sup> damage to mitochondria and the endoplasmic reticulum through activation of apoptosis,<sup>6</sup> dysregulation of mitochondrial calcium homeostasis,<sup>7</sup> autoimmune factors, interference with mRNA processing, and translation<sup>8</sup> and inflammation.<sup>9,10</sup> A number of studies, including a report by our own group, have looked at the pharmacogenetic characterization of BiPN.<sup>11,12</sup> In the study carried out by our group, the comparison between early onset (within one treatment cycle) BiPN and late onset (after two or three treatment cycles) BiPN revealed that genes for apoptosis contribute to early onset BiPN, whereas genes that have a role in inflammatory pathways and DNA repair contribute to the development of late onset BiPN, indicating that distinct genetic factors are involved in the development of early onset and late onset forms of this side effect.<sup>11</sup> Recently, Favis *et al.* reported on the association between SNPs and the time to Bortezomib induced peripheral neuropathy within the VISTA trial with associated SNPs including a SNP in the gene *CTLA4*.<sup>12</sup>

In this study, we further explore the genetic risk factors associated with the development of BiPN in patients with MM who had not been previously treated with Bortezomib. A large dataset from the IFM 2005-01 trial was used as discovery set. In addition, a dataset based on the patients from the HOVON-65/GMMG-HD4 trial were used as a validation set.<sup>11</sup>

---

# MATERIALS AND METHODS

## Patients

The study was performed on patients who had been included in two randomized clinical trials, i.e. the Institutional Review Board-approved HOVON-65/GMMG-HD4 (ISRCTN64455289) trial for newly diagnosed patients with MM ( $n = 833$ ), and the IFM 2005-01 trial (NCT00200681;  $n = 493$ ) approved by the ethics committee of the University of Nantes, both of which compared standard induction treatment (VAD) with a Bortezomib combination prior to high-dose therapy (HDT) and stem cell transplantation (online Figure S1a). In addition, as part of the cooperative program of the International Myeloma Foundation (IMF) and International Myeloma Working Group (IMWG), a set of 56 patients (i.e. 56 unique DNA samples), uniformly treated with Bortezomib and Dexamethasone at relapse, were obtained. In addition, a prospectively collected set of samples ( $n = 56$ ) from the Babak Research Institute (Czech Republic) was included as part of the cooperative program of the IMF and IMWG. All patients gave written informed consent for this genetic study. Patients with amyloidosis or monoclonal gammopathy of undetermined significance (MGUS) were excluded. Adverse events (AEs) were prospectively assessed using standard National Cancer Institute Common Toxicity Criteria for Adverse Events, version 3.0 (CTCAE 3.0). To ensure homogeneity of allelic frequencies, 15 patients of non-European descent were excluded from the study. In total, 238 of 246 patients from IFM 2005-01, 183 of 412 patients from HOVON-65/GMMG-HD4 and 48 of 56 from the Czech Republic who were randomized for treatment with Bortezomib were included in the analysis. Samples were divided into a discovery and validation set (online Figure S1B and online Table S1).

## Genotyping

DNA was extracted from peripheral blood nucleated cells or CD138 negative bone marrow cells. Genotyping was performed using an Affymetrix targeted genotyping custom built panel, comprising 3404 SNPs. These were selected using a hypothesis-driven strategy, targeting genes and SNPs with previously described

associations or putative functional effects.<sup>13</sup>

## Statistical analysis

After imputation and applying SNP exclusion criteria (minor allele frequency (MAF)  $< 0.05$ , Hardy Weinberg equilibrium  $< 1 \times 10^{-5}$ ), a panel containing 2149 SNPs was analyzed by univariate association analysis using the software package PLINK.<sup>14</sup> Categorical comparisons with respect to frequencies were performed with the  $\chi^2$  or Fisher's exact test, and continuous variables were analyzed using the Mann-Whitney U test (online Table S1).

SNP association analysis comparing grade 1–4 BiPN with no BiPN patients in the discovery set (IFM 2005-01) was performed as previously described.<sup>11</sup>

The associated gene sets were subjected to Ingenuity Pathway Analysis (Ingenuity System Inc., USA) using 2149 SNPs as a reference set. Only the top three associated pathways with a FDR  $\leq 20\%$  are reported.

As validation, a Cochran Mantel-Haenszel stratified association test was performed in an independent dataset comprised of patients from the HOVON-65/GMMG-HD4 trial and patients from the Czech Republic to evaluate cross validating SNP associations and odds ratios (ORs). Specifically, ORs from significant SNPs (pointwise  $p < 0.05$ ) in the discovery set were selected for validation. A one-sided test for OR was performed to test whether the observed effects in the validation set were associated with the same effect direction as observed in the discovery set.

Based on the numbers of the discovery and validation set, a conservative power calculation for both sets was performed. According to this calculation, ORs need to be higher than 2.28 or lower than 0.44 to be found at a significance level of  $\alpha = 0.05$  for SNPs with a MAF of 0.5. These ORs diverge as the MAF decreases (online Figures S2 and S3, online Tables S1 and S2). Please note this is a conservative analysis in which multiplicity correction is performed by Bonferroni correction and no linkage is taken into account.

---

## RESULTS AND DISCUSSION

The BiPN rates and clinical characteristics of both the discovery set ( $n = 238$ ) and the validation set ( $n = 231$ ) are shown in the online Table S1. In the discovery set, 27 patients developed BiPN grade 1, 57 grade 2, 11 grade 3, and 4 grade 4. Online Figure S4 shows the time to BiPN for each grade separately in patients from the HOVON-65/GMMG-HD4 trial, who are included in the validation set. The median time to BiPN grade 1 was six weeks, and seven weeks to grade 2, 3 or 4. The peripheral neuropathy rates in the VAD treatment arm (i.e. not Bortezomib) of the HOVON-65/GMMG-HD4 trial, will not be discussed further here (online Table S3).

After imputation and applying PLINK exclusion filters, a panel containing 2149 SNPs was analyzed for association by conducting a  $\chi^2$  association analysis. None of the SNPs were found to be significantly associated with BiPN using the permuted  $p$ -value correction for multiple testing in the discovery set (IFM2005-01; Table 1). The highest ranking SNP, with corrected  $p$ -value of 0.3, is in the locus of the cell cycle gene *CDKN1B*. This SNP, *rs3759217*, has been evaluated in a number of cancer studies, but was not reported to be significantly associated with any cancer type.<sup>15</sup> Using the pointwise, uncorrected  $p$ -value, 56 SNPs were found to be associated with BiPN in this set (Table 1).

The results of the analysis performed in the discovery set (IFM 2005-01 trial) were validated using an independent dataset from the Czech Republic combined with the dataset from the HOVON-65/GMMG-HD4 trial (online Figure S1). A Cochran Mantel-Haenszel stratified association test was performed. Associated SNPs (pointwise  $p < 0.05$ ) in this validation set are shown in online Table S5. To investigate whether associated SNPs (pointwise  $p < 0.05$ ) in the discovery set and available in the validation set ( $n = 51$ ) had the same direction of effect, a one-sided test for ORs was performed in the validation set. This resulted in one pointwise significantly cross validating SNP; *rs619824* in *CYP17A1* (online Table S6).

*CYP17A1*, cytochrome P-450c17 $\alpha$ , is involved in steroid hormone biosynthesis, and has both steroid 17 $\alpha$ -hydroxylase activity and 17,20-lyase activity.<sup>16</sup> Steroids have been shown to affect nerve cells, and have even been suggested for



use as a therapeutic option to prevent the development of neuropathy.<sup>17</sup> Treatment with progesterone has been reported to increase the expression of myelin protein zero in both rat sciatic nerve and Schwann cells.<sup>17</sup> Due to the paucity of cross validated SNPs, we have examined the SNPs with a significant pointwise  $p$ -value in the discovery set (Table 1). Foremost, we have performed a pathway analysis based on this set of SNPs. This analysis showed enrichment of genes involved in cardiovascular disease (11 genes), genetic disorder (22 genes) and neurological disease (21 genes). The latter include the genes NEFL, PON1, PTGS2 and ABCG2, which have been reported frequently in relation to neurological disease such as Alzheimer's. Previous studies showed that Bortezomib is primarily metabolized by cytochrome P450 isoforms CYP3A4, CYP2C19, CYP1A2, with a minor contribution of CYP2D6 and CYP2C9.<sup>18</sup> The results show an enrichment of the major Bortezomib metabolizing genes within the top 56 SNPs ( $p= 0.0013$ ).

Previously, genes involved in inflammation were found to be associated with late onset BiPN.<sup>11</sup> Indeed, one of the most associated SNPs, *rs3136516* (pointwise  $p= 0.008$ ) was an intronic SNP located in prothrombin (coagulation factor II; F2), which has been reported in relation to the neuro-toxic cascade leading to neurodegenerative diseases.<sup>19</sup> Two SNPs that lie within or in close proximity to the TNF $\alpha$  gene (*rs2857605* and *rs2228088*; online Figure S5) were associated with BiPN. TNF $\alpha$  has been implicated in the pathogenesis of several neurodegenerative diseases, including multiple sclerosis, Alzheimer's disease, and human immunodeficiency virus-related encephalopathy.<sup>20</sup> Additionally, the TNF $\alpha$  system is activated in diabetic polyneuropathy, which leads to increased microvascular permeability, hypercoagulability and even direct nerve damage. Improvement of diabetic polyneuropathy following suppression of TNF $\alpha$  has been shown in several animal models.<sup>21</sup> Furthermore, neuropathic pain, one of the determinants of the CTCAE-neuropathy score, and thus of BiPN severity, is mediated through TNF-mediated induction of stress-activated kinasesap like p38 MAPK.<sup>22</sup>

The NF $\kappa$ B pathway is central to the immune response and two associated SNPs are located in the *IKBKAP* gene; *rs10979601* and *rs10759326*. This is a particularly relevant association because hereditary sensory and autonomic neuropathy type III, or familial dysautonomia (FD), can be caused by mutations in the *IKBKAP* gene, leading to poor development, reduced survival, and progressive de-

**Table 1. SNPs associated with BIPN.** Shown are  $\chi^2$  associations with pointwise  $p < 0.05$ . The genomic inflation factor  $\lambda$  is 1.0201.

SNP	CHR	Alleles	OR [95%CI]	$p(\chi^2)$		Gene	SNP Type	In LD with
				pointwise	permuted			
rs3759217	12	C > T	2.76 [1.58 – 4.84]	<0.001	0.3291	CDKN1B	Locus	
rs11466155	17	C > T	1.87 [1.25 – 2.80]	0.004	0.9744	NGFR	nonsynonymous	
rs6033	1	A > G	2.53 [1.30 – 4.94]	0.006	0.9993	F5	nonsynonymous	rs6018, rs6027
rs2228088	6	G > T	0.56 [0.36 – 0.87]	0.006	1	TNF	nonsynonymous, TAGSNP: TNF 3'UTR	
rs2686184	8	G > A	1.72 [1.19 – 2.49]	0.006	0.9966	FDFT1	nonsynonymous	
rs12721516	1	C > T	0.55 [0.34 – 0.90]	0.007	1	CSF1	nonsynonymous	
rs6945306	7	G > C	1.71 [1.17 – 2.52]	0.007	0.9999	STK31	nonsynonymous	
rs228851	20	G > T	0.59 [0.41 – 0.86]	0.008	0.9998	NFATC2	Intron	
rs3136516	11	A > G	0.61 [0.42 – 0.88]	0.008	1	F2	Intron	
rs584589	17	A > G	2.01 [1.16 – 3.47]	0.009	1	NGFR	Promotor	
rs4148949	10	C > T	0.60 [0.41 – 0.88]	0.010	1	CHST3	Untranslated	rs4148946
rs619824	10	G > T	0.64 [0.44 – 0.93]	0.010	1	CYP17A1	3'UTR	
rs338599	19	G > C	2.97 [1.24 – 7.08]	0.011	1	CYP2S1	nonsynonymous	
rs121	7	A > G	1.61 [1.11 – 2.32]	0.011	1	OSBPL2	Intron	
rs17169	1	T > C	1.65 [1.14 – 2.39]	0.012	1	SLC16A1	Untranslated	rs1049434
rs2239330	16	C > T	0.59 [0.39 – 0.90]	0.012	1	ABCC1	nonsynonymous	rs212090, rs212087
rs2295155	22	C > A	0.43 [0.23 – 0.81]	0.012	1	GARD10	Intron	
rs2976437	8	A > G	1.63 [1.13 – 2.37]	0.013	1	NEFL	Promotor	rs2976436
rs2033178	12	C > T	2.42 [1.23 – 4.74]	0.014	1	IGF1	Intron	
rs878201	1	G > A	1.54 [1.04 – 2.29]	0.015	1	Admixture	Admixture	
rs1149901	10	C > T	1.62 [1.07 – 2.45]	0.015	1	GATA3	Locus, untranslated	
rs2973015	5	A > G	0.63 [0.44 – 0.91]	0.017	1	GHR	Intron	
rs2227956	6	T > C	0.52 [0.30 – 0.88]	0.018	1	HSPA1L	nonsynonymous	
rs504122	13	C > T	0.63 [0.43 – 0.93]	0.018	1	SPRY2	nonsynonymous	
rs1641536	17	G > A	0.43 [0.22 – 0.86]	0.021	1	SHBG	3'UTR	
rs2472299	15	G > A	0.62 [0.42 – 0.92]	0.022	1	CYP1A1	Promotor	
rs9885672	6	T > C	1.86 [1.08 – 3.21]	0.024	1	KIAA0274	nonsynonymous	
rs163078	2	C > T	0.63 [0.43 – 0.92]	0.026	1	CYP1B1	Intron, TagSNP: CYP1B1	rs163077
rs20432	1	T > G	0.59 [0.35 – 0.97]	0.027	1	PTGS2	Intron	
rs762551	15	A > C	0.63 [0.42 – 0.93]	0.027	1	CYP1A2	Intron, TagSNP: CYP1A cluster	
rs3776432	5	G > A	1.52 [1.04 – 2.24]	0.028	1	NSUN2	Intron	
rs3817074	19	C > T	1.95 [1.06 – 3.60]	0.029	1	BAX	Intron	
rs1126526	1	C > T	1.41 [0.96 – 2.08]	0.029	1	ATF3	5'UTR	
rs1805405	1	C > A	0.56 [0.33 – 0.95]	0.030	1	PARP1	Intron	rs1805407, rs2280712
rs1002153	1	T > C	0.56 [0.33 – 0.95]	0.030	1	PARP1	Intron	rs1805408
rs4799055	18	G > T	1.61 [1.10 – 2.35]	0.030	1	NFATC1	Intron	

Table 1. continued.

SNP	CHR	Alleles	OR [95%CI]	$p(\chi^2)$	Gene	SNP Type	In LD with
rs854556	7	C>T	0.64 [0.44 – 0.95]	0.031	PON1	Intron, TagSNP: PON1	
rs1052637	2	G>C	0.66 [0.45 – 0.97]	0.031	DDX18	nonsynonymous	
rs440454	6	C>T	0.62 [0.39 – 0.97]	0.032	RDBP	Locus, intron	
rs854555	7	C>A	1.53 [1.05 – 2.24]	0.032	PON1	Intron, TagSNP: PON1	
rs854556	7	C>T	0.64 [0.44 – 0.95]	0.031	PON1	Intron, TagSNP: PON1	
rs1052637	2	G>C	0.66 [0.45 – 0.97]	0.031	DDX18	nonsynonymous	
rs440454	6	C>T	0.62 [0.39 – 0.97]	0.032	RDBP	Locus, intron	
rs854555	7	C>A	1.53 [1.05 – 2.24]	0.032	PON1	Intron, TagSNP: PON1	
rs2857605	6	A>G	0.57 [0.36 – 0.92]	0.034	TNF	Intron, TagSNP: TNF	
rs6768093	3	T>A	0.66 [0.45 – 0.96]	0.036	ATR	Locus	rs2227930, rs2227928
rs1405655	19	T>C	1.56 [1.05 – 2.32]	0.036	NR1H2	Intron	
rs3733890	5	G>A	0.66 [0.45 – 0.98]	0.037	BHMT	nonsynonymous	
rs1801105	2	C>T	1.95 [1.06 – 3.60]	0.041	HNMT	nonsynonymous	
rs2231142	4	C>A	2.12 [1.04 – 4.31]	0.042	ABCG2	nonsynonymous	
rs3212254	14	C>A	2.12 [1.04 – 4.31]	0.042	RIPK3	nonsynonymous	
rs6940663	7	A>G	0.67 [0.46 – 0.98]	0.042	PTPN12	nonsynonymous	
rs1050152	5	C>T	0.68 [0.47 – 0.99]	0.044	SLC22A4	nonsynonymous	
rs2007231	1	T>C	0.66 [0.44 – 0.97]	0.044	NRAS	Intron	
rs1296028	8	A>G	0.64 [0.42 – 0.99]	0.045	FDFT1	3'UTR	
rs3758881	10	G>A	2.35 [1.12 – 4.97]	0.047	CYP2C19	nonsynonymous	
rs2124459	21	T>C	0.66 [0.45 – 0.96]	0.047	CBS	Intron	
rs2228233	14	C>T	0.65 [0.43 – 0.98]	0.048	NFATC4	synonymous	
rs10759326	9	T>G	1.57 [0.99 – 2.48]	0.048	IKBKAP	nonsynonymous	rs10979601
rs2074351	7	G>A	1.51 [1.01 – 2.26]	0.050	PON1	Intron, TagSNP: PON1	

---

generation of the sensory and autonomic nervous system.<sup>23</sup>

Mutations in neurofilament light polypeptide (NEFL) cause Charcot-Marie-Tooth Neuropathy Type 2E/1F, the most common inherited peripheral neuropathy.<sup>24</sup> Two promoter SNPs (*rs2976437* and *rs2976436*) in *NEFL* were associated with BiPN. Two SNPs were located in the nerve growth factor receptor (*NGFR*; *rs11466155* and *rs584589*), a gene particularly important with respect to neurological functions. The NGFR signals via NF $\kappa$ B activation and binds neurotrophin precursors that stimulate neuronal cell survival and differentiation. These results support the finding in our previous study that late onset BiPN is associated with genes involved in the development and function of the nervous system.<sup>11</sup> In a recent paper, the time to BiPN was found to be associated with the occurrence of the SNP *rs4553808* in the gene *CTLA4*.<sup>12</sup> Comparison with that study is not feasible, due to the fact that the SNP set tested had only minimal overlap with our SNP set (2% overlap).

7 We evaluated genetic risk factors associated with BiPN in MM patients who had not been previously treated with Bortezomib in the largest study to date using a hypothesis-driven approach. This method is limited by the possibility of population heterogeneity. However, a limited set of patients with different genetic backgrounds were selected out, as described in the Material and Methods section and as reported previously.<sup>11</sup> Further limitations are: i) the inability of assessing SNPs outside the candidate panel; and ii) the possibility of finding false-positive associations as a result of multiple testing. To address both issues, we are currently performing a genome-wide scan that will clarify and possibly confirm the associations reported in this study. The power analysis indicated in this study has sufficient power to detect associations with an OR of less than 0.44 or an OR of more than 2.28 and diverging with MAF. It is unlikely that smaller effects can be found. Using the custom BOAC SNP array in a discovery set of 238 patients, no SNP was found to be significantly associated to BiPN at the corrected  $p < 0.05$  significance level. However, based on the highest-ranking SNPs found using the uncorrected  $p$ -value in the discovery set, pathway analysis did demonstrate clear enrichment of neurological disease SNPs.

## REFERENCES

1. Richardson PG, Sonneveld P, Schuster MW, *et al.* Bortezomib or high-dose dexamethasone for relapsed multiple myeloma. *N Engl J Med* . 2005; **352**(24):2487–2498.
2. Richardson PG, Briemberg H, Jagannath S, *et al.* Frequency, characteristics, and reversibility of peripheral neuropathy during treatment of advanced multiple myeloma with bortezomib. *J Clin Oncol* . 2006; **24**(19):3113–20.
3. Richardson PG, Xie W, Mitsiades C, *et al.* Single-agent bortezomib in previously untreated multiple myeloma: efficacy, characterization of peripheral neuropathy, and molecular correlations with response and neuropathy. *J Clin Oncol* . 2009; **27**(21):3518–25.
4. Delforge M, Blade J, Dimopoulos MA, *et al.* Treatment-related peripheral neuropathy in multiple myeloma: the challenge continues. *Lancet Oncol* . 2010; **11**(11):1086–95.
5. Richardson PG, Barlogie B, Berenson J, *et al.* A phase 2 study of bortezomib in relapsed, refractory myeloma. *N Engl J Med* . 2003; **348**(26):2609–2617.
6. Cavaletti G, Gilardini A, Canta A, *et al.* Bortezomib-induced peripheral neurotoxicity: a neurophysiological and pathological study in the rat. *Exp Neurol* . 2007; **204**(1):317–25.
7. Landowski TH, Megli CJ, Nullmeyer KD, Lynch RM, & Dorr RT. Mitochondrial-mediated dysregulation of Ca<sup>2+</sup> is a critical determinant of Velcade (PS-341/bortezomib) cytotoxicity in myeloma cell lines. *Cancer Res* . 2005; **65**(9):3828–36.
8. Casafont I, Berciano MT, & Lafarga M. Bortezomib induces the formation of nuclear poly(A) RNA granules enriched in Sam68 and PABPN1 in sensory ganglia neurons. *Neurotox Res* . 2010; **17**(2):167–78.
9. Cavaletti G & Marmiroli P. Chemotherapy-induced peripheral neurotoxicity. *Nat Rev Neurol* . 2010; **6**(12):657–66.
10. Ravaglia S, Corso A, Piccolo G, *et al.* Immune-mediated neuropathies in myeloma patients treated with bortezomib. *Clin Neurophysiol* . 2008; **119**(11):2507–12.
11. Broyl A, Corthals SL, Jongen JL, *et al.* Mechanisms of peripheral neuropathy associated with bortezomib and vincristine in patients with newly diagnosed multiple myeloma: a prospective analysis of data from the HOVON-65/GMMG-HD4 trial. *Lancet Oncol* . 2010; **11**(11):1057–65.
12. Favis R, Sun Y, van de Velde H, *et al.* Genetic variation associated with bortezomib-induced peripheral neuropathy. *Pharmacogenet Genomics* . 2011; **21**(3):121–9.
13. Van Ness B, Ramos C, Haznadar M, *et al.* Genomic variation in myeloma: design, content, and initial application of the Bank On A Cure SNP Panel to detect associations with progression-free survival. *BMC Med* . 2008; **6**:26.
14. Purcell S, Neale B, Todd-Brown K, *et al.* PLINK: a tool set for whole-genome association and population-based linkage analyses. *Am J Hum Genet* . 2007; **81**(3):559–75.
15. Gayther SA, Song H, Ramus SJ, *et al.* Tagging single nucleotide polymorphisms in cell cycle control genes and susceptibility to invasive epithelial ovarian cancer. *Cancer Res* . 2007; **67**(7):3027–35.
16. Sharp L, Cardy AH, Cotton SC, & Little J. CYP17 gene polymorphisms: prevalence and as-

- 
- sociations with hormone levels and related factors. a HuGE review. *Am J Epidemiol* . 2004; **160**(8):729–40.
17. Roglio I, Giatti S, Pesaresi M, *et al*. Neuroactive steroids and peripheral neuropathy. *Brain Res Rev* . 2008; **57**(2):460–9.
  18. Curran MP & McKeage K. Bortezomib: a review of its use in patients with multiple myeloma. *Drugs* . 2009; **69**(7):859–88.
  19. Mhatre M, Nguyen A, Kashani S, Pham T, Adesina A, & Grammas P. Thrombin, a mediator of neurotoxicity and memory impairment. *Neurobiol Aging* . 2004; **25**(6):783–93.
  20. Sriram K & O'Callaghan JP. Divergent roles for tumor necrosis factor-alpha in the brain. *J Neuroimmune Pharmacol* . 2007; **2**(2):140–53.
  21. Gonzalez-Clemente JM, Mauricio D, Richart C, *et al*. Diabetic neuropathy is associated with activation of the TNF-alpha system in subjects with type 1 diabetes mellitus. *Clin Endocrinol (Oxf)* . 2005; **63**(5):525–9.
  22. Boyle DL, Jones TL, Hammaker D, *et al*. Regulation of peripheral inflammation by spinal p38 MAP kinase in rats. *PLoS Med* . 2006; **3**(9):e338.
  23. Anderson SL, Coli R, Daly IW, *et al*. Familial dysautonomia is caused by mutations of the IKAP gene. *Am J Hum Genet* . 2001; **68**(3):753–8.
  24. Jordanova A, de Jonghe P, Boerkoel CF, *et al*. Mutations in the neurofilament light chain gene (NEFL) cause early onset severe Charcot-Marie-Tooth disease. *Brain* . 2003; **126**(Pt 3):590–7.

## **A Genome-Wide Association Study Identifies a Novel Locus for Bortezomib-Induced Peripheral Neuropathy in European Patients with Multiple Myeloma**

Florence Magrangeas, Rowan Kuiper, Hervé Avet-Loiseau,  
Wilfried Gouraud, Catherine Guérin-Charbonnel, Ludovic Ferrer,  
Alexandre Aussem, Haytham Elghazel, Jérôme Suhard,  
Henri Der Sakissian, Michel Attal, Nikhil C. Munshi, Pieter Sonneveld,  
Charles Dumontet, Philippe Moreau, Mark van Duin,  
Loïc Campion & Stéphane Minvielle

---

## ABSTRACT

Painful peripheral neuropathy is a frequent toxicity associated with bortezomib therapy. This study aimed to identify loci that affect susceptibility to this toxicity. A genome-wide association study (GWAS) of 370605 SNPs was performed to identify risk variants for developing severe bortezomib-induced peripheral neuropathy (BiPN) in 469 patients with multiple myeloma who received bortezomib-dexamethasone therapy prior to autologous stem cell in randomized clinical trials of the Intergroupe Francophone du Myélome (IFM) and findings were replicated in 114 patients with multiple myeloma of the HOVON-65/GMMG-HD4 clinical trial. An SNP in the *PKNOX1* gene was associated with BiPN in the exploratory cohort (*rs2839629*; OR=1.9, 95% confidence interval: [1.5-2.4];  $p= 7.6 \times 10^{-6}$ ) and in the replication cohort (OR= 2.0 [1.1-3.3];  $p= 8.3 \times 10^{-3}$ ). In addition, *rs2839629* is in strong linkage disequilibrium ( $r^2 = 0.87$ ) with *rs915854*, located in the intergenic region between *PKNOX1* and cystathionine- $\beta$ -synthetase (*CBS*). Expression quantitative trait loci mapping showed that both *rs2839629* and *rs915854* genotypes have an impact on *PKNOX1* expression in nerve tissue, whereas *rs2839629* affects *CBS* expression in skin and blood. The use of GWAS in multiple myeloma pharmacogenomics has identified a novel candidate genetic locus mapping to *PKNOX1* and in the immediate vicinity of *CBS* at 21q22.3 associated with the severe bortezomib-induced toxicity. The proximity of these two genes involved in neurologic pain whose tissue-specific expression is modified by the two variants provides new targets for neuroprotective strategies.



## INTRODUCTION

Some patients with multiple myeloma have subclinical or even clinical peripheral neuropathy at diagnosis. This peripheral neuropathy can be related to comorbidities, such as diabetes mellitus, or associated with the M-protein itself. In the course of the disease, peripheral neuropathy is mostly induced by therapies, especially thalidomide (thalidomide-induced peripheral neuropathy, TiPN) and bortezomib (bortezomib-induced peripheral neuropathy, BiPN), which may be considered as distinct clinical entities.<sup>1</sup> TiPN may arise after prolonged administration of thalidomide (in 30–55% of patients treated for 12 months, including 15–25% with grade 2 or higher peripheral neuropathy) and appears to be due to a cumulative effect. Initial symptoms include sensory changes, such as paresthesia and hyperesthesia, later followed by motor symptoms and autonomic dysfunction. BiPN is characterized by neuropathic pain and a length dependent distal sensory neuropathy with suppression of reflexes. Motor neuropathy may follow and infrequently results in mild to severe distal weakness in the lower limbs. There may also be a significant autonomic component, which manifests as dizziness, hypotension, diarrhea or constipation, and/or extreme fatigue. BiPN is thought to occur at a certain threshold of treatment (within five cycles but rarely beyond) in 40 – 60% of the patients, including 15 – 40% who will develop severe peripheral neuropathy (grade 2 or higher). This drug-induced toxicity is well known by physicians and nurses, and patients are now systematically informed about these potential side effects. The use of subcutaneous bortezomib reduces the incidence of BiPN but does not abrogate this toxicity.<sup>2</sup> As no effective prophylactic treatment is available, prompt action in case of symptoms, including dose reduction and weekly administration of bortezomib, is crucial to manage this severe toxicity, which may dramatically affect the quality of life.<sup>3–5</sup> Therefore, the identification of patients at risk of developing BiPN or TiPN is an important issue. This is especially true because the triplet combination of bortezomib–thalidomide–dexamethasone is considered one of the best induction regimens prior to high-dose therapy and autologous stem cell transplantation for the treatment of younger patients with de novo multiple myeloma.<sup>6</sup> The interindividual differences in the onset of BiPN or TiPN is in agreement with an underlying

---

genetic susceptibility to this toxicity. Rare variants in bortezomib or thalidomide target proteins could affect the patient's sensitivity to these drugs. Among the pharmacogenomic methods to discover genetic loci associated with drug-induced toxicities, the candidate gene approach has shown a significant genetic contribution to the risk of developing TiPN or BiPN.<sup>7-10</sup> However, a genome-wide association study (GWAS) has the capacity to identify new genetic variants that will have a direct or indirect effect on drug sensitivity. Here we report the results of a GWAS of 583 patients with multiple myeloma treated with bortezomib to discover genetic variants associated with severe BiPN. This is the first GWA pharmacogenomic study of bortezomib treatment toxicity and provides novel insights into bortezomib-related pathways.

## MATERIALS AND METHODS

### Clinical samples

Peripheral blood DNA samples were collected from 598 patients with newly diagnosed multiple myeloma who received bortezomib–dexamethasone (VD) induction therapy. Patients were treated in randomized clinical trials of the Intergroupe Francophone du Myélome (IFM; IFM 2005-01, IFM2007-02) or routine practice in France ( $n = 482$ ) and in a randomized clinical trial of the Dutch/Belgian Haemato-Oncology Foundation for Adults in du the Netherlands (HOVON) and the German-Speaking Myeloma Multicenter Group (GMMG; HOVON-65/GMMG-HD4;  $n = 116$ ). The IFM VD treatment consisted of four 3-week cycles of bortezomib  $1.3 \text{ mg}/\text{m}^2$  administered intravenously on days 1, 4, 8, and 11 plus dexamethasone  $40 \text{ mg}$  on days 1 to 4 (all cycles) and days 9 to 12 (cycles 1 and 2). The HOVON-65/GMMG-HD4 VD treatment consisted of three cycles of bortezomib  $1.3 \text{ mg}/\text{m}^2$  administered intravenously on days 1, 4, 8, and 11 plus dexamethasone  $40 \text{ mg}$  on days 1 to 4, 9 to 12, and 17 to 20 (patients enrolled in the HOVON-65/GMMG-HD4 trial received doxorubicin  $9 \text{ mg}/\text{m}^2/\text{day}$  on days 1 to 4, in addition to VD according to the bortezomib, doxorubicin, and dexamethasone (PAD) regimen. Adverse events including peripheral neuropathy were graded by NCI Common Toxicity Criteria Version 3.0. All patients provided written informed consent for both the treatment and companion protocols.

### Genotyping

Data quality assessment and control steps carried out during GWAS are summarized in online Figure S1. A total of 482 multiple myeloma samples in the exploratory IFM cohort and 116 multiple myeloma samples in the Dutch and German replication cohort were genotyped using Affymetrix SNP6.0 Human DNA chips. Affymetrix CEL files were analyzed either by using Affymetrix Genotyping Console software v4.0 (GTC 4.0), followed by application of the Affymetrix Birdseed algorithm v2.0 to generate SNP genotype calls for the IFM exploratory cohort (GEO accession GSE65777) or by application CRLMM v2 algorithm to generate SNP genotype calls for the replication cohort (GEO accession GSE66903).

---

## Samples quality control

Stringent quality control (QC) thresholds were applied to filter out poorly genotyped subjects: if contrast QC < 0.4, call rate < 97% and outlying heterozygosity rate ( $\text{het\_rate} > \text{mean het\_rate} + 3\text{SD}$ ), the individual was removed. Principal component analysis (PCA) was performed to visualize the genetic ancestry of the IFM samples that passed the QC and assess whether population adjustment should be made (online Figure S2). Random 60000 genotypes of IFM subjects (IFM,  $n = 469$ ) and unrelated individuals from three HapMap phase III populations representing Northwest European (CEU,  $n = 162$ ), African (YRI,  $n = 163$ ), and Chinese (CHB,  $n = 82$ ) ancestries were combined to calculate the PCA. This method identified samples not clustering with the Northwestern European individuals (IFM outliers,  $n = 34$ ), given that these patients were equally distributed between the case and control groups (Fisher exact test  $p = 0.36$ ), no adjustment was needed, and therefore they were kept for the GWAS. Inspection of the observed and expected distribution of the neuropathy association statistic showed absence of hidden population substructure (Cochran–Armitage test of association; genomic inflation factor  $\lambda = 1.05$ ).

## Marker QC

SNP QC was conducted in four steps to remove suboptimal markers of the GWA data (Figure S1). i) unannotated SNPs according to hg19 na32 SNP6.0 Affymetrix annotations ( $n = 130$ ) along with SNPs from mitochondrial and sex chromosomes ( $n = 37326$ ) were not considered in the study, ii) SNPs with missing genotype in more than 5% of the subjects ( $n = 16743$ ), iii) SNPs of low minor allele frequency (MAF) less than 5% ( $n = 483984$ ), iv) SNPs showing extensive deviation from Hardy–Weinberg equilibrium (HWE) with an HWE  $p < 1 \times 10^{-5}$  ( $n = 834$ ).

## Statistical analysis

Statistical analyses were performed using SNPTEST v2.5.<sup>11</sup> First, we compared 370605 genotypes from 155 grade  $\geq 2$  BiPN IFM patients to 314 control IFM patients defined as grade 1 BiPN or no BiPN. Second, we performed a validation us-

ing the HOVON-65/GMMG-HD4 cohort for the highest associated SNPs ( $p_{\text{trend}} < 1 \times 10^{-5}$ ) as identified in the exploratory cohort. We compared 41 bortezomib-treated grade  $\geq 2$  BiPN patients with 75 bortezomib-treated control patients. We applied a one-sided logistic regression with 10000 label-swapping permutations to correct for multiple testing to confirm BiPN association in this independent cohort. The predictive value of the SNP validated in the external series was assessed on the overall population ( $n = 583$ , i.e. 195 cases and 388 controls) with  $1 \times 10^7$  label-swapping permutations.

---

## RESULTS

We conducted a pharmacogenomic GWA study to identify genetic variants associated with bortezomib toxicity in newly diagnosed patients with multiple myeloma who received VD induction therapy. Using SNP6.0 Affymetrix arrays, we genotyped 909622 tagging SNPs in 482 multiple myeloma cases. Of the 482 DNA samples genotyped, 469 cases passed strict QC criteria (online Figure S1). We considered only the 370605 autosomal SNPs with homozygosity in at least 5% of patients, a genotype call in at least 95% of patients and with an HWE  $p > 1 \times 10^{-5}$ . We compared the genetic contribution of patients who developed BiPN of grade  $\geq 2$  ( $n = 155$ ) with that of patients who did not develop severe BiPN or without BiPN ( $n = 314$ ). We separated grade 0 and 1 versus grade 2 or more based on the clinical impact of such a toxicity. Grade 1 neuropathy requires a careful follow-up, but doses of bortezomib are not modified. Doses of bortezomib in the routine clinical practice must be adapted (from  $1.3 \text{ mg}/\text{m}^2$  to  $1.0 \text{ mg}/\text{m}^2$ , or from the bi-weekly to the weekly schedule administration) according to the onset of grade 2 peripheral neuropathy, or stopped in case of grade 3 or more, and resumed in case of recovery. The GWA study showed association for six SNPs with  $\text{OR} > 1.8$  and  $p_{\text{trend}} < 1 \times 10^{-5}$  (Table 1 and online Table S1; online Figure S3 and S4), although none reached the actual significance in a GWA study ( $\frac{0.05}{37065} = 1.35 \times 10^{-7}$ ). To replicate these findings, a validation was performed using SNP6.0 Affymetrix arrays in 114 newly diagnosed patients with multiple myeloma enrolled in the HOVON-65/GMMG-HD4 clinical trial who received VD induction therapy. A significant association was seen for *rs2839629* ( $\text{OR} = 2.04$ ; 95%CI [1.11–3.33] ( $p = 8.3 \times 10^{-3}$ ; Table 2) which maps within the 3'UTR of *PKNOX1* (transcription factor PBX/knotted 1 homeobox 1). The overall estimate for *rs2839629* was an OR of 1.89 [1.45–2.44];  $p = 5 \times 10^{-7}$ ). Moreover, *rs2839629* is in strong linkage disequilibrium (LD) with *rs76516641* ( $r^2 = 0.94$ ) and *rs915854* ( $r^2 = 0.86$ ) which map within the intergenic region of 19.5kb between *PKNOX1* and cystathionine- $\beta$ -synthetase (*CBS*; Figure 1).

Both *PKNOX1* and *CBS* appear to be strong candidates for BiPN susceptibility genes. *PKNOX1* is known to modulate transcriptional activity of chemokine monocyte chemoattractant protein-1 (*MCP-1*) gene.<sup>12–15</sup> Through interaction

**Table 1. Six highest associated SNPs.** SNPTTEST results for exploratory population for the six highest associated SNPs

SNP	CHR	BIPN ≥ 2			BIPN < 2			Odds ratio [95%CI]			$p_{\text{trend}}$
		A B	#AA #AB #BB	#AA #AB #BB	AB/AA	BB/AA	global				
rs10862339	12	A C	40 79 36	147 135 32	2.2 <sub>[1.4-3.4]</sub>	4.1 <sub>[2.3-7.5]</sub>	2.1 <sub>[1.6-2.7]</sub>				$5.47 \times 10^7$
rs1344016	12	A G	41 79 35	145 135 34	2.1 <sub>[1.3-3.2]</sub>	3.6 <sub>[2.0-6.5]</sub>	1.9 <sub>[1.5-2.6]</sub>				$3.81 \times 10^6$
rs2414277	15	T C	21 70 64	86 155 73	1.9 <sub>[1.3-3.0]</sub>	3.6 <sub>[2.0-6.3]</sub>	1.9 <sub>[1.5-2.6]</sub>				$6.17 \times 10^6$
rs2839629	21	G A	33 79 43	128 137 49	1.5 <sub>[0.93-2.5]</sub>	3.5 <sub>[2.0-5.9]</sub>	1.9 <sub>[1.5-2.5]</sub>				$7.64 \times 10^6$
rs4776196	15	T C	21 70 64	85 155 74	1.9 <sub>[1.2-2.9]</sub>	3.5 <sub>[2.0-6.3]</sub>	1.9 <sub>[1.4-2.5]</sub>				$9.31 \times 10^6$
rs11145770	9	G A	46 72 37	141 144 29	2.6 <sub>[1.5-4.6]</sub>	3.9 <sub>[2.2-7.1]</sub>	1.9 <sub>[1.4-2.5]</sub>				$9.70 \times 10^6$

with its cognate receptor CCR2, MCP-1 contributes to paclitaxel CIPN through changes in dorsal root ganglion neurons.<sup>16</sup> *MCP-1* is universally increased in different models of neuropathic pain and may be considered as a biomarker of chronic pain.<sup>17</sup> *MCP-1* is an important mediator of macrophage-related neural damage in different animal models of inherited neuropathies and acute inflammatory demyelinating neuropathy.<sup>18,19</sup> *CBS* encodes the endogenous H<sub>2</sub>S-producing enzyme CBS. CBS-H<sub>2</sub>S signaling pathway is implicated in the pathogenesis of a variety of neurodegenerative and inflammatory disorders, diabetic gastric hypersensitivity and plays a crucial role in inflammatory pain in temporomandibular joint.<sup>20-23</sup> To explore the possibility that this association might be mediated through differential expression of *PKNOX1* or *CBS* or both, we examined the correlations between *rs2839629*, *rs76516641*, and *rs915854* genotypes and tissue-specific gene expression levels by using the expression quantitative trait locus analysis available on the SNIIPA portal ([www.snipa.org](http://www.snipa.org)) that used GTEx Portal v6 and MuTHER consortium as primary sources.<sup>24-26</sup> *PKNOX1* expression was significantly associated with *rs2839629* and *rs915854* genotypes in tibial nerve tissue ( $p = 5.6 \times 10^{-8}$  and  $p = 1.9 \times 10^{-7}$ , respectively; online Tables S2 and S3) with higher expression associated with *rs2839629* risk alleles (Figure

**Table 2. Logistic regression results** One-sided logistic regression in the validation cohort to test whether the direction of association found in the exploratory cohort can be confirmed. OR<sub>global</sub>, odds ratio estimate;  $p$ , uncorrected parametric  $p$ -value;  $p_{\text{pointwise}}$ , pointwise  $p$ -value as determined by permutation;  $p_{\text{FWER}}$ , permuted  $p$ -value (familywise error rate correction).

SNP	OR <sub>global</sub> [95%CI]	$p$	$p_{\text{pointwise}}$	$p_{\text{FWER}}$
rs10862339	1.02 <sub>[0.58-1.79]</sub>	0.53	0.54	0.96
rs1344016	1.05 <sub>[0.60-1.85]</sub>	0.43	0.44	0.91
rs2414277	1.20 <sub>[0.71-2.08]</sub>	0.24	0.22	0.66
rs2839629	2.04 <sub>[1.11-3.33]</sub>	$9.6 \times 10^{-3}$	$8.3 \times 10^{-3}$	0.036
rs4776196	1.19 <sub>[0.71-2.08]</sub>	40.24	0.27	0.70
rs11145770	1.43 <sub>[0.75-2.33]</sub>	0.14	0.13	0.46

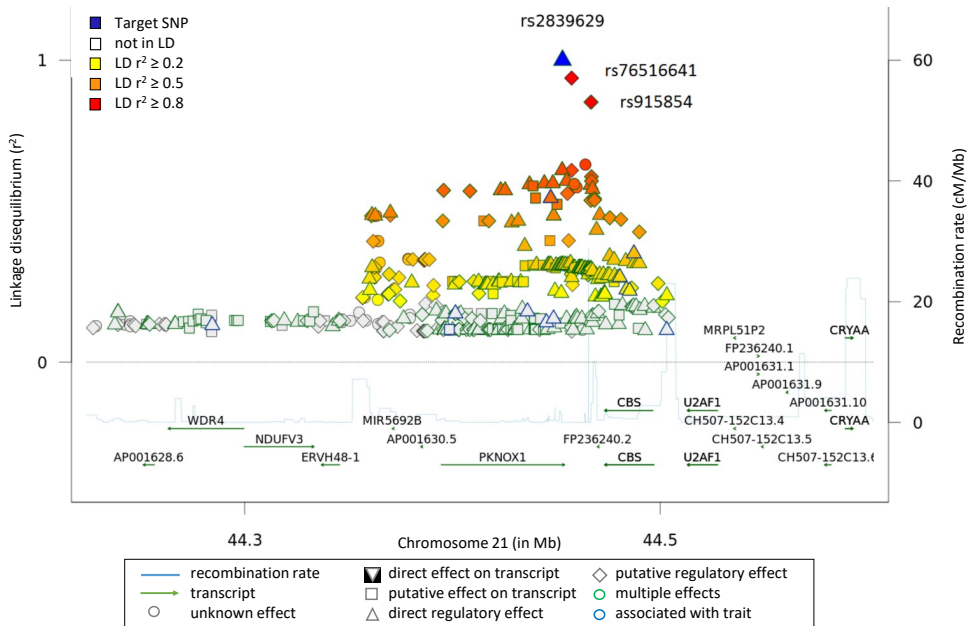


**Figure 1. SNP associations with BiPN on the 21q22.3 locus.** Showing genome-wide level of evidence of BiPN in multiple myeloma. Illustration of the locus with the local LD and recombination rate over 500kb centred on *rs2839629* (blue triangle). Each diamond, triangle, circle, or square represents an SNP found in this locus, *rs76516641* and *rs915854* are indicated (red diamond). The figure was generated using the web-based tool SNIpa ([www.snipa.org](http://www.snipa.org); ref. 24).

8

2), whereas *CBS* expression was significantly associated only with *rs2839629* in skin ( $p = 2.6 \times 10^{-15}$ ) and in blood ( $p = 3.1 \times 10^{-8}$ ; online Table S2). *rs915854* is annotated with a regulatory feature cluster characterized by histone marks H3K27ac and H3K4me1 enrichment in blood and cervix cells (online Table S3). In addition, a *rs915854* minor allele is predicted to disrupt the binding site for the general pioneer factor FOXA1, this could render the enhancer less active for target gene expression such as *PKNOX1* (Figure 3). Conversely, the *rs76516641* genotype has no significant effect on the gene expression of both *PKNOX1* and *CBS* (data not shown).

As we show that the risk allele A for *rs2839629* is associated with higher levels of *PKNOX1* expression and previous report have demonstrated that PKNOX1 binds preferentially to the -2578G (*rs1024611G*) polymorphism leading to increase *MCP-1* levels,<sup>14</sup> we analyzed the relationship between *rs2839629A* and



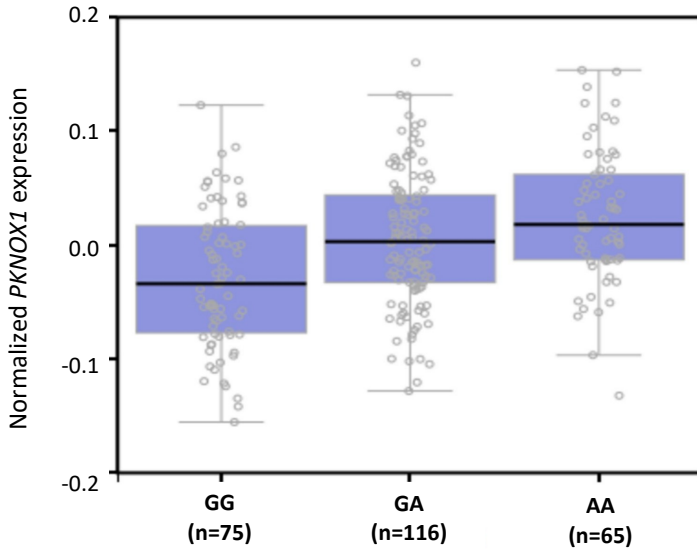


**Figure 2. *PKNOX1* expression vs. *rs2839629* genotype.** Relationship between tibial nerve *PKNOX1* expression and *rs2839629* genotype from the GTEx Portal v6 ([www.gtexportal.org](http://www.gtexportal.org); ref. 25).

*rs1024611G* in the IFM exploratory cohort. We found a significant association between the *rs2839629* A/A homozygous genotype and the *rs1024611G*-bearing allele (Fisher exact-test  $p=0.01$ ) suggesting a possible epistatic interaction between *rs2839629* and *rs1024611* to regulate *MCP-1* expression. The current pharmacogenomic GWA study also confirmed the modest association of the *rs619824* genotype with BiPN ( $p=0.043$ ) previously identified by Corthals *et al.*<sup>8</sup> Although there has been no overlap with a previous study on late-onset of BiPN-associated variants reported by Broyl *et al.*<sup>10</sup> as shown in online Table S4. This lack of overlap could reflect the potential complexity of predisposition to BiPN. More importantly, the design of the custom SNP chip used previously only contained 3404 SNPs in 983 hypothesis-driven genes which were thought to be functionally relevant in abnormal cellular functions, inflammation and immunity, as well as drug responses rather than adverse drug reactions which are less obvious candidates.<sup>27</sup>

---

## DISCUSSION

To date there are no established predictors of BiPN, it is impossible to predict which patient will develop neuropathy. Previous studies performed by our group and others using candidate gene approach have revealed significant association between SNP and BiPN; however, the clinical relevance of these findings is not clear.<sup>8-10</sup> To increase our chance to discover variants that might provide new insights in the mechanisms underlying gene phenotype, we used a hypothesis-free approach. GWAS in cancer pharmacogenomics is challenging and few reports have been published to date. This is mainly due to insufficient statistical power in studies.<sup>28</sup> To partially overcome these limitations, we designed our analysis to identify high-effect SNP ( $OR > 1.8$ ) with MAFs greater than 0.05, in a large cohort of IFM patients with multiple myeloma ( $n = 469$ ) uniformly treated to achieve convincing statistical power<sup>29</sup> and we verified our findings in an independent cohort of Dutch and German patients with multiple myeloma. Furthermore, our GWAS approach eliminates selection case-control bias as both case-control studies included patients in cohort studies, i.e. IFM or HOVON/GMMG clinical trials cohorts. When evaluating toxicity, it is sometimes difficult to distinguish between BiPN and neuropathic pain in general. It is also recognized that the sole use of the NCI CTC for assessment of sensory peripheral neuropathy is suboptimal. It is also recognized that detailed patient-reported symptom data and a quality-of-life assessment more accurately describes this toxicity and that physician-reported NCI-CTC grading underreports peripheral neuropathy. These systematic evaluations are difficult to apply in a multicenter study in the context of pharmacogenomics analyses. Of note, our study has enrolled patients without peripheral neuropathy at baseline, and patients were treated with the doublet combination of bortezomib and dexamethasone, and did not receive other neurotoxic agents.

Our analysis revealed a SNP associated with BiPN (*rs2839629*;  $OR = 1.89$ ;  $p = 7.6 \times 10^{-6}$ ) that was replicated in an independent cohort ( $OR = 2.04$ ;  $p = 8.3 \times 10^{-3}$ ) in high LD with SNP *rs915854*. Both variants are in noncoding regions; *rs2839629* is located in the 3'UTR of *PKNOX1*, and *rs915854* is in the intergenic region between *PKNOX1* and *CBS*. Expression quantitative trait loci showed that these variants alter *PKNOX1* and *CBS* expression presumably via cis-regulatory

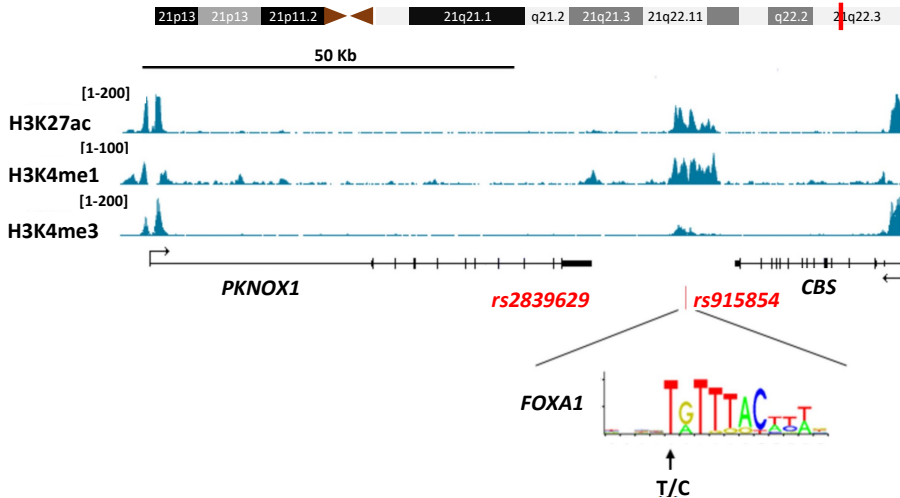


Fig-

**Figure 3. Histone marks *PKNOX1* locus.** UCSC Genome Browser views of histone marks H3K27ac and H3K4me1 enrichment and H3K4me3 depletion within the region covering *PKNOX1* and *CBS* in HeLa cells. Arrow indicates the variant sequence and location in position-weight matrix for *FOXA1*.

elements in the case of *rs915854* as it falls within a regulatory region (Figure 3). Finally, we found a significant association between *rs2839629A* and *rs1024611G* that could have an impact on *MCP-1* expression levels. Given that these genes encode proteins, directly or indirectly, involved in neuropathic<sup>16</sup> and inflammatory<sup>23</sup> pain, the functional significance of these predictive SNPs is established. This discovery opens the way to investigate novel pathways linked to *PKNOX1* and *CBS* activities for a better understanding of mechanisms underlying this neurotoxicity. This work generated a new hypothesis regarding neurotoxicity mechanisms and provides new targets for neuroprotective strategies; however, additional international collaborative efforts including non-European countries are warranted to confirm or refute these findings and examine the impact of differential expression of both *PKNOX1* and *CBS* effects on bortezomib exposure in cell model. Our results are preliminary and cannot be proposed yet for a systematic use in the routine clinical practice. Nevertheless, our findings are one of the first steps that may allow for the identification of patients at increased risk of severe BiPN, and these patients may benefit from the use of alternative drugs, such as carfilzomib, and/or a more focused clinical management of this toxicity.

---

## REFERENCES

1. Cavaletti G & Marmiroli P. Chemotherapy-induced peripheral neurotoxicity. *Nat Rev Neurol* . 2010; **6**(12):657–66.
2. Moreau P, Pylypenko H, Grosicki S, *et al*. Subcutaneous versus intravenous administration of bortezomib in patients with relapsed multiple myeloma: a randomised, phase 3, non-inferiority study. *Lancet Oncol* . 2011; **12**(5):431–40.
3. Delforge M, Blade J, Dimopoulos MA, *et al*. Treatment-related peripheral neuropathy in multiple myeloma: the challenge continues. *Lancet Oncol* . 2010; **11**(11):1086–95.
4. Mohty B, El-Cheikh J, Yakoub-Agha I, Moreau P, Harousseau JL, & Mohty M. Peripheral neuropathy and new treatments for multiple myeloma: background and practical recommendations. *Haematologica* . 2010; **95**(2):311–9.
5. Richardson PG, Delforge M, Beksac M, *et al*. Management of treatment-emergent peripheral neuropathy in multiple myeloma. *Leukemia* . 2012; **26**(4):595–608.
6. Moreau P, San Miguel J, Ludwig H, *et al*. Multiple myeloma: ESMO Clinical Practice Guidelines for diagnosis, treatment and follow-up. *Ann Oncol* . 2013; **24 Suppl 6**:vi133–7.
7. Johnson DC, Corthals SL, Walker BA, *et al*. Genetic factors underlying the risk of thalidomide-related neuropathy in patients with multiple myeloma. *J Clin Oncol* . 2011; **29**(7):797–804.
8. Corthals SL, Kuiper R, Johnson DC, *et al*. Genetic factors underlying the risk of bortezomib induced peripheral neuropathy in multiple myeloma patients. *Haematologica* . 2011; **96**(11):1728–32.
9. Favis R, Sun Y, van de Velde H, *et al*. Genetic variation associated with bortezomib-induced peripheral neuropathy. *Pharmacogenet Genomics* . 2011; **21**(3):121–9.
10. Broyl A, Corthals SL, Jongen JL, *et al*. Mechanisms of peripheral neuropathy associated with bortezomib and vincristine in patients with newly diagnosed multiple myeloma: a prospective analysis of data from the HOVON-65/GMMG-HD4 trial. *Lancet Oncol* . 2010; **11**(11):1057–65.
11. Marchini J, Howie B, Myers S, McVean G, & Donnelly P. A new multipoint method for genome-wide association studies by imputation of genotypes. *Nat Genet* . 2007; **39**(7):906–13.
12. Rovin BH, Lu L, & Saxena R. A novel polymorphism in the MCP-1 gene regulatory region that influences MCP-1 expression. *Biochem Biophys Res Commun* . 1999; **259**(2):344–8.
13. Wright J E K, Page SH, Barber SA, & Clements JE. Prep1/Pbx2 complexes regulate CCL2 expression through the -2578 guanine polymorphism. *Genes Immun* . 2008; **9**(5):419–30.
14. Page SH, Wright J E K, Gama L, & Clements JE. Regulation of CCL2 expression by an upstream TALE homeodomain protein-binding site that synergizes with the site created by the A-2578G SNP. *PLoS One* . 2011; **6**(7):e22052.
15. Pham MH, Bonello GB, Castiblanco J, *et al*. The rs1024611 regulatory region polymorphism is associated with CCL2 allelic expression imbalance. *PLoS One* . 2012; **7**(11):e49498.
16. Zhang H, Boyette-Davis JA, Kosturakis AK, *et al*. Induction of monocyte chemoattractant protein-1 (MCP-1) and its receptor CCR2 in primary sensory neurons contributes to paclitaxel-induced peripheral neuropathy. *J Pain* . 2013; **14**(10):1031–44.
17. Zhang J & De Koninck Y. Spatial and temporal relationship between monocyte chemoattractant

- protein-1 expression and spinal glial activation following peripheral nerve injury. *J Neurochem* . 2006; **97**(3):772–83.
18. Groh J, Heintz K, Kohl B, *et al.* Attenuation of MCP-1/CCL2 expression ameliorates neuropathy in a mouse model for Charcot-Marie-Tooth 1X. *Hum Mol Genet* . 2010; **19**(18):3530–43.
  19. Yuan F, Yosef N, Lakshmana Reddy C, *et al.* CCR2 gene deletion and pharmacologic blockade ameliorate a severe murine experimental autoimmune neuritis model of Guillain-Barre syndrome. *PLoS One* . 2014; **9**(3):e90463.
  20. Wang Y, Qu R, Hu S, Xiao Y, Jiang X, & Xu GY. Upregulation of cystathionine beta-synthetase expression contributes to visceral hyperalgesia induced by heterotypic intermittent stress in rats. *PLoS One* . 2012; **7**(12):e53165.
  21. Schemann M & Grundy D. Role of hydrogen sulfide in visceral nociception. *Gut* . 2009; **58**(6):744–7.
  22. Zhang HH, Hu J, Zhou YL, *et al.* Promoted interaction of nuclear factor-kappaB with demethylated cystathionine-beta-synthetase gene contributes to gastric hypersensitivity in diabetic rats. *J Neurosci* . 2013; **33**(21):9028–38.
  23. Miao X, Meng X, Wu G, *et al.* Upregulation of cystathionine-beta-synthetase expression contributes to inflammatory pain in rat temporomandibular joint. *Mol Pain* . 2014; **10**:9.
  24. Arnold M, Raffler J, Pfeuffer A, Suhre K, & Kastenmuller G. SNIPA: an interactive, genetic variant-centered annotation browser. *Bioinformatics* . 2015; **31**(8):1334–6.
  25. GTEx Consortium. Human genomics. The Genotype-Tissue Expression (GTEx) pilot analysis: multitissue gene regulation in humans. *Science* . 2015; **348**(6235):648–60.
  26. Grundberg E, Small KS, Hedman AK, *et al.* Mapping cis- and trans-regulatory effects across multiple tissues in twins. *Nat Genet* . 2012; **44**(10):1084–9.
  27. Van Ness B, Ramos C, Haznadar M, *et al.* Genomic variation in myeloma: design, content, and initial application of the Bank On A Cure SNP Panel to detect associations with progression-free survival. *BMC Med* . 2008; **6**:26.
  28. Low SK, Takahashi A, Mushiroda T, & Kubo M. Genome-wide association study: a useful tool to identify common genetic variants associated with drug toxicity and efficacy in cancer pharmacogenomics. *Clin Cancer Res* . 2014; **20**(10):2541–52.
  29. Wang WY, Barratt BJ, Clayton DG, & Todd JA. Genome-wide association studies: theoretical and practical concerns. *Nat Rev Genet* . 2005; **6**(2):109–18.



**CHAPTER**

**9**

**General discussion**

---

This thesis focuses on gene expression profiling (GEP) to identify multiple myeloma (MM) patients with high-risk disease. Currently, prognostication of MM is based on the international staging system (ISS) and presence of selected cytogenetic aberrations, either separately or combined into the revised ISS (R-ISS).<sup>1,2</sup> We have shown the usefulness, solid performance and reproducibility of GEP based prognostication.

## Development of the EMC92 classifier

In Chapter 2 we described the development of the EMC92 risk classifier, which classifies patients into high-risk or standard-risk. The HOVON65/GMMG-HD4 clinical trial was used as the training set. We were able to validate the EMC92 classifier in independent datasets obtained from the clinical trials MRC-IX, TT2, TT3 and APEX.<sup>3-6</sup> The risk of death at any time is three times higher for high-risk patients compared to standard-risk patients. The proportion of EMC92 high-risk patients was stable across validation sets with an average of 18%. The EMC92 classifier compared favorably to other GEP classifiers, with the UAMS70-gene classifier demonstrating comparable performance in terms of effect size. However, the proportion of patients classified as high-risk was larger using the EMC92 classifier (15-20% vs. 3-15%).<sup>7,8</sup> The EMC92 classifier was shown to effectively classify patients treated with different treatments, including Thalidomide (MRC-IX, TT2) and Bortezomib (APEX, TT3). The validation sets also included patients of different age categories and disease stage; newly diagnosed as well as relapsed patients, suggesting the classifier is applicable to all MM patients.

9

Together with comorbidities, physical and cognitive condition, age is a major factor in distinguishing fit from frail patients.<sup>9</sup> Patients aged 65 years and older are often considered ineligible for intensive treatments such that they receive a fundamentally different treatment than younger patients. The EMC92 classifier was only validated in a limited group of elderly patients in Chapter 2. Therefore, in Chapter 5 we addressed the value of the EMC92 classifier specifically in a group of elderly patients. In this population the classifier also passed validation, confirming the general usefulness of the EMC92 classifier.<sup>10,11</sup> Moreover, we showed in a multivariate model that the EMC92 classifier was independent of the revised ISS. This finding needs to be confirmed in future studies, with larger



sample size. Four additional datasets confirmed the value of the EMC92 classifier in: newly diagnosed patients in the UK NCRI Myeloma XI trial, relapse patients treated within the total therapy regime of TT6, a cohort of patients included in the multiple myeloma genomics initiative (MMGI) and a cohort of Czech MM patients.<sup>10,12</sup> It is important to emphasize here that there must be a clearly defined separation between the set of patients needed for identifying factors of prognostic value (training set), and an independent set of patients needed to evaluate the general applicability of the identified factors (validation set). For this reason, we systematically excluded the training set when testing the performance of a classifier. When a classifier is not validated in independent data, no conclusions can be drawn on the performance of that classifier, and results can and should only be reported as an observed association.<sup>13-15</sup> Another shortcoming in some gene classifier reports is an insufficient description of the algorithm, thereby preventing a correct use of that classifier.<sup>16-18</sup> Therefore, guidelines which stipulate adequate validation and thorough description of classifiers must be met.<sup>19,20</sup> Next, we evaluated and extended a non-parametric measure of concordance aiming to compare the stability of classifiers (Chapter 6). Samples were tested under varying operational conditions (e.g., varying reagent lots, operator or scanner) to determine reproducibility by comparing the concordance between risk scores. The currently most widely accepted GEP classifiers UAMS70 and the EMC92 performed equally well in this analysis, demonstrating that both classifiers can be used in a clinical context, at least in terms of assay stability. The possible future use and availability of the EMC92 classifier is discussed below.

## Combining prognostic markers

Our next question was how the EMC92 classifier would perform in comparison to and in combination with other markers. To this end, a series of GEP classifiers, serum markers and FISH markers were structurally combined in a pairwise manner, classifying patients into an a priori unspecified number of risk groups (Chapter 3). Strikingly, high-risk patients are much better identified by molecular markers while low-risk patients seemed to be ideally identified by the ISS stage I. This suggests that disease promoting factors are driven by tumor intrinsic factors while disease suppression is likely more systemic in nature; i.e., as a result

---

of a higher tumor load, immune cells are further depleted and the microenvironment is increasingly altered.<sup>21-24</sup> The lowest ISS stage turned out to be highly additive to many FISH and GEP markers. Combining EMC92 with ISS resulted in the identification of a large subset of low-risk patients (38%) with a median overall survival (OS) that was not reached at eight years of follow-up and a high-risk group (17%) with a median OS of 24 months. The high-risk patients were 5 to 7 times more likely to die at any point in time than lowest-risk patients. In contrast to ISS or EMC92 alone in which a 2 to 3 times higher chance is observed. The remaining patients (45%) were part of two intermediate-risk groups with a median OS of 47 and 61 months. A disadvantage of this combined EMC92-ISS marker is the identification of 4 risk groups, with unclear clinical consequences, especially for the intermediate-risk patients. It would therefore be interesting to extend the analyses to optimally identify the high-risk or low-risk patients specifically.

## Practical use of GEP classifiers

Correct use of GEP classifiers - like most other markers - is dependent on a number of requirements. Most importantly, it is necessary to reduce differences between the samples to classify and the samples used to build the classifier (training set). Variation between labs, technicians, protocols and reagents are the main sources of these differences.<sup>25</sup> Naturally, sources of variation should be avoided as much as possible, whilst adequate batch correction can be applied to remove remaining differences. The training set should then be used as a reference.<sup>26</sup> To aid this process, and to generate gene classifier scores for the research setting, we developed the geneClassifiers software package as part of the R Bioconductor project.<sup>27</sup> For use in clinical practice, however, thorough standardization of procedures is required. This process is laborious and expensive, and may hinder the translation of useful findings to the clinic.<sup>28,29</sup> GEP classifiers currently in use are the MammaPrint (Breast cancer, Agendia) and MyPRS (MM, UAMS70, Signal-Genetics). Also the SKY92 is currently offered as part of the MMprofiler™ assay (SkylineDx).<sup>30-33</sup> The MMprofiler is a standard Affymetrix Plus 2.0 microarray, with a standard algorithm to generate the risk score. In order to perform an MMprofiler assay, enough plasma cell derived RNA must be obtained ( $\geq 100$ ng RNA from  $>80\%$  plasma cells after purification).

## Clinical utility and risk based treatment

GEP classifiers such as SKY92 and UAMS70 turn out to have a significant contribution to prognosis for both high- and low-risk classifications. As a result GEP based prognostics are now recommended in the guidelines.<sup>34,35</sup> For many patients, prognostic markers may clarify important questions dealing with life expectancy, possibly resulting in an improved quality of life.<sup>36</sup> As discussed below, treatment decisions may be changed as a result of prognostic insight, and this may ultimately lead to improved survival. Currently prognostic markers have limited effect on clinical decision making. For now, the focus to reach improved survival as well as improved quality of life is on the development of drugs, also taking into account administration schemes and different options of transplantation.<sup>37,38</sup> New drugs are continuously under development and include monoclonal antibodies, novel proteasome inhibitors and targeted therapies directed against specific mutated proteins. The role for the patients' immune system will become increasingly important, and it is thought that this may allow for treatment of early disease. Examples of immune therapies include bispecific T-cell engagers (BiTE), chimeric antigen receptor (CAR) T-cells and immune checkpoint inhibitors.<sup>39-41</sup>

The effect of some aspects of drug administration in relation to risk status has been investigated. Elderly newly diagnosed MM patients were treated with either a sequential (i.e., all VMP cycles before all Rd cycles or vice versa) or an alternating scheme in which VMP and Rd administration were combined within each cycle. No difference in survival and response was observed.<sup>42</sup> A preliminary analysis reported however that the sequential scheme overcame the poor survival of patients with del(17p), t(4;14) or t(14;16).<sup>43</sup> The time of transplantation is another option to consider. It has been proposed to maintain an early transplant for high-risk patients and to postpone the transplantation for standard-risk patients as part of salvage therapy.<sup>44</sup> This idea is contradicted by recent data from the EMN02 trial, showing a benefit of early transplantation for all subgroups.<sup>45</sup> Confirmation of this data requires longer follow up.

In contrast to the retrospective associations above, some trials are specifically designed to use GEP based risk stratification. The total therapy 5 (TT5) study only included UAMS70 based high-risk patients. A reduced drug dosing

---

was given in one arm with shorter intervals between cycles with the aim of preventing inter-cycle relapse. Although this regimen effectively reduced early mortality and relapse, it failed to improve progression free survival (PFS) and OS due to relapse early during maintenance.<sup>46</sup> Standard-risk patients not included in the TT5, were included in the TT4 which aimed to determine whether a reduction in the intensity of Total Therapy reduces toxicity and maintains efficacy. Although there was no difference in response and OS between the regimes after 4.5 years of follow up in 289 patients, the less intense treatment had in fact a shorter duration of complete response than the standard treatment. The results further failed to show a decrease in toxicities and treatment-related mortalities.<sup>47</sup> The British Institute of Cancer Research (ICR) has launched the Myeloma UK nine phase II trial (MUK9 OPTIMAL trial; ISRCTN16847817) in which MM and patients with plasma cell leukemia will be stratified according to cytogenetics and SKY92 risk status. Within the high-risk population – which are thought not to benefit fully from current treatment approaches - combinations of multiple novel agents will be evaluated and optimized. Another trial currently being designed is the SWOG S1211 phase I/II trial (NCT01668719) for RvD with or without the SLAMF7 antibody elotuzumab in high-risk patients based on the SKY92 and other risk definitions.<sup>48</sup> An important aspect of the clinical utility is the biological variability of GEP classifiers over time, and at different tumor sites in the body of a given patient (longitudinal, spatial variation). Both aspects require further studies, particularly regarding the SKY92 classifier, as all current knowledge on these aspects of variability is based on UAMS70 data.<sup>49,50</sup>

## 9

### Predictive markers

With increasing choice of treatment options for MM, markers which can identify the most optimal treatment for a specific patient are becoming increasingly important.<sup>51</sup> Examples of such predictive markers are known for other disease entities. In patients with myelodysplastic syndrome, deletion of 5q has long been recognized to be a predictive marker to select Lenalidomide treatment, for which multiple mechanisms have been proposed including the recent findings involving effects of Lenalidomide on the Cereblon-MCT1-CD147 axis.<sup>52-58</sup> The treatment of BCR-ABL–positive chronic myeloid leukemia patients with imatinib is another

example of patient characteristics giving rise to a specific treatment.<sup>59</sup> In non-small-cell lung cancer, EGFR mutation status has emerged as an important predictor of response to the EGFR tyrosine kinase inhibitors such as erlotinib<sup>60,61</sup> and overexpression of the growth factor receptor gene HER2 is found in 20 to 30% of early stage breast cancer patients, responding well to treatment with an antibody against HER2.<sup>62</sup> In myeloma, there is currently no established predictive marker. There is provisional evidence that response to venetoclax - a selective inhibitor of the anti-apoptotic protein BCL-2 - is almost exclusively limited to those MM patients that have a t(11;14) translocation. Still, only half of all t(11;14) patients respond. Instead, only patients with increased BCL-2 mRNA expression - often absent in patients without t(11;14) - and low expression of other anti-apoptotic molecules such as BCL2L1 or MCL-1, seem to be responsive to venetoclax treatment.<sup>63-68</sup> Responses were independent of cytogenetic status as determined by interphase FISH. These findings were confirmed in a phase II trial of venetoclax treatment in combination with Bortezomib (which indirectly inhibits MCL-1) and Dexamethasone.<sup>69</sup> In response to the identification of CRBN as the target protein of Thalidomide and other immunomodulatory drugs,<sup>70</sup> we analyzed the effect of CRBN gene expression in MM tumor cells on survival and response in HOVON-65 maintenance patients (Chapter 7). Interestingly, a weak association was found for PFS in Thalidomide treated patients while absent in Bortezomib treated patients. This corresponds well to the report of reduced CRBN expression in > 85% of MM patients who were Lenalidomide resistant.<sup>71</sup> With the exception of treatments for which a clear biological cause and effect relation is known, finding predictive markers is difficult. The number of patients available for analysis is often small, considering that only a subgroup of all patients receives the specific treatment, of which only a part will respond. Small effect sizes of treatment benefits can be expected, and will make it difficult to obtain adequately powered discovery and validation data. Recently, the algorithm TOPSPIN has been developed which classifies patients as responders or non-responders to treatment using a non-linear separation based on gene sets.<sup>72</sup> Although large numbers of patients in at least two treatments arms are required, reported results look promising. As an alternative to predictive markers based on tumor cell biology, the genetic predisposition of patients to specific toxicities

---

may help to guide treatment choices. In Chapters 7 and 8 we described analyses of common germ-line variants in relation to peripheral neuropathy especially after Bortezomib treatment (BiPN). Being the dose limiting toxicity, with grade 2-4 BiPN seen in 15-40% of patients treated with Bortezomib, it constitutes a serious adverse event. In Chapter 7, newly diagnosed MM patients were studied using an early custom design chip detecting 3400 single nucleotide polymorphisms (SNPs). No association of BiPN with an individual SNP could be found. A variant in CYP17A1 was among highest associations in both the discovery and validation set. A similar analysis was performed in the VISTA trial. An analysis of 2000 variants found the CTLA4 and PSMB1 genes - which are described in relation with immune function and drug binding - to be associated with time to onset of BiPN.<sup>73</sup> As there was almost no overlap in the SNPs included in both studies, a comparison between the two studies was not possible. As a result of evolving microarray technology, we were able to perform a genome wide association study (Chapter 8). Despite a much larger number of variants that were genotyped, the small sample size precluded solid conclusions. A SNP in the gene PKNOX1 that was associated with BiPN was the most promising finding. However, a modest association of the CYP17A1 genotype with BiPN was confirmed in Chapter 8. The difficulty in finding a clear association underlines the need for collaboration in consortia for performing this type of analyses, as well as a clear definition of the trait studied.<sup>74</sup>

## Future of treatment decisions

### 9

In summary, today the patient specific factors used for treatment decisions are primarily age, the presence of comorbidities, frailty and renal failure. As a result, almost all newly diagnosed MM patients receive similar treatment. This treatment has been shown to be effective in the MM patient group as a whole. However, some patients respond only minimally or do not respond at all requiring treatment adjustments. This approach therefore fails to produce the best response in each patient. Future molecular biomarkers are likely to guide treatment decisions (Figure 1). The aim is to identify treatment specific markers for both toxicities and response. In the absence of reliable predictions, treatments can be adapted based on risk stratification. In this way, a most optimal treatment



---

## REFERENCES

1. Greipp PR, San Miguel J, Durie BG, *et al.* International staging system for multiple myeloma. *J Clin Oncol* . 2005; **23**(15):3412–20.
2. Palumbo A, Avet-Loiseau H, Oliva S, *et al.* Revised International Staging System for Multiple Myeloma: A Report From International Myeloma Working Group. *J Clin Oncol* . 2015; **33**(26):2863–9.
3. Mulligan G, Mitsiades C, Bryant B, *et al.* Gene expression profiling and correlation with outcome in clinical trials of the proteasome inhibitor bortezomib. *Blood* . 2007; **109**(8):3177–3188.
4. Morgan GJ, Davies FE, Gregory WM, *et al.* Long-term follow-up of MRC Myeloma IX trial: Survival outcomes with bisphosphonate and thalidomide treatment. *Clin Cancer Res* . 2013; **19**(21):6030–8.
5. Barlogie B, Pineda-Roman M, van Rhee F, *et al.* Thalidomide arm of Total Therapy 2 improves complete remission duration and survival in myeloma patients with metaphase cytogenetic abnormalities. *Blood* . 2008; **112**(8):3115–3121.
6. Pineda-Roman M, Zangari M, Haessler J, *et al.* Sustained complete remissions in multiple myeloma linked to bortezomib in total therapy 3: comparison with total therapy 2. *Br J Haematol* . 2008; **140**(6):625–634.
7. Reme T, Hose D, Theillet C, & Klein B. Modeling risk stratification in human cancer. *Bioinformatics* . 2013; **29**(9):1149–57.
8. Shaughnessy JJ D, Zhan F, Burington BE, *et al.* A validated gene expression model of high-risk multiple myeloma is defined by deregulated expression of genes mapping to chromosome 1. *Blood* . 2007; **109**(6):2276–2284.
9. Palumbo A, Brinthen S, Mateos MV, *et al.* Geriatric assessment predicts survival and toxicities in elderly myeloma patients: an International Myeloma Working Group report. *Blood* . 2015; **125**(13):2068–74.
10. van Vliet M, Ubels J, de Best L, van Beers EH, & Sonneveld P. The combination of SKY92 and ISS provides a powerful tool to identify both high risk and low risk multiple myeloma cases, validation in two independent cohorts [abstract]. *Blood* . 2015; **126**(23):2970.
11. van Beers E, van Vliet M, Kuiper R, *et al.* Prognostic validation of SKY92 and its combination with International Staging System in an independent cohort of Multiple Myeloma patients. *Clinical Lymphoma, Myeloma and Leukemia* . 2017; **17**(9):555–562.
12. Sherborne A, Begum D, Price A, *et al.* Identifying Ultra-High Risk Myeloma By Integrated Molecular Genetic and Gene Expression Profiling [abstract]. *Blood* . 2016; **128**(22):4407.
13. Simon R, Radmacher MD, Dobbin K, & McShane LM. Pitfalls in the use of DNA microarray data for diagnostic and prognostic classification. *J Natl Cancer Inst* . 2003; **95**(1):14–8.
14. Simon R. Roadmap for developing and validating therapeutically relevant genomic classifiers. *J Clin Oncol* . 2005; **23**(29):7332–41.
15. Brenton JD, Carey LA, Ahmed AA, & Caldas C. Molecular classification and molecular forecasting of breast cancer: ready for clinical application? *J Clin Oncol* . 2005; **23**(29):7350–60.



16. Kostka D & Spang R. Microarray based diagnosis profits from better documentation of gene expression signatures. *PLoS Comput Biol* . 2008; **4**(2):e22.
17. Chng WJ, Chung TH, Kumar S, *et al*. Gene signature combinations improve prognostic stratification of multiple myeloma patients. *Leukemia* . 2015; **30**(5):1071–8.
18. Dickens NJ, Walker BA, Leone PE, *et al*. Homozygous deletion mapping in myeloma samples identifies genes and an expression signature relevant to pathogenesis and outcome. *Clin Cancer Res* . 2010; **16**(6):1856–1864.
19. Repetitive flaws. *Nature* . 2016; **529**(7586):256.
20. McNutt M. Journals unite for reproducibility. *Science* . 2014; **346**(6210):679.
21. Pinzon-Charry A, Maxwell T, & Lopez JA. Dendritic cell dysfunction in cancer: a mechanism for immunosuppression. *Immunol Cell Biol* . 2005; **83**(5):451–61.
22. Ostrand-Rosenberg S, Sinha P, Beury DW, & Clements VK. Cross-talk between myeloid-derived suppressor cells (MDSC), macrophages, and dendritic cells enhances tumor-induced immune suppression. *Semin Cancer Biol* . 2012; **22**(4):275–81.
23. Glavey SV, Naba A, Manier S, *et al*. Proteomic characterization of human multiple myeloma bone marrow extracellular matrix. *Leukemia* . 2017; **21**(11):2426.
24. Quail DF & Joyce JA. Microenvironmental regulation of tumor progression and metastasis. *Nat Med* . 2013; **19**(11):1423–37.
25. Kitchen RR, Sabine VS, Simen AA, Dixon JM, Bartlett JM, & Sims AH. Relative impact of key sources of systematic noise in Affymetrix and Illumina gene-expression microarray experiments. *BMC Genomics* . 2011; **12**(1):589.
26. Kitchen RR, Sabine VS, Sims AH, *et al*. Correcting for intra-experiment variation in Illumina BeadChip data is necessary to generate robust gene-expression profiles. *BMC Genomics* . 2010; **11**:134.
27. Gentleman RC, Carey VJ, Bates DM, *et al*. Bioconductor: open software development for computational biology and bioinformatics. *Genome Biol* . 2004; **5**(10):R80.
28. Wehling M. Translational medicine: can it really facilitate the transition of research "from bench to bedside"? *Eur J Clin Pharmacol* . 2006; **62**(2):91–5.
29. Tajeja N. Bridging the translation gap - new hopes, new challenges. *Fundam Clin Pharmacol* . 2011; **25**(2):163–71.
30. van 't Veer LJ, Dai H, van de Vijver MJ, *et al*. Gene expression profiling predicts clinical outcome of breast cancer. *Nature* . 2002; **415**(6871):530–6.
31. van Laar R, Flinckum R, Brown N, *et al*. Translating a gene expression signature for multiple myeloma prognosis into a robust high-throughput assay for clinical use. *BMC Med Genomics* . 2014; **7**:25.
32. Kuiper R, Broyl A, de Knegt Y, *et al*. A gene expression signature for high-risk multiple myeloma. *This thesis and Leukemia* . 2012; **26**(11):2406–13.
33. Wittner BS, Sgroi DC, Ryan PD, *et al*. Analysis of the MammaPrint breast cancer assay in a predominantly postmenopausal cohort. *Clin Cancer Res* . 2008; **14**(10):2988–93.
34. Mikhael JR, Dingli D, Roy V, *et al*. Management of newly diagnosed symptomatic multiple mye-

---

loma: updated Mayo Stratification of Myeloma and Risk-Adapted Therapy (mSMART) consensus guidelines 2013. *Mayo Clin Proc* . 2013; **88**(4):360–76.

35. Chng WJ, Dispenzieri A, Chim CS, *et al*. IMWG consensus on risk stratification in multiple myeloma. *Leukemia* . 2014; **28**(2):269–77.
36. Shay LA, Parsons HM, & Vernon SW. Survivorship Care Planning and Unmet Information and Service Needs Among Adolescent and Young Adult Cancer Survivors. *J Adolesc Young Adult Oncol* . 2017; **6**(2):327–332.
37. Ludwig H, Sonneveld P, Davies F, *et al*. European Perspective on Multiple Myeloma Treatment Strategies in 2014. *Oncologist* . 2014; **19**(9):829–844.
38. Crawley C, Iacobelli S, Bjorkstrand B, Apperley JF, Niederwieser D, & Gahrton G. Reduced-intensity conditioning for myeloma: lower nonrelapse mortality but higher relapse rates compared with myeloablative conditioning. *Blood* . 2007; **109**(8):3588–94.
39. Huehls AM, Coupet TA, & Sentman CL. Bispecific T-cell engagers for cancer immunotherapy. *Immunol Cell Biol* . 2015; **93**(3):290–6.
40. Maus MV, Grupp SA, Porter DL, & June CH. Antibody-modified T cells: CARs take the front seat for hematologic malignancies. *Blood* . 2014; **123**(17):2625–35.
41. Pardoll DM. The blockade of immune checkpoints in cancer immunotherapy. *Nat Rev Cancer* . 2012; **12**(4):252–64.
42. Mateos MV, Martinez-Lopez J, Hernandez MT, *et al*. Sequential vs alternating administration of VMP and Rd in elderly patients with newly diagnosed MM. *Blood* . 2016; **127**(4):420–5.
43. Mateos MV, Gutierrez NC, Martin ML, *et al*. Bortezomib Plus Melphalan and Prednisone (VMP) Followed By Lenalidomide and Dexamethasone (Rd) in Newly Diagnosed Elderly Myeloma Patients Overcome the Poor Prognosis of High-Risk Cytogenetic Abnormalities (CA) Detected By Fluorescence in Situ Hybridization (FISH). *Blood* . 2015; **126**(23):4243.
44. Brioli A. First line vs delayed transplantation in myeloma: Certainties and controversies. *World J Transplant* . 2016; **6**(2):321–30.
45. Cavo M, Palumbo A, Zweegman S, *et al*. Upfront autologous stem cell transplantation (ASCT) versus novel agent-based therapy for multiple myeloma (MM): A randomized phase 3 study of the European Myeloma Network (EMN02/HO95 MM trial). *Journal of Clinical Oncology* . 2016; **34**:8000–8000.
46. Jethava Y, Mitchell A, Zangari M, *et al*. Dose-dense and less dose-intense total therapy 5 for gene expression profiling-defined high-risk multiple myeloma. *Blood Cancer J* . 2016; **6**:e471.
47. Jethava YS, Mitchell A, Epstein J, *et al*. Adverse Metaphase Cytogenetics Can Be Overcome by Adding Bortezomib and Thalidomide to Fractionated Melphalan Transplants. *Clin Cancer Res* . 2017; **23**(11):2665–2672.
48. Usmani SZ, Sexton R, Ailawadhi S, *et al*. Phase I safety data of lenalidomide, bortezomib, dexamethasone, and elotuzumab as induction therapy for newly diagnosed symptomatic multiple myeloma: SWOG S1211. *Blood Cancer J* . 2015; **5**:e334.
49. Rasche L, Chavan SS, Stephens OW, *et al*. Spatial genomic heterogeneity in multiple myeloma revealed by multi-region sequencing. *Nat Commun* . 2017; **8**(1):268.

50. Zhou Y, Barlogie B, & Shaughnessy J J D. The molecular characterization and clinical management of multiple myeloma in the post-genome era. *Leukemia* . 2009; **23**(11):1941–56.
51. Ballman KV. Biomarker: Predictive or Prognostic? *J Clin Oncol* . 2015; **33**(33):3968–71.
52. Fenaux P, Giagounidis A, Selleslag D, *et al*. A randomized phase 3 study of lenalidomide versus placebo in RBC transfusion-dependent patients with Low-/Intermediate-1-risk myelodysplastic syndromes with del5q. *Blood* . 2011; **118**(14):3765–76.
53. List A, Kurtin S, Roe DJ, *et al*. Efficacy of lenalidomide in myelodysplastic syndromes. *N Engl J Med* . 2005; **352**(6):549–57.
54. List A, Dewald G, Bennett J, *et al*. Lenalidomide in the myelodysplastic syndrome with chromosome 5q deletion. *N Engl J Med* . 2006; **355**(14):1456–65.
55. Giagounidis A, Mufti GJ, Fenaux P, Germing U, List A, & MacBeth KJ. Lenalidomide as a disease-modifying agent in patients with del(5q) myelodysplastic syndromes: linking mechanism of action to clinical outcomes. *Ann Hematol* . 2014; **93**(1):1–11.
56. Stahl M & Zeidan AM. Lenalidomide use in myelodysplastic syndromes: Insights into the biologic mechanisms and clinical applications. *Cancer* . 2017; **123**(10):1703–1713.
57. Wei S, Chen X, Rocha K, *et al*. A critical role for phosphatase haplo deficiency in the selective suppression of deletion 5q MDS by lenalidomide. *Proc Natl Acad Sci U S A* . 2009; **106**(31):12974–9.
58. Eichner R, Heider M, Fernandez-Saiz V, *et al*. Immunomodulatory drugs disrupt the cereblon-CD147-MCT1 axis to exert antitumor activity and teratogenicity. *Nat Med* . 2016; **22**(7):735–43.
59. Druker BJ, Guilhot F, O'Brien SG, *et al*. Five-year follow-up of patients receiving imatinib for chronic myeloid leukemia. *N Engl J Med* . 2006; **355**(23):2408–17.
60. Wang Y, Schmid-Bindert G, & Zhou C. Erlotinib in the treatment of advanced non-small cell lung cancer: an update for clinicians. *Ther Adv Med Oncol* . 2012; **4**(1):19–29.
61. Gazdar AF. Personalized medicine and inhibition of EGFR signaling in lung cancer. *N Engl J Med* . 2009; **361**(10):1018–20.
62. King CR, Kraus MH, & Aaronson SA. Amplification of a novel v-erbB-related gene in a human mammary carcinoma. *Science* . 1985; **229**(4717):974–6.
63. Touzeau C, Dousset C, Le Gouill S, *et al*. The Bcl-2 specific BH3 mimetic ABT-199: a promising targeted therapy for t(11;14) multiple myeloma. *Leukemia* . 2014; **28**(1):210–2.
64. Kumar S, Kaufman JL, Gasparetto C, *et al*. Efficacy of venetoclax as targeted therapy for relapsed/refractory t(11;14) multiple myeloma. *Blood* . 2017; **130**:2401–2409.
65. Ross J, Chyla B, Goswami R, *et al*. BCL2 expression is a potential predictive biomarker of response to venetoclax in combination with bortezomib and dexamethasone in patients with relapsed/refractory multiple myeloma [abstract P682]. *Haematologica* . 2017; **102**(s2):272.
66. Gupta VA, Newman S, Bahlis NJ, *et al*. B-Cell Markers Predict Response to Venetoclax in Multiple Myeloma. *Blood* . 2016; **128**(22):2108.
67. Wu J, Ross J, Peale J F V, *et al*. A Favorable BCL-2 Family Expression Profile May Explain the Increased Susceptibility of the t(11;14) Multiple Myeloma Subgroup to Single Agent Venetoclax. *Blood* . 2016; **128**(22):5613.

- 
68. Matulis SM, Gupta VA, Nooka AK, *et al.* Dexamethasone treatment promotes Bcl-2 dependence in multiple myeloma resulting in sensitivity to venetoclax. *Leukemia* . 2016; **30**(5):1086–1093.
  69. Moreau P, Chanan-Khan A, Roberts AW, *et al.* Promising efficacy and acceptable safety of venetoclax plus bortezomib and dexamethasone in relapsed/ refractory MM. *Blood* . 2017; **130**:2392–2400.
  70. Ito T, Ando H, Suzuki T, *et al.* Identification of a primary target of thalidomide teratogenicity. *Science* . 2010; **327**(5971):1345–50.
  71. Zhu YX, Braggio E, Shi CX, *et al.* Cereblon expression is required for the antimyeloma activity of lenalidomide and pomalidomide. *Blood* . 2011; **118**(18):4771–9.
  72. Ubels J, Sonneveld P, van Beers EH, Broijl A, van Vliet MH, & de Ridder J. Predicting treatment benefit in multiple myeloma through simulation of alternative treatment effects. *Nat Commun* . 2017; **9**(1):2943.
  73. Favis R, Sun Y, van de Velde H, *et al.* Genetic variation associated with bortezomib-induced peripheral neuropathy. *Pharmacogenet Genomics* . 2011; **21**(3):121–9.
  74. Mitchell JS, Li N, Weinhold N, *et al.* Genome-wide association study identifies multiple susceptibility loci for multiple myeloma. *Nat Commun* . 2016; **7**:12050.

**CHAPTER**

**10**

**Summaries**

---

## English summary

The studies in this thesis cover two main topics: development and comparison of prognostic markers in Multiple Myeloma (MM) (chapters 2-6), and characterization of the genetic basis of peripheral neuropathy, an important toxicity of MM treatment (chapters 7 and 8).

**Chapter 2** (Kuiper *et al.* 2012): By gene expression profiling of 290 MM patients included in the HOVON-65/GMMG-HD4 clinical trial, a 92 gene classifier (EMC92) was developed, enabling the classification of patients into high- or standard risk. This classifier was validated in four external patient cohorts (newly diagnosed and relapsed) in which its performance was shown to be independent of other prognostic factors.

**Chapter 3** (Kuiper *et al.* 2015): By exploiting the value of twenty known prognostic factors, which were systematically combined pair-wisely, we selected those combinations that improved prognostication. Among the most promising was the EMC92-ISS combination, enabling the classification of patients into four risk groups. The combinations that were found in the discovery phase were then validated in a similar group of patients that were left out of the discovery phase prior to the analysis.

**Chapter 4** (submitted): Although approximately 65% of newly diagnosed MM patients are older than 65 years and thus likely non-transplant eligible, the EMC92-gene classifier has been validated using mainly newly diagnosed transplant eligible or relapsed patients. Only in a subset of the MRC-IX, newly diagnosed non-transplant eligible patients were included. Therefore, we applied the EMC92-gene classifier to 178 patients included in the HOVON-87 trial with a median age of 73 years. Also in this setting the classifier has a strong performance, independent of other prognostic factors.

**Chapter 5** (submitted): The most important aspect of a prognostic predictor is its prognostic value. Precision is also important, i.e. upon repeatedly classifying a patient under similar conditions, the resulting outcome should remain the same. We have described a method to quantify the concordance between repeated measurements and a test for equal concordances.

**Chapter 6** (Broyl *et al.* 2013): Recently, cereblon (CRBN) expression was

found to be essential for the activity of the immune modulatory drugs, thalidomide and lenalidomide. Using 96 thalidomide treated patients of the HOVON-65/GMMG-HD4 trial, we showed that higher levels CRBN expression were significantly associated with longer progression-free survival. In contrast, no association between CRBN expression and survival was observed in the arm with bortezomib maintenance.

**Chapter 7** (Corthals *et al.* 2011): Peripheral neuropathy (PNP) is the dose limiting toxicity for bortezomib. Patients with higher grades of PNP require dose-reduction or even discontinuation of the treatment. Identification of an increased risk before start of the treatment could help treatment decisions. Therefore we tested the association between germline single nucleotide polymorphisms (SNPs) and the occurrence of PNP during bortezomib treatment in the IFM-2015-01 clinical trial. The SNPs were detected using an early SNP chip (with hypothesis driven design) containing 3400 features of which 56 were found to be univariately associated in the discovery set. However, neither in the discovery set, nor in the HOVON-65/GMMG-HD4 validation set, any of these reached significance after multiple testing correction. Based on the highest-ranking SNPs found using the uncorrected p-value in the discovery set, pathway analysis did demonstrate clear enrichment of neurological disease SNPs, possibly indicative for a combination of many small effects.

**Chapter 8** (Magrangeas *et al.* 2016): The bortezomib treated HOVON65/GMMG-HD4 patients have been re-genotyped using a more recent type of SNP array (with unbiased design) containing more than 900.000 SNPs. Similar analyses were performed with a slight alteration in the phenotype definition: PNP grades 0 and 1 versus grades >1. A SNP mapping to the 3' UTR of PKNOX1 was among the highest associations in the IFM discovery cohort that could be validated in the HOVON-65/GMMG-HD4 validation data in which it reached significance after multiple testing correction.

---

## Nederlandse samenvatting

De studies in dit proefschrift beschrijven twee hoofdlijnen, namelijk: de ontwikkeling en vergelijking van prognostische markers in multiple myeloma (MM; hoofdstukken 2 tot en met 6), en onderzoek naar de genetische basis van perifere neuropathie, wat een ernstige en veel geziene bijwerking is tijdens de behandeling van MM (hoofdstukken 7 en 8).

**Hoofdstuk 2** (Kuiper *et al.* 2012): Een prognostische classificator op basis van 92 genen is ontwikkeld in gen expressie profielen van 290 MM patiënten die waren geïncludeerd in de HOVON-65/GMMG-HD4 klinische studie. De classificator is gevalideerd in vier externe cohorten (zowel nieuw gediagnostiseerde als recidief patiënten) waarin de onafhankelijke prognostische waarde ten opzichte van bestaande prognostische markers aangetoond kon worden.

**Hoofdstuk 3** (Kuiper *et al.* 2015): Door twintig bekende prognostische markers systematisch paarsgewijs met elkaar te combineren is getracht die combinaties te selecteren die een verbeterde voorspelling gaven van de prognose. De beste prestaties werden onder meer bereikt door de EMC92/ISS combinatie die patiënten categoriseerde in een van vier risico groepen. Deze classificator is gevalideerd in een onafhankelijke subset van de data.

**Hoofdstuk 4** (submitted): Ondanks dat 65% van de nieuw gediagnostiseerde patiënten ouder zijn dan 65 jaar en dus waarschijnlijk ongeschikt zijn om beenmerg transplantatie te ondergaan, is de EMC92 classificator voornamelijk gevalideerd op jongere nieuw gediagnosticeerde patiënten die wel een transplantatie ondergingen. Daarom is de EMC92 toegepast op 178 patiënten die zijn geïncludeerd in de HOVON87 studie. Deze patiënten hebben een mediane leeftijd van 73 jaar. Ook in deze setting bleef de prognostische waarde van de EMC92 behouden.

**Hoofdstuk 5** (submitted): Naast het onderscheidend vermogen is ook precisie een belangrijk aspect van een classificator. Dat wil zeggen, het herhaaldelijk classificeren van een patiënt zou tot consistente uitkomsten moeten leiden. Wij hebben een algemene methode beschreven om de mate van overeenkomst tussen herhaaldelijke metingen te kwantificeren en de mate van overeenkomst tussen methodes te vergelijken.

**Hoofdstuk 6** (Broyl *et al.* 2013): Onlangs bleek dat het tot expressie komen



van cereblon (CRBN) essentieel is voor de effectiviteit van zogenaamde ‘immune modulatory’ drugs zoals thalidomide en lenalidomide. Daarom hebben we gekeken naar de overleving op thalidomide of bortezomib onderhoudsbehandeling in HOVON65 patiënten ten opzichte van de gemeten CRBN expressie bij diagnose. Een toegenomen CRBN expressie was significant geassocieerd met langere progressie vrije overleving bij thalidomide onderhoudsbehandeling. Bij bortezomib was dit verband afwezig.

**Hoofdstuk 7** (Corthals *et al.* 2011): Perifere neuropathie (PNP) is de dosisbeperkende toxiciteit voor bortezomib. Patiënten met ernstige neuropathie moeten behandeld worden met lagere dosis of de behandeling zal zelfs beëindigd moeten worden. Het herkennen van een verhoogd risico op PNP voor de start van de behandeling van belang zou gewenst zijn. Daarom hebben we gezocht naar verbanden tussen het optreden van PNP en het hebben van specifieke genotypes genaamd ‘single nucleotide polymorphisms’ (SNPs) bij patiënten in de IFM-2015-01 klinische studie. Met behulp van een van de eerste SNP chips konden we 3400 (hypothese gedreven) SNPs per patiënt bepalen. Hiervan werden er 56 univariaat gelinkt aan PNP in de IFM data. Geen van deze was echter significant na correctie voor multiple testing. De hoogst gerangschikte SNPs waren verrijkt met SNPs die in eerdere studies in verband werden gebracht met neurologische aandoeningen. Dit duidt mogelijk op het aanwezig zijn van vele SNPs die zwak geassocieerd zijn met PNP en dus enkel gevonden kunnen worden in studies met meer patiënten.

**Hoofdstuk 8** (Magrangeas *et al.* 2016): Patiënten zijn opnieuw gegenotypeerd op een nieuwere SNP chip met meer dan 900.000 SNPs. Soortgelijke analyses zijn gedaan met een kleine aanpassing in de definitie van het fenotype: PNP grades 0 en 1 zijn vergeleken met grades >1. Een univariaat significant verband tussen hogere graads PNP en een variant in het PKNOX1 gen werd gevonden in de IFM data. Deze bevinding kon worden gevalideerd in de HOVON65 validatie data waarin de SNP significant was na correctie voor multiple testing.

---

## List of publications

1. Kuiper R, Broyl A, de Knegt Y, *et al.* A gene expression signature for high-risk multiple myeloma. *Leukemia*. 2012;**26**(11):2406-2413.
2. Kuiper R, van Duin M, van Vliet MH, *et al.* Prediction of high- and low-risk multiple myeloma based on gene expression and the International Staging System. *Blood*. 2015;**126**(17):1996-2004
3. Broyl A, Kuiper R, van Duin M, *et al.* High cereblon expression is associated with better survival in patients with newly diagnosed multiple myeloma treated with Thalidomide maintenance. *Blood*. 2013;**121**(4):624-627.
4. Corthals SL, Kuiper R, Johnson DC, *et al.* Genetic factors underlying the risk of Bortezomib induced peripheral neuropathy in multiple myeloma patients. *Haematologica*. 2011;**96**(11):1728-1732.
5. Magrangeas F, Kuiper R, Avet-Loiseau H, *et al.* A Genome-Wide Association Study Identifies a Novel Locus for Bortezomib-Induced Peripheral Neuropathy in European Patients with Multiple Myeloma. *Clin Cancer Res*. 2016;**22**(17):4350-4355.
6. Broyl A, Corthals SL, Jongen JL, *et al.* Mechanisms of peripheral neuropathy associated with Bortezomib and vincristine in patients with newly diagnosed multiple myeloma: a prospective analysis of data from the HOVON-65/GMMG-HD4 trial. *Lancet Oncol*. 2010;**11**(11):1057-1065.
7. Corthals SL, Sun SM, Kuiper R, *et al.* MicroRNA signatures characterize multiple myeloma patients. *Leukemia*. 2011;**25**(11):1784-1789.
8. Pedotti P, t Hoen PA, Vreugdenhil E, *et al.* Can subtle changes in gene expression be consistently detected with different microarray platforms? *BMC Genomics*. 2008;9:124.
9. Wu P, Walker BA, Broyl A, *et al.* A gene expression based predictor for high risk myeloma treated with intensive therapy and autologous stem cell rescue. *Leuk Lymphoma*. 2014:1-8.
10. Mitchell JS, Li N, Weinhold N, *et al.* Genome-wide association study identifies multiple susceptibility loci for multiple myeloma. *Nat Commun*.

---

2016;7:12050.

11. Broijl A, Kuiper R, van Duin M, *et al.* Hoog- en laagrisico multipel myeloom kunnen worden voorspeld met de combinatie van EMC92 en ISS. *Ned Tijdschr Hematol.* 2017.
12. van Beers EH, van Vliet MH, Kuiper R, *et al.* Prognostic Validation of SKY92 and Its Combination With ISS in an Independent Cohort of Patients With Multiple Myeloma. *Clin Lymphoma Myeloma Leuk.* 2017; **17**(9):555-562.
13. Went M, Sud A, Försti A, *et al.* Identification of multiple risk loci and potential regulatory mechanisms influencing susceptibility to multiple myeloma. Accepted by *Nat Commun* Jun 2018.
14. Went, M., Sud, A., Law, P.J. *et al.* Assessing the effect of obesity-related traits on multiple myeloma using a Mendelian randomisation approach. *Blood cancer j.* 2017;**7**(6):e573.
15. Kuiper R, Zweegman S, van Duin M, *et al.* Gene expression classifier SKY92 identifies high-risk multiple myeloma in elderly patients of the HOVON-87/NMSG-18 study. Submitted 2018.
16. Kuiper R, Huisman SMH, Hoogenboezem R, *et al.* Nopaco: A Non-Parametric test for concordance in unbalanced data. Submitted 2018.
17. Kuiper R, van Duin M, van Vliet MH, *et al.* Two group risk classification in multiple myeloma: validation of EMC92 gene expression signature as high risk marker and the EMC92-ISS combination as low risk marker. Submitted 2018.



## Curriculum vitae

Rowan Kuiper werd geboren op 8 maart 1981 te Vlaardingen. Hij heeft in 1998 zijn HAVO diploma behaald aan de school de Angelus Merula te Spijkenisse. In datzelfde jaar is hij gestart met de opleiding tot scheepsbouwkundig ingenieur aan de Hogeschool Rotterdam. Na het behalen van het diploma in 2002 en een kortstondige periode ergotherapie te hebben gestudeerd, is hij in 2004 begonnen aan de opleiding tot bioinformaticus aan de Hogeschool Leiden waar hij in 2008 cum laude afstudeerde op het onderwerp proteïn modelling. In 2009 begon hij zijn promotie onderzoek op de afdeling hematologie van de Erasmus Universiteit Rotterdam onder supervisie van prof. dr. P. Sonneveld en dr. Mark van Duin waarvan de resultaten zijn beschreven in dit proefschrift. Momenteel is hij werkzaam als bioinformaticus bij SkylineDx te Rotterdam waar hij zijn onderzoek naar toegepaste prognostiek in MM en andere aandoeningen voortzet.

---

## Dankwoord

Na een intensieve periode van bijna tien jaar, wil ik afsluiten met dit dankwoord.

Allereerst wil ik mijn promotor prof. dr. Pieter Sonneveld bedanken. Beste Pieter, dank voor het in mij gestelde vertrouwen om het promotietraject te kunnen beginnen. Mede door jou kon ik beschikken over data van hoge kwaliteit. In combinatie met je kritische commentaar hebben deze analyses uiteindelijk geresulteerd in een aantal interessante uitkomsten.

Dr. Mark van Duin, mijn copromotor. Je bent altijd beschikbaar voor vragen, die je vervolgens vaak heel pragmatisch beantwoord. Daarnaast heb ik vaak vertrouwd op je goede Engels waarmee je een belangrijke bijdrage hebt gehad aan alle artikelen. Beste Mark, ik wil je enorm bedanken voor je behulpzaamheid en goede samenwerking!

De leden van de kleine commissie, prof. dr. Ruud Delwel, prof. dr. Sonja Zweegman en prof. dr. André Uitterlinden wil ik hartelijk bedanken voor het beoordelen van mijn proefschrift. Prof. dr. Ron van Schaik, prof. dr. Marcel Reinders, dr. Peter Valk, dr. Bronno van der Holt en dr. Jeroen de Ridder wil ik bedanken voor het plaatsnemen in de grote commissie.

Verder wil ik het HOVON data centrum bedanken voor het aanleveren van alle patiëntendata en in het bijzonder de al eerder genoemde dr. Bronno van der Holt en dr. Kazem Nasserinejad voor het meedenken bij statistische vragen.

Binnen de Sonneveld-groep heb ik kunnen werken aan verschillende technieken. Samen met Sophie Corthals heb ik aan de SNP analyses gewerkt en samen met Annemiek Broijl aan de HOVON-65 microarray gen expressie analyses. Dank aan Davine Hofste op Bruinink die zorgde voor mijn eerste concrete kennismaking met next generation sequencing. Dank allen voor de fijne samenwerking, het meedenken tijdens werkbesprekingen en de leuke avonden rondom congressen zoals het zonnige etentje op een eiland in het Lago Maggiore.

Natuurlijk niet te vergeten, dank aan alle analisten, Yvonne de Knecht, Martijn Schoester, Jasper Koenders, Michael Vermeulen en Chelsea den Hollander binnen het EMC en Belinda Dumeé, Lizanne Bosman, Daphne Huigh, Sena Zümürütçü en Deborah Bokx bij Skyline, zonder wie ik geen data gehad zou hebben om te analyseren.

Veel pauzes heb ik doorgebracht met de bio-informatici. Hier heb ik voor het eerst kennis gemaakt met het statistische begrip 'Lasso'. Hier ging het over assembly, processoren, videokaarten en harddisks waar ik nog altijd niet veel van begrepen heb. En hier heb ik te horen gekregen dat mijn leven nog veel duurzamer kan - wat ik betwijfel maar wat ik wel een goed streven vind. Dank aan Erdogan Taskesen, Mathijs Sanders, Remco Hoogeboezem, Roger Mulet en Elodie Stoetman.

Mijn onderzoek vond plaats binnen het BioChip project van CTMM, dat als doel had resultaten uit onderzoek beschikbaar te maken voor de patiënt. In dit verband heb ik sinds het begin van mijn onderzoek contact gehad met Martin van Vliet en Erik van Beers van SkylineDx. Hier hebben we het 'het 92-gen signature' verder ontwikkeld tot een product dat op dit moment beschikbaar is voor patiënten in de EU en VS. Sinds vier jaar ben ik zelf werkzaam voor SkylineDx waar ik in de mogelijkheid ben geweest om een deel van mijn werk voor Skyline te combineren met het onderzoekstraject, waarvoor dank aan Dharminder Chahal.

Alle dank aan mijn vader en moeder voor de jaren dat ik heb kunnen studeren. Mijn moeder heeft samen met mij moeten stressen over presentaties, deadlines en de slepende laatste loodjes van dit proefschrift. Mijn oma wil ik bedanken voor haar nuchtere kijk op de wetenschap. Volgens haar is er meer tussen hemel en aarde. Verder was ik zonder de hulp van mijn zus niet tot deze lay-out gekomen. De cover van dit proefschrift is geheel het werk van mijn moeder. Mijn zus en haar man hebben de organisatie van het feest voor hun rekening genomen. Beste familie, al met al waren het extreem hectische jaren. Een diep dal maar zeker ook leuke gebeurtenissen met als hoogtepunt de komst van Toon en Mia, mijn neefje en nichtje.

Allen bedankt!





# PhD Portfolio

Name PhD student:	Rowan Kuiper	PhD period:	Jan 2009 - Oct 2018
Erasmus MC department:	Hematology	Promotor:	Prof. dr. P. Sonneveld
Research school:	Molecular Medicine	Co-promotor:	Dr. M. van Duin

## 1. PhD training

	Year	ECTS
<b>Courses</b>		
SNPs and Human Diseases (MolMed)	2009	1.9
Partek training course	2009	1.3
Molecular and Cell Biology	2009	6
Regression analysis	2009	1.9
Introduction to Data-analysis	2009	1
Matlab fundamentals and statistical methods	2009	1

### Workshops and seminars

Erasmus Hematology Lectures	2009-2014	1
-----------------------------	-----------	---

### Presentations

6 × Hematology Lectures	2009 - 2014	3
3 × Journal clubs	2009 - 2014	1.5
3 × AIO-postdoc meetings	2009 - 2014	1.5
4 × CTMM workpackage 1 meetings	2009 - 2014	4
4 × European Myeloma Network Baveno	2013,14,16,17	4
2 × Myeloma Preclinical Day	2012-2013	2
1 × European Hematology Association Amsterdam	2012	2
1 × Dutch Hematology Conference Papendal	2012	2

### (Inter)national conferences

American Society of Hematology New Orleans (poster)	2009	1
American Society of Hematology San Diego (poster)	2011	1
International Myeloma Workshop Parijs (poster)	2012	1
CTMM Annual Meeting Utrecht (poster)	2010	1
CTMM Annual Meeting Utrecht (poster)	2011	1
14 <sup>th</sup> Molecular Medicine Day (poster)	2010	0.5
15 <sup>th</sup> Molecular Medicine Day (poster)	2011	0.5
International Myeloma Workshop Kyoto (poster)	2013	1
CTMM Annual Meeting Utrecht (poster)	2013	1
European Hematology Association Madrid (poster)	2017	1
European Hematology Association Stockholm (2 posters)	2018	2

## 2. Teaching

European Myeloma Network Gene Expression Workshop	2009	1
Assistant clustering practicum	2013	0.25

<b>Total</b>		<b>46.35</b>
--------------	--	--------------



# Abbreviations

<b>Term</b>	<b>Definition</b>
95%CI	95% Confidence interval
AE	Adverse event
ANOVA	Analysis of variance
ASCT	Autologous stem cell transplantation
B2m	Beta-2-microglobulin
BiPN	Bortezomib induced Peripheral Neuropathy
BiTE	Bispecific T-cell Engagers
BOR	Drug: Bortezomib
CAR	Chimeric Antigen Receptor
CD1, CD2	Cluster: Cyclin D1 or D2 gene translocation
cDNA	Complementary DNA
CE	Conformité Européene
CEU	Central European
CHB	Han Chinese in Beijing
CHR	Chromosome
CRAB	Diagnostic criteria for MM: hyperCalcemia, Renal failure, Anemia, or lytic Bone lesions
CTA	Cluster: Cancer Testis Antigens
CTCAE	Common Toxicity Criteria for Adverse Events
CTDa	Treatment: attenuated Cyclophosphamide, Thalidomide, Dexamethasone
CVAD	Treatment: Cyclophosphamide, Vincristine, Doxorubicin, Dexamethasone
DNA	Deoxyribonucleic acid
EFS	Event free survival
EMC92	Erasmus Medical Center 92-gene classifier
FDR	False Discovery Rate

<b>Term</b>	<b>Definition</b>
FISH	Fluorescence in Situ Hybridization
FRMA	Frozen Robust Multi-Array normalization
FWER	Family-Wise Error Rate
GCRMA	Guanine Cytosine adjusted Robust Multi-Array normalization
GEO	Gene Expression Omnibus
GEP	Gene Expression Profiling
GMMG	German-Speaking Myeloma Multicenter Group
GPI50	Gene Proliferation Index 50-gene classifier
GWAS	Genome Wide Association Study
HDM	High dose Melphalan
HM19	Heidelberg-Montpellier 19-gene classifier
HO-<xx>	HOVON study with trial number <xx>
HOVON	Haemato Oncology Foundation for Adults in the Netherlands
HR	Hazard ratio or High-risk
HWE	Hardy-Weinberg equilibrium
HY	Cluster: Hyperdiploid
ICC	Intra Class Correlation coefficient
IFM15	Intergroupe Francophone du Myélome 15-gene classifier
IgH, IgH	Immunoglobulin-H or G
IMiD	Immunomodulatory Drug
IMWG	International Myeloma Working Group
Interm	Intermediate
ISS	International Staging System
IVD	In Vitro Diagnostic
LB	Cluster: Bone disease
LD	Linkage disequilibrium
LDH	Lactate dehydrogenase
MPR-R	Treatment: Melphalan, Prednisone, Lenalidomide plus Lenalidomide maintenance

<b>Term</b>	<b>Definition</b>
M-protein	Monoclonal protein
MAF	Minor allele frequency or MAF gene
MAS5	Microarray suite 5.0 gene expression normalization method
MDE	Myeloma Defining Events
MF	Cluster: MAF gene translocation cluster
MGUS	Monoclonal Gammopathy of Undetermined Significance
MM	Multiple Myeloma
MP	Treatment: Melphalan Prednisone
MPT-T	Treatment: Melphalan, Prednisone, Thalidomide plus Thalidomide maintenance
MRCIX6	Medical Research Council IX 6-gene classifier
mRNA	messenger RNA
MS	Cluster: MMSET gene translocation cluster
mSMART	Mayo Stratification for Myeloma And Risk-adapted Therapy
n.r.	Median not reached
NA	Not Applicable or Not Available
NCBI	National Center for Biotechnology
Neg	Negative
NMSG	Nordic Myeloma Study Group
Nopaco	Non-parametric concordance coefficient
OR	Odds Ratio
OS	Overall Survival
PAD	Treatment: Bortezomib, Adriamycin, Dexamethasone
PANP	Presence-Absence Calls from Negative Strand Matching Probesets
PCA	Principal Component Analysis
PCL	Plasma Cell Leukemia
PCLI	Plasma Cell Labeling Index
PFS	Progression Free Survival

<b>Term</b>	<b>Definition</b>
PI	Proteasome Inhibitor
PNP	Peripheral Neuropathy
Pos	Positive
PR	Cluster: Proliferation cluster
Prop.	Proportion
QC	Quality Control
R-ISS	Revised International Staging System
Rd	Treatment: Lenalidomide, low dose Dexamethasone
RMA	Robust Multi-array Averaging gene expression normalization
RNA	Ribonucleic acid
RS	Rank Score
RT-PCR	Real-Time Polymerase Chain Reaction
SD	Standard Deviation
SKY92	Skyline 92-gene classifier
SMM	Smoldering Multiple Myeloma
SNP	Single Nucleotide Polymorphism
SR	Standard-risk
SWOG	Southwest Oncology Group
TC-classification	Translocation and Cyclin-D classification system
Thal	Thalidomide
TiPN	Thalidomide induced Peripheral Neuropathy
TT2, TT3	Total therapy 2, Total therapy 3
Tx	Treatment
UAMS17 -70 -80	University of Arkansas for Medical Sciences 17, 70 or 80 gene classifiers
UTR	Untranslated Region
VAD	Treatment: Vincristine, Adriamycin, Dexamethasone
VCD	Treatment: Bortezomib, Cyclophosphamide and Dexamethasone
VD	Treatment: Vincristine, Dexamethasone

<b>Term</b>	<b>Definition</b>
VMD	Treatment: Bortezomib, Melphalan, Dexamethasone
VMP	Treatment : Bortezomib, Melphalan, Prednisone
VTD	Treatment: Bortezomib, Thalidomide, Dexamethasone
WHO	World Health Organization
YRI	Yoruba from Ibadan







